THE INTEGRATOR SUBUNITS FUNCTION IN HEMATOPOIESIS BY MODULATING SMAD/BMP SIGNALING

TAO SHIJIE

TEMASEK LIFE SCIENCES LABORATORY

NATIONAL UNIVERSITY OF SINGAPORE

2009

THE INTEGRATOR SUBUNITS FUNCTION IN HEMATOPOIESIS BY MODULATING SMAD/BMP SIGNALING

TAO SHIJIE
(B. Sci., SUN YAT-SEN University)

A THESIS SUBMITTED

FOR THE DEGREE OF DOCTOR OF PHILOSOPHY

TEMASEK LIFE SCIENCES LABORATORY

DEPARTMENT OF BIOLOGICAL SCIENCES

NATIONAL UNIVERSITY OF SINGAPORE

2009

ACKNOWLEDGEMENTS

I would like to express my wholehearted gratitude to my supervisor Dr. Karuna Sampath for offering me the opportunity to pursue the Ph.D. degree in her laboratory. I deeply appreciate Dr. Sampath for her excellent supervision, consistent encouragement, and great support throughout the course of my research work, and also for her invaluable amendments to my thesis.

My sincere thanks also go to my graduate supervisory committee members: Dr Cai Yu, Dr. Mike Jones and Dr. Sudipto Roy for their invaluable suggestions and great encouragement during the course of my work.

I would like to thank the past and present members in Dr. Sampath laboratory: Aniket Gore, Leong Lisun Srinivas Ramasamy, Tang Lan, Tian Jing, Albert Cheong, Helen Ngoc Bao Quach, Dr. Ruan Hua, Dr. Gilligan Patrick Clemente, Jiao Binwei, Lim Shimin, Tran Duc Long and Kumari Pooja for their kind help, technical assistance, helpful discussion and priceless friendship.

I cherish the critical comments from Dr. Gilligan Patrick Clemente, Lim Shi Min and Kumari Pooja for my thesis. Many thanks also go to my attachment student Jiang Guanying for her technical support for this work.

I thank all the TLL facilities, especially fish facility and sequencing facility for the great service and support they supplied, such that this project was able to proceed smoothly.

Last, my deepest appreciation goes to my parents and my husband, Chen Zhong, for their love, encouragement and support for all these years.

Tao Shijie

Feb, 2010

TABLE OF CONTENTS

LIST OF FIGURES

LIST OF TABLES

LIST OF ABREVIATIONS

ActR-II	Actin type II receptor
AGM	aorta-gonad-mesonephros
AM	acceptor morpholino
BC	blood cell
BMP	bone morphogenetic protein
BMPR-II	type II bone morphogenetic protein receptor
CDMP	cartilage-derived morphogenetic protein
CE	convergence-extension
CHIP	chromatin immunoprecipitation
chd	*chordin*
Ci	cubitus interruptus
Co-Smad	co-mediator SMAD
cPML	cytoplasmic promyelocytic leukemia protein
CPSF	cleavage and polyadenylation specificity factor
CTD	C-terminal domain
Dad	Daughters against Dpp
DBA	Diamond-Blackfan anemia
DEPC	Diethylpyrocarbonate
DHH	Desert hedgehog
DIG	Digoxigenin
din	*chordin*
DL	Dorsal
dlx3	*distal-less homeobox 3*
DM	donor morpholino
Dpp	Decapentaplegic
DSS1	Deleted in split hand/split foot 1
EB	Embryoid body
EC	endothelia cells

Epo	erythropoietin
eve1	*even-skipped 1*
FGF	fibroblast growth factor
Flt-3	fms-like tyrosine kinase 3
FLU	Fluorescein
GDF	Growth-differentiation factor
GM-CSF	granulocyte-macrophage colony-stimulating-factor
GTPase	guanosine triphophatases
GS	Gly-Ser
gsc	*goosecoid*
H1	α-helix 1
HCC	hepatocellular carcinoma
HEK	human embryonic kidney
HH	Hedgehog
hpf	hour post fertilization
HSC	hematopoietic stem cell
hyb	hybridization
ICM	intermediate cell mass
IGF	Insulin-like growth factor
IHH	Indian hedgehog
IL-3	Interleukin-3
IL-5	Interleukin-5
IL-3R	Interleukin-3 receptor
Ints	the Integrator subunit
I-Smad	inhibitory SMAD
JAK	Janus family tyrosine protein kinase
JNK	c-Jun N-terminal kinase
JM	juxtamembrane
KD	kinase domain

KI	kinase insert
laf	*lost a fin*
LPM	lateral plate mesoderm
MAB	Maleic acid buffer
MAPK	mitogen-activated protein kinase
MAPKKK	mitogen-activated protein kinase kinase kinase
mes	*mercedes*
mfn	*minifin*
MH1	Mad homology domain 1
MH2	Mad homology domain 2
MIS	mullerian inhibiting substance
Mpo	Myeloperoxidase
NOD/SCID	nonobese diabetic/severe combined immune deficient
ntl	*no tail*
OD	optical density
ogo	*ogon*
OP	osteogenic protein
PBS	phosphate buffered saline
PC	proprotein convertase
PFA	paraformaldehyde
pgy	*piggytail*
PI-3-kinase	phosphatidylinositol 3-kinase
PKB	Protein kinase B
PPH	primary pulmonary hypertension
Ptch	Patched
PY	PPXY sequence
RACE	Rapid Amplification Of cDNA Ends
RBCs	red blood cells
RBI	rostral blood island

RNAPII	Deleted in split hand/split foot 1
RPS19	ribosomal protein S19
rRNA	ribosomal RNA
R-Smad	receptor-activated SMAD
RTK	Receptor tyrosine kinase
RT-PCR	Reverse Transcription-Polymerase Chain Reaction
SARA	SMAD anchor for receptor activation
sbn	*somitobun*
scl	*stem cell leukemia*
SH2	Src homology 2
SHH	Sonic hedgehog
siRNA	small interfering RNA
SMA	spinal muscular atrophy
SMC	smooth muscle cell
SMN	survival motor neuron
SMO	smoothened
snh	*snailhouse*
SNO	spindle-shaped N-cadherin^{+}CD45^{-} osteoblastic
snRNP	small nuclear ribonucleoparticles
SOCS	suppressor of cytokine signaling
spt	*spadetail*
SSC	standard sodium citrate
swr	*swirl*
TAK-1	TGF-β activated kinase 1
TβR1	Type I TGF-β receptor
TβRII	Type II TGF-β receptor
TGF-β	transforming growth factor-β
TILLING	Targeting Induced Local Lesions In Genomes
TM	transmembrane

VEGF	vascular endothelial growth factor
VEGFR	vascular endothelial growth factor receptor
VRAP	VEGFR associated protein
vWA	von Willebrand factor type A
VWM	vanishing white matter disease
WISH	whole mount *in situ* hybridization
WT	wild type

LIST OF PUBLICATION

Tao, S., Cai, Y., Sampath, K. (2009). The Integrator subunits function in hematopoiesis by modulating Smad/BMP signaling. *Development* **136**, 2757-2765.

Summary

Hematopoiesis, the dynamic process of blood cell development, is regulated by the activity of the Bone Morphogenetic Protein (BMP) signaling pathway, and many transcription factors. However, the molecules and the mechanisms that regulate BMP/Smad signaling in hematopoiesis are largely unknown. In our study, we show that the Integrator complex, an evolutionarily conserved group of proteins, functions in zebrafish hematopoiesis by modulating Smad/BMP signaling. The Integrator complex proteins are known to directly interact with RNA polymerase II to mediate 3'end processing of U1 and U2 snRNAs. We have identified several subunits of the Integrator complex in zebrafish. Anti-sense morpholino mediated knock-down of the Integrator subunit 5 (Ints5) in zebrafish embryos causes aberrant splicing of *smad1* and *smad5* RNA, and reduced expression of the hematopoietic genes, *stem cell leukemia* (*scl*) and *gata1*. Blood smears from *ints5* morphant embryos show arrested red blood cell differentiation, similar to *scl*-deficient embryos. Interestingly, targeting other Integrator subunits also leads to defects in *smad5* RNA splicing and arrested hematopoiesis, suggesting that the Int proteins function as a complex to regulate the BMP pathway during hematopoiesis. Our work establishes a link between the RNA processing machinery and the downstream effectors of BMP signaling, and reveals a new group of proteins that regulate the switch from primitive hematopoietic stem cell identity and blood cell differentiation by modulating Smad function.

Chapter I

Introduction

1.1 THE INTEGRATOR COMPLEX

1.1.1 Discovery Of The Integrator Complex

A subunit of the Integrator complex (Integrator subunit 5, Ints5) was recently identified from a genetic screen for genes that function in *Drosophila* oogenesis. Depletion of *ints5* in the *Drosophila* germarium causes failure in production of mature oocytes (Cai et al., unpublished data). Identification and characterization of the fly mutant showed that the gene encoded a component of the Integrator complex. The Integrator complex was originally discovered in human embryonic kidney (HEK) 293 cells by the Shiekhattar group (Baillat et al., 2005). They were interested in the function of Deleted in split hand/split foot 1 (DSS1), the product of a candidate gene for split hand/split foot. DSS1 was initially identified as a small acidic protein that could directly interact with the C-terminal domain (CTD) of the BRCA2 protein (Marston et al., 1999). To elucidate the molecular mechanism by which DSS1 induces its functional effects, Baillat et al isolated the DSS1-containing complexes from HEK293-derived cell lines stably expressing Flag-DSS1 and identified its components by mass spectrometry. They showed that DSS1 is a component of multiple, distinct complexes. They identified the 19S proteasome subunits as the main component of DSS1-associated polypeptides. In addition, they obtained peptide sequences corresponding to BRCA2, RNA polymerase II (RNAPII), and a number of uncharacterized human open reading frames, which included the novel subunits of a large complex that they named as Integrator (for integrating the CTD of RNAPII largest subunit with the 3' end processing of small nuclear RNAs, snRNA, U1 and U2) (Baillat et al., 2005).

The Integrator subunits (Ints) were found to stably associate with RNAPII. Analysis of Ints6, Ints7, and Ints12 protein sequences and structures revealed the presence of a von Willebrand factor type A (vWA) domain, an ARM repeat, and a PHD domain, respectively (Baillat et al., 2005). More interestingly, Ints11 and Ints9 display sequence homology to the subunits of the cleavage and polyadenylation specificity factor CPSF-73 and CPSF-100, respectively (Dominski et al., 2005). Importantly, Ints11 contains the putative catalytic β-lactamase domain, so it is predicted to function as an RNA-specific endonuclease (Callebaut et al., 2002). Although the Integrator subunits do not display any homology to yeast genes, nearly all of them have homologues in metazoans.

1.1.2 The Integrator Complex Is Recruited To The U1 And U2 snRNA Genes And Mediates RNA Polymerase II Dependent snRNA Transcription.

Baillat *et al.* showed that although the Integrator complex directly bound to the CTD of RNAPII, neither ectopic expression nor depletion of Integrator subunits using small interfering RNA (siRNA) transfection resulted in alteration of mRNA expression level. Moreover, they could not detect the Integrator complex at the promoters of protein coding genes, using chromatin immunoprecipitation (ChIP). This led them to examine other genes (besides protein coding genes), whose expression is also mediated by RNAPII (Baillat et al., 2005).

It is known that the CTD of RNAPII is also required for the transcription and processing of U1 and U2 snRNAs (Uguen and Murphy, 2003). Therefore, they examined the promoter and coding region of U1 and U2 genes for the presence of the Integrator complex and RNAPII using ChIP. The ChIP experiments demonstrated that the Integrator-RNAPII complex specifically recruited to U1 and U2 snRNA genes.

Furthermore, Ints11 associates with RNAPII and other subunits of the Integrator complex and also specifically binds to both the promoter and 3' end of U1, U2 snRNA genes. (Baillat et al., 2005).

snRNAs are core components of the spliceosome, a complex assembly of ribonucleoparticles involved in pre-mRNA processing (Jurica and Moore, 2003). The majority of snRNAs are transcribed by RNAPII to yield short nonpolyadenylated 3' extended precursors (Wieben et al., 1985). These precursors are then exported to the cytoplasm for further 3' trimming and incorporated into the small nuclear ribonucleoparticles (snRNPs). The formation of proper snRNA precursors depends on the 3' box, located 9–19 nucleotides downstream of the 3' end of the mature snRNA and the presence of a snRNA-compatible promoter at the 5' end of the gene (Egloff et al., 2008; Uguen and Murphy, 2003) (Figure 1.1).

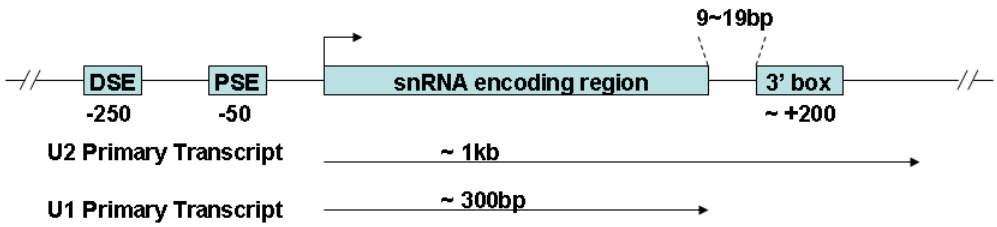
9~19bp
DSE
PSE
snRNA encoding region
3' box
-250
-50
~ +200
U2 Primary Transcript
~ 1kb
U1 Primary Transcript
~ 300bp

Figure 1.1 The structure of human U1, U2 snRNA genes transcribed by pol II.
The diagram shows the DSE and PSE *cis*-acting promoter elements and the RNA-processing element, 3'box. Their position relative to the transcription start site is noted. The start site of transcription is marked with an arrow above the line and the extent of the transcription unit of the U1 and U2 genes is indicated below the line by an arrow. (Adapted from Egloff *et al*., 2008, with slight modification.)

1.1.3 The Integrator Complex Mediates the 3' End Processing of U1 And U2 snRNAs

Analysis of U1 and U2 primary transcripts after the deletion of Ints1 (the largest subunit of the Integrator complex) and Ints11 (the subunit with predicted catalytic activity) revealed a pronounced accumulation of primary transcripts, consistent with a defect in processing the 3' end of U1 and U2 snRNA transcripts (Baillat et al., 2005). This accumulation represents a failure to cleave the primary transcript at its natural processing site located upstream of the 3' box (Wieben et al., 1985). However, the defect in 3'end processing did not result in decreased levels of mature U1 and U2 transcripts, possibley because RNAPII-transcribed spliceosomal snRNAs (U1, U2, U4, and U5) have long half-lives, exceeding 60 hours (Baillat et al., 2005; Fury and Zieve, 1996) (Figure 1.2).

1.1.4 Function Of The Integrator Subunits

As the Integrator complex plays a vital role in transcription and processing of snRNA, dysfunction of the Integrator subunits can lead to various developmental defects. In fact, recent work has shown that disruption of the murine Integrator subunit 1 causes growth arrest and eventual apoptosis at early blastocyst stages (Hata and Nakayama, 2007). Integrator subunit 3 may be involved in the development and/or progression of hepatocellular carcinoma (HCC) tumors (Inagaki et al., 2008). More intriguingly, integrator subunit 5 (Ints5) has been recently identified with an important function in *Drosophila* oogenesis. It is found that depletion of *ints5* in *Drosophila* germarium affects Decapentaplegic (Dpp, the homologue of bone morphogenetic protein, BMP) signaling activities, which in turn leads to maturation defects in oocytes (Cai et al., unpublished data). Therefore, it is possible that Ints5 or Integrator complex are required for proper

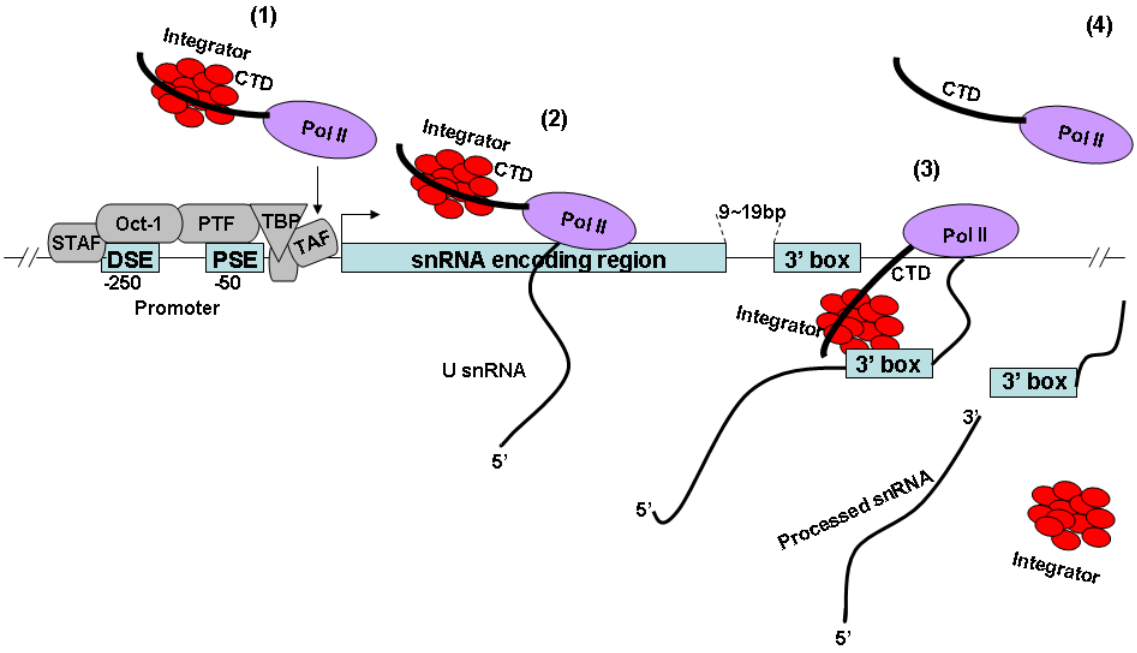
(1)
Integrator
CTD
Pol II
(2)
Integrator
CTD
Pol II
(3)
CTD
Pol II
(4)
CTD
Pol II
STAF
Oct-1
PTF
TBP
TAF
DSE
-250
PSE
-50
Promoter
snRNA encoding region
9~19bp
3' box
U snRNA
5'
Integrator
3' box
CTD
Pol II
3' box
3'
5'
Processed snRNA
Integrator
5'

Figure 1.2 The Integrator complex plays important role in 3'Box-dependent processing of snRNA.
(1) The Integrator complex interacts with RNA polymerase II (Pol II) at the promoter of snRNAs genes. Various transcription activators (grey) are involved in recognizing the promoter of snRNA gene and recruitment of Pol II to initiate snRNA transcription. (2) The Integrator complex travels with Pol II till the 3' box is transcribed. (3) Cleavage occurs at the upstream of the 3' box after the Integrator complex binds to the exposed 3'box. (4) Termination occurs after release of the Integrator complex and the cleaved snRNA. (Modified from Baillat *et al*., 2005 and Egloff *et al*., 2008)

BMP function during vertebrate development as well. Here, I am interested in studying the function of Integrator subunits, especially Ints5, and in elucidating the link between Ints5 and BMP signaling during early development of zebrafish. The study presented in this thesis shows that the Integrator complex functions in zebrafish hematopoiesis to regulate the switch from primitive hematopoietic stem cell identity and blood cell differentiation by modulating BMP/Smad signaling. This work may provide insights into the mechanism by which the Integrator complex and individual subunits may function in development and possibly in other events.

1.2 BMP SIGNALING

Since Ints5 affects Dpp (the homologue of bone morphogenetic protein, BMP) signaling in the *Drosophila* germarium (Cai et al., unpublished data), it is possible that Ints5 and the Integrator complex are also required for proper BMP function during vertebrate development.

Bone morphogenetic proteins (BMPs) form a large subgroup within the transforming growth factor-β (TGF-β) superfamily, which is a group of secreted peptide growth factors in metazoans comprising the TGF-βs, Activins/Inhibin/Nodal and related proteins (Serra, 2002).The activity of BMPs was first identified in the 1960s, but the proteins responsible for bone induction remained unknown until the purification and sequence of bovine BMP-3 (osteogenin) and cloning of human BMP-2 and 4 in the late 1980s (Wozney et al., 1988). To date, about 20 BMP family members have been identified and characterized, and can be subdivided into several groups based on their structures and functions. BMP-2, BMP-4, and the *Drosophila* Dpp are classified as BMP-2/4 group. BMP-5, BMP-6, BMP-7 (also termed osteogenic protein-1, OP-1), BMP-8 (OP-2), and the *Drosophila* gbb-60A gene product form the BMP-5 subgroup (also known as OP-1 group). Growth-differentiation factor-5 (GDF-5, also termed cartilage-derived morphogenetic protein-1, CDMP-1), GDF-6 (CDMP-2 or BMP-13), and GDF-7 (BMP-12) form the third group. Members of the BMP family have distinct expression profiles and the biological activities are not identical among members. One of the reasons is that they bind to BMP receptors with different affinities (Miyazono et al., 2005; Serra, 2002).

The current model of induction of signaling responses by BMP factors is a linear pathway from the type II and type I receptor kinases to Smad activation, resulting in ligand-

stimulated transcriptional activation or repression (Figure 1.3). The SMADs are critical for TGF-β/BMP family signaling (Derynck and Zhang, 2003; Kitisin et al., 2007). However, more recent data also suggests that SMAD-independent pathways exist. For instance, TGF-β rapidly activates Rho family guanosine triphophatases (GTPases) and mitogen-activated protein kinases (MAPKs) through their upstream kinase activators such as TAK1 (TGF-β activated kinase 1) and protein kinase B (PKB, also called Akt). However, no clear link between these pathways to receptors has been identified, and this area remains to be investigated (Attisano and Wrana, 2002; Derynck and Zhang, 2003; Zhang, 2009).

In addition, the proper functioning of BMP signaling also depends on its constitutive and extensive communication with other signaling pathways, such as TGF-β, MAPK, PI3/Akt, Wnt, Hedgehog, Notch, and the interleukin/interferon-gamma/tumor necrosis factor-alpha cytokines induced signaling pathways. This interplay between TGF-β/BMP and other pathways is context dependent and tightly regulated both spatially and temporally, leading to the remarkable complexity and diversity of BMP functions and eventually desirable biological outcomes (Guo and Wang, 2009; Miyazono et al., 2005; Nakayama et al., 2000).

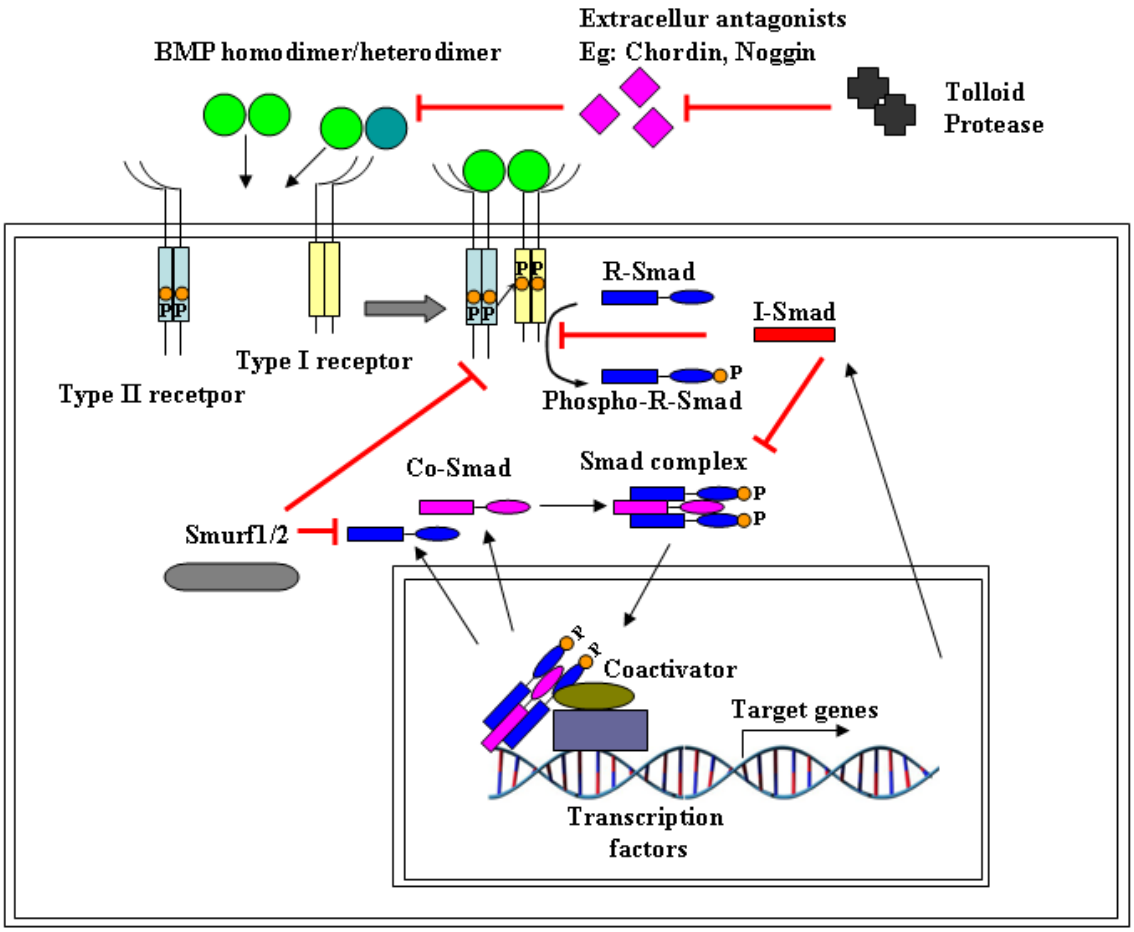
Extracellur antagonists
Eg: Chordin, Noggin
BMP homodimer/heterodimer
Tolloid
Protease
R-Smad
I-Smad
Type I receptor
Type II recetpor
Phospho-R-Smad
Co-Smad
Smad complex
Smurf1/2
Coactivator
Target genes
Transcription
factors

Figure 1.3 BMP signaling pathway.
BMP signaling is transduced through Smad proteins. BMP homodimer or heterodimer ligand binds to type II receptor, whose kinase activity is constitutively active. Ligand binding induces the association of type I and type II receptors, which leads to a unidirectional phosphorylation event in which the type II receptor phosphorylates the type I receptor, thereby activating its intracellular kinase domain and induce phosphorylation of R-Smads. R-Smads form complexes with Co-Smad, and move into the nucleus, where they regulate transcription of target genes. One of the targets of Smad signaling is I-Smads, which suppress Smad signaling by interacting with activated receptors and inhibiting the complex formation between R-Smads and Co-Smad. E3 ubiquitin ligase Smurf1/2 target poly-ubiquitination and proteasomal degradation of R-Smad and the activated receptor complex. BMP activity is also negatively regulated by extracelullar antagonists, such as Chordin, Noggin, Follistatin, and Cerberus. Another level of regulation of this pathway is achieved through the proteolytic activity of the metalloprotease-Tolloid, which cleaves BMP antagonist, such as Chordin and in turn releases the BMP signals. (Reviewed by Miyazono *et al*., 2005 and Itoh and ten Dijke, 2007.)

1.2.1 BMP/Smad Signaling Pathway (Figure 1.3)

Parallel work in files, worms and vertebrates has revealed a conserved BMP signaling pathway (Attisano and Wrana, 2002; Roberts and Derynck, 2001). The cell-surface receptor that carries the BMP signal into the cell is a complex of single-pass transmembrane serine and threonine kinases. This receptor complex consists of two distinct proteins, known as the type I and type II receptors. The BMP ligand binds to type II receptor, whose kinase activity is constitutively active. Ligand binding induces the association of type I and type II receptors, which leads to a unidirectional phosphorylation event in which the type II receptor phosphorylates the type I receptor, thereby activating its intracellular kinase domain (Attisano and Wrana, 2002).

The activated type I receptor then signals to the SMAD family of intracellular mediators. Vertebrate SMADs can be divided into three functional classes: (1) receptor-activated SMADs (R-Smads), (2) co-mediator SMAD 4 (Co-Smads), and (3) inhibitory SMADs 6 and 7 (I-Smads). The type I receptors are critical to determine the specificity of the downstream SMAD. BMP type I receptors specifically phosphorylate R-Smads: Smad 1, 5, and 8. In contrast, TGF-β/Activins/Nodal signaling pathway function through R-Smads: Smad2 and 3 (Attisano and Wrana, 2002; Jurica and Moore, 2003; Miyazono et al., 2005; Moustakas et al., 2001) (Figure 1.4).

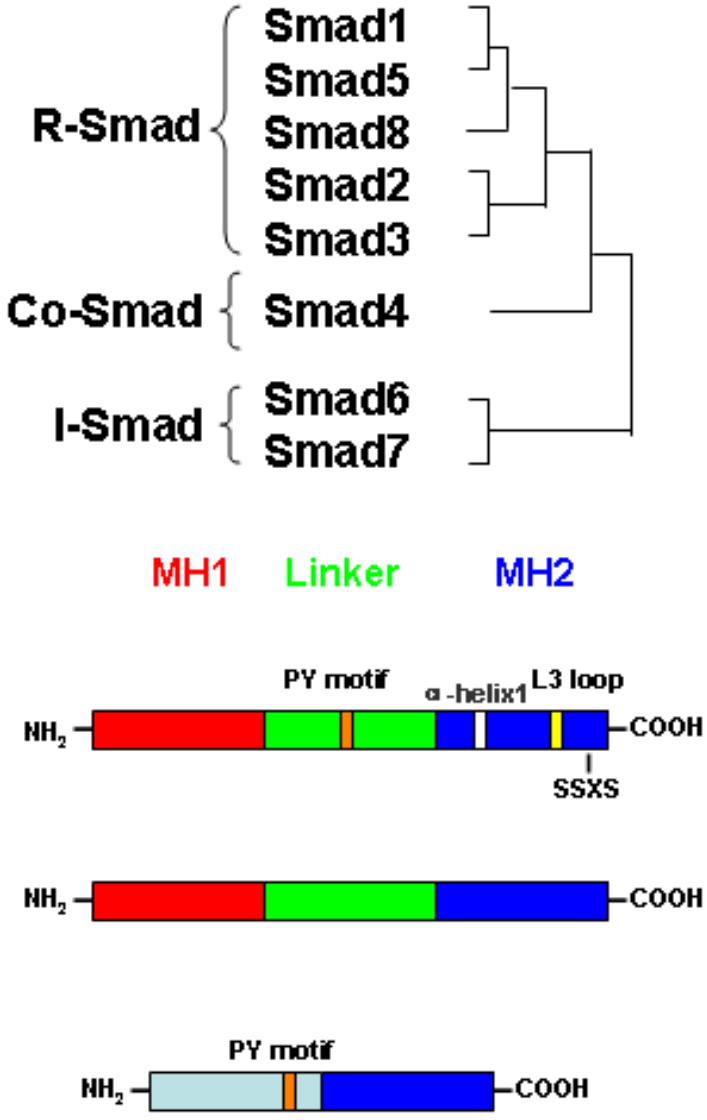
R-Smad
Smad1
Smad5
Smad8
Smad2
Smad3
Co-Smad
Smad4
I-Smad
Smad6
Smad7
MH1
Linker
MH2
PY motif
α -helix1
L3 loop
NH2
COOH
SSXS
NH2
COOH
PY motif
NH2
COOH

Figure 1.4 The classification and schematic representation of Smad family members. There are three classes of Smad proteins. R-Smads contain an SSXS motif at the C-terminus, where the last two Ser residues are phosphorylated by the type I receptor. Both R-Smads and Co-Smads have highly conserved MH1 domains (red) and MH2 domains (blue). MH1 and MH2 domains are separated by linker region with various lengths (green). I-Smads shows limited homology with R-Smads and Co-Smads, and this homology is restricted to the MH2 domain. PY motif is found in both R-Smad and I-Smad. L3 loop and α-helix 1 (H1) in MH2 domain of R-Smad are required for the interaction between R-Smad and type I receptor. (Reviewed by Nakayama *et al*., 2000 and Miyazono *et al*., 2005.)

The receptor regulated SMADs (R-Smads), are directly phosphorylated by the type I receptors on two conserved serines at the COOH-terminus. Phosphorylation of R-Smads induces release from the receptor complex as well as from cytoplasmic anchor proteins, including SARA (SMAD anchor for receptor activation) and cytoplasmic PML (promyelocytic leukemia protein) (Figure 1.5). Phosphorylation also stimulates R-Smads to interact with Co-Smads, Smad4 and accumulate together in the nucleus as heteromeric complexes. In the nucleus, the Smads associate with various DNA binding partners and transcriptional coactivators or corepressors to positively or negatively regulate target gene expression (Attisano and Wrana, 2002; Heldin et al., 1997; Massague et al., 2000).

I-SMADs (Smad6 and 7), counteract the effects of R-Smads and thus negatively regulate BMP signaling (Moustakas et al., 2001; Wrana, 2000). BMP signaling is also opposed extracellularly by antagonists originated from the organizer, including Chordin, Noggin, Follistatin, and Cerberus, all of which are able to bind BMPs and block activation of their receptors (Iemura et al., 1998; Piccolo et al., 1999; Piccolo et al., 1996; Zimmerman et al., 1996). Another level of regulation of this pathway is achieved through the proteolytic activity of the metalloprotease-Tolloid, which cleaves BMP antagonist, such as Chordin and in turn releases the BMP signals (Blader et al., 1997; Piccolo et al., 1997).

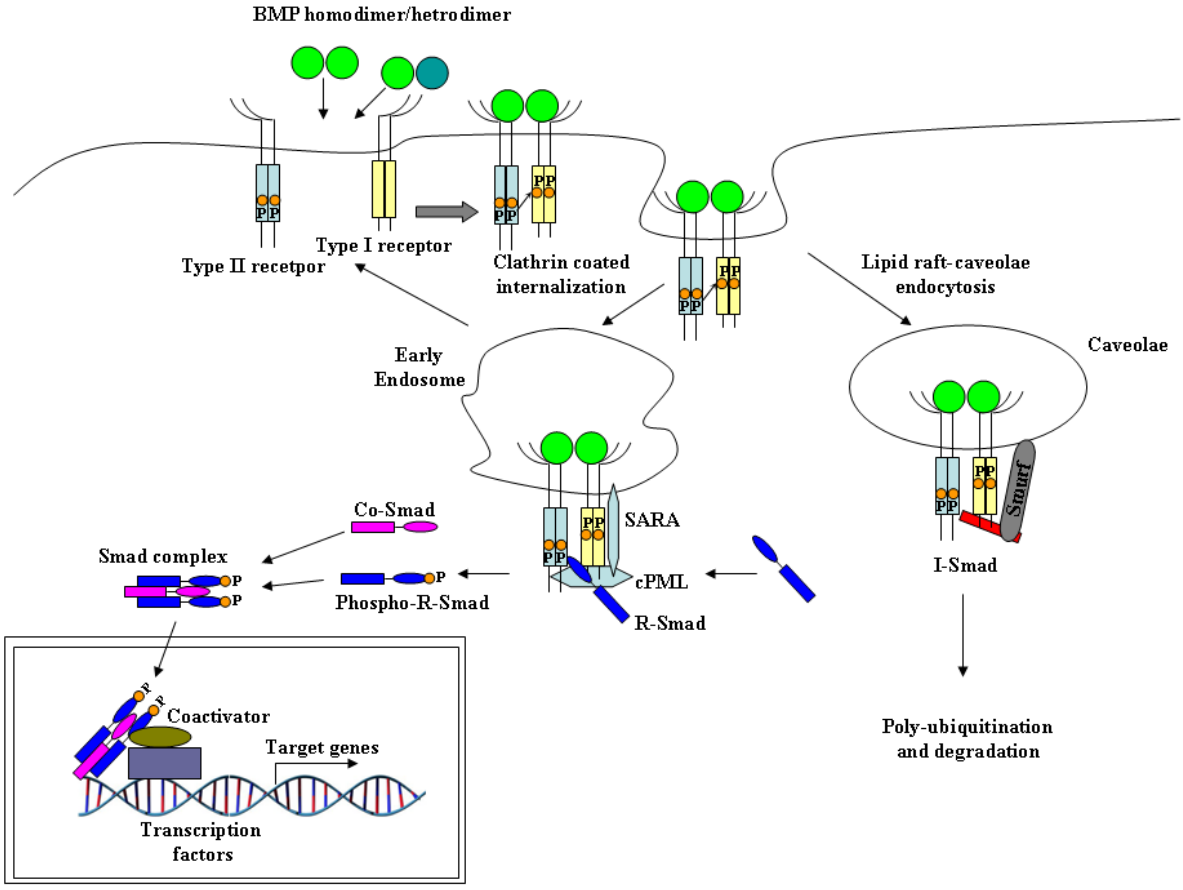
BMP homodimer/hetrodimer
Type II recetpor
Type I receptor
Clathrin coated internalization
Lipid raft-caveolae endocytosis
Caveolae
Early Endosome
Co-Smad
Smad complex
Phospho-R-Smad
SARA
cPML
R-Smad
Smurf
I-Smad
Coactivator
Target genes
Transcription factors
Poly-ubiquitination and degradation

Figure 1.5 Turnover of BMP receptors.
Internalization of the receptor complex can occur via two pathways: (i) the clathrin- and (ii) lipid raft-caveolae endocytic routes. Early endosomes bind SARA, which can, together with cytoplamic PML (cPML), recruit R-Smads, Smad 1,5, 8 to the activated receptor. R-Smads are phosphorylated by the type I receptor, and in turn can form heteromeric complexes with the Co-Smad, Smad4.These activated Smad complexes accumulate in the nucleus, where they directly or indirectly bind to specific promoter region on target genes together with transcription factor and/or co-activators/repressors. On the other hand, receptor complexes that are endocytosed into lipid rafts-caveolae microdomains are predestined to be degraded. I-Smads (Smad6 and Smad7) can recruit E3 ubiquitin ligase Smurf1/2 that target poly-ubiquitination and proteasomal degradation of the activated receptor complex. (Adapted from Itoh and ten Dijke, 2007, with modification.)

1.2.1.1 BMP Ligands

BMP ligands are synthesized as inactive precursors that become activated after proteolytic cleavage. The cleavage occurs after the multi-basic amino acid motifs -Arg-Ser-Lys-Arg- to generate C-terminal mature proteins before they are secreted as homidimers or heterodimers (Aono et al., 1995; Cui et al., 1998; Nishimatsu and Thomsen, 1998). This processing event has been proposed to regulate the diffusion of BMPs, thereby controlling the range over which these molecules can signal during embryonic development (Cui et al., 2001). Members of a family of higher eukaryotic endoproteases, named proprotein convertases (PCs), are good candidates for endogenous BMP convertases. In mammals, seven members of this family have been characterized and designated as Furin, PC2, PC3, PACE-4, PC4, PC5/PC6A and B, and LPC/PC7/ PC8 (Steiner, 1998). Individual PCs exhibit overlapping, but distinct, substrate specificities (Breslin et al., 1993; Creemers et al., 1993). Furin, the first characterized member of PC family, is a membrane-localized, calcium-dependent serine endoprotease that cleaves proprotein molecules following the consensus sequence Arg- X-X-Arg (Molloy et al., 1992). Many precursor proteins, including those for TGF-βs share this cleavage site and can be efficiently cleaved by Furin in vivo and *in vitro* (Bresnahan et al., 1990; Dubois et al., 1995; Nakayama, 1997).

1.2.1.2 Receptors Of BMP Signaling Pathway

Members of the BMP family bind to two distinct serine/threonine kinase type I and type II receptors. The constitutively activated type II receptors phosphorylate Gly-Ser (GS) domains of the type I receptors upon ligand binding, leading to the activation of type I receptor kinases (Heldin et al., 1997; Miyazono et al., 2005; Shi and Massague, 2003).

Then, the specificity of downstream intracellular signals is mainly dependent on type I receptors. Of the four type I receptors for BMPs, BMP-2/4 preferentially bind to ALK-3 and ALK-6, whereas members of the BMP-5 group bind to ALK-2 and ALK-6. In contrast, those of the GDF-5 group bind to ALK-6, but not efficiently to other receptors (Derynck and Zhang, 2003). In addition to the members of the BMP family, mullerian inhibiting substance (MIS) has been shown to bind to ALK-2 in the presence of MIS type II receptor, and to mediate BMP-like signaling in target cells (Clarke et al., 2001; Visser et al., 2001). Mutations in the ALK-3 gene have been found in some patients with juvenile polyposis (Howe et al., 2001).

There are three different type II receptors, BMPR-II, ActR-II, and ActR-IIB (Derynck and Zhang, 2003). BMPR-II has a long C-terminal tail following the serine/ threonine kinase domain. Hassel *et al.* reported the proteomics analyses of BMPR-II interacting proteins, and found that several cytoskeletal components interact with the C-terminal tail as well as the kinase domain of BMPR-II (Hassel et al., 2004). Thus, the C-terminal tail of BMPR-II may play important roles in the regulation of cytoskeletal protein functions. In fact, truncations of BMPR-II in the C-terminal tail have been found in some patients with familial primary pulmonary hypertension (PPH) (Deng et al., 2000; Lane et al., 2000).

Besides, the turnover of receptor complex is important for the regulation and termination of signaling events. After type I receptor activation, receptor internalization can occur via two pathways: the clathrin-endocytic and lipid raft-caveolae endocytic routes (Figure 1.5). Clathrin coated internalization guides receptor complex to early endosomes that are enriched for phosphatidylinositol 3-phosphate. Early endosomes bind FYVE domain

protein SARA, which can, together with PML, recruit R-Smads to the activated receptor. R-Smads are then phosphorylated by type I receptor, and participate in downstream signaling. The receptors can travel back to the cell surface. In contrast, receptor complexes that are endocytosed into lipid rafts-caveolae vesicles are lead to be degraded. I-Smads bind to activated receptors in the coveolae, and serve as adapters to recruit E3 ubiquitin ligase, Smurfs for poly-ubiquitination and proteasomal degradation of TGF-β receptor complex (Itoh and ten Dijke, 2007).

1.2.1.3 Smads Of BMP Signaling Pathway

R-Smads and Co-Smads have highly similar amino-acid sequences at their N- and C-termini, which are termed as Mad homology (MH)1 and MH2 domains, respectively. The two domains are separated by a divergent proline-rich linker region with variable lengths. The MH1 domain of R-Smads and Co-Smads can bind to the specific DNA sequences and also repress the function of MH2 domain. In contrast, the MH2 domain plays important roles in protein interactions. For example, MH2 domain of R-Smads directly binds to type I receptors, forms oligomer with Co-Smads, and interacts with coactivators for transcriptional activation. In addition, only R-Smads have a Ser-Ser-X-Ser (SSXS) motif at their COOH-terminal ends, serving as the phosphorylation site by type I receptors (Massague et al., 2005; Miyazono et al., 2005) (Figure 1.4).

The L45 loop within the type I receptor kinase domain and the L3 loop in the MH2 domains of R-Smads determine the specificity of intracellular signaling induced by TGF-βs. BMP-Smads, Smad1, 5 and 8 are phosphorylated by BMP type I receptors (ALK-1, ALK-2, ALK-3 and ALK-6), whereas TGF-β/Activin-Smads, Smad2 and 3 are activated by TGF-β and activin type I receptors (ALK-4 and ALK-5) and orphan type I receptor

ALK-7. For the interaction of Smad1 with AlK-1 and ALK-2, not only its L3 loop, but also the α-helix 1 (H1) in MH2 domain is required (Chen and Massague, 1999; Itoh and ten Dijke, 2007; Miyazono et al., 2005) (Figure 1.4).

The Co-Smad, Smad4 can form heteromeric complexe with all activated R-Smads and is thus a shared component in TGF-β, activin and BMP signal transduction. Work by Kawabata *et al*, together with the finding that MH2 domain of Smad4 forms a trimer in solution, suggests that the hetero-oligomers may be heterotrimers, composed of two R-Smads and one Smad4, or one R-Smad and two Smad4 (Kawabata et al., 1998; Shi et al., 1997). Although phosphorylated R-Smads can form oligomers and translocate into the nucleus even in the absence of Co-Smad, Co-Smad stabilizes the structures of the Smad oligomers. Therefore, Co-Smads guarantee the efficient transcriptional activity of the Smad complexes (Shi and Massague, 2003).

I-Smads, Smad6 and Smad7, are distantly related members of the Smad family. Expression of I-Smads is induced by ligand stimulation. For example, *Drosophila* homologue of Smad6/7, Daughters against Dpp (Dad), is induced by Dpp (*Drosophila* homologue of Bmp2/4) signal. This finding indicates that I-Smads regulate TGF-β/BMP signaling by a negative feedback loop (Christian and Nakayama, 1999; Miyazono et al., 2005; Tsuneizumi et al., 1997). I-Smads contain a conserved MH2 domain that interacts with type I receptors to compete with R-Smads for receptor binding. It is also shown that Smad6 binds to activated Smad1, and prevents complex formation between Smad1 and Smad4 (Hata et al., 1998; Heldin et al., 1997; Murakami et al., 2003). Both Smad6 and Smad7 inhibit BMP signaling, while Smad7 is more potent in inhibiting TGF-β/activin signals than Smad6.The N-terminal regions of I-Smads show a weak similarity to MH1

domains of R- and Co-Smads, and may have a role in determining signal specificity (Miyazono et al., 2005).

The linker region of R-Smads has consensus sequences phosphorylated by MAPK. MAPK phosphorylation inhibits R-Smads nuclear localization, thereby antagonizing TGF-β signaling (Kretzschmar et al., 1997). In *Xenopus* embryos, MAPK induced phosphorylation of Smad1 linker region by IGF and FGF (fibroblast growth factor) plays an important role in neural induction (Pera et al., 2003). Although mice with mutations in the linker region of Smad1 (Smad1L/L) exhibit less severe phenotypes compared to Smad1-null mice or those with a mutation in the C-terminus of Smad1, Smad1L/L mice exhibit defects in gastric epithelial homeostasis and formation of primordial germ cells, suggesting the functional importance of MAPK-mediated Smad1 phosphorylation in vivo (Aubin et al., 2004). In addition, the PPXY sequence (also called PY motif), which interacts with WW domain containing proteins, such as E3 ligase-Smurf, is present in the linker regions of most R- and I-Smads (Ebisawa et al., 2001; Kavsak et al., 2000) (Figure 1.4).

1.2.1.4 Regulation of R-Smads

Ubiquitin–proteasome-mediated degradation controls the levels of R-Smads post-translationally. R-SMAD protein is regulated by the ubiquitin proteasome pathway through association with E3 ubiquitin ligases such as Smurf1 and Smurf2. Smurf proteins are members of the HECT domain containing E3 ubiquitin ligases. The WW domains of Smurfs bind to the PY motifs of R-SMADs. Smurf1 interacts with Smad1 and Smad5, thereby affecting BMP responses, whereas Smurf2 interacts more broadly with different R-Smads, allowing interference with BMP and TGF-β/activin signaling. Nevertheless,

Xenopus embryo assays indicate that Smurf1 and Smurf2 primarily target the BMP pathway (Derynck and Zhang, 2003; Miyazono et al., 2005).

Recent work has revealed that the Smads are also post-transcriptionally regulated. Jiang *et al*. identified a ubiquitously expressed novel isoform, SMAD5β, encodes a 351 amino acid protein with a truncated MH2 domain and a unique C-terminal tail of 18 amino acids. The expression level of the *smad5β* isoform is higher in CD34+ hematopoietic stem cells than in terminally differentiated peripheral blood leukocytes, thereby implicating the function of β form in hematopoietic stem cell homeostasis (Jiang et al., 2000). It is also indicated that the alternative splicing of *smad5* is differentially regulated during maturation of hematopoietic cells. Therefore, the post-transcriptional processing of Smads is important for their function. However, the mechanisms of this process are poorly understood.

The elucidation of BMP signal transduction pathways might provide insights into human diseases. Various human syndromes and illnesses, both hereditary and spontaneous, have been attributed to mutations in BMP pathway components. Especially, mutations in SMADs have been associated with cancers and anemia (de Caestecker et al., 2000; Massague et al., 2000).

1.2.2 Function Of BMP Signaling In Dorso-ventral Patterning

The activities of BMPs are achieved by regulating proliferation, differentiation, migration and apoptosis of different cell types. Studies from transgenic and knock-out mice and from other animals and humans with naturally occurring mutations in BMPs and related genes have shown that BMP signaling plays multiple roles at different developmental

stages (Abe, 2006; Dale and Jones, 1999; de Caestecker et al., 2000; Guo and Wang, 2009; Larsson and Karlsson, 2005; Maxson and Ishii, 2008; Miyazono et al., 2005; Nakayama et al., 2000). Here I mainly introduce the function of BMP signaling in patterning the dorso-ventral axis of vertebrate embryos.

One of the earliest and best documented roles for BMPs is in patterning the dorso-ventral axis (Graff, 1997) (Figure 1.6). In vertebrate, maternally deposited determines leads to the establishment of dorsal organizer. One of the essential organizer factors is nodal related protein. Nodal also belongs to TGF-β superfamily and occurs in deuterostoms and serves as mesoderm and endoderm inducers. During gastrulation, the organizer induces dorsal fates within mesoderm, anterior fates within endoderm, and neural fates within ectoderm. The organizer seems to cause these events primarily by opposing morphogenetic activities from the ventro–lateral regions of the embryo (De Robertis et al., 2000). Intriguingly, Studies in Xenopus have revealed the existence of BMP signaling pathway, which specifies the ventral and lateral fate of the embryo, together with Wnt pathways (Harland and Gerhart, 1997).The role of BMP signaling in dorso–ventral patterning of the gastrula embryo is highly conserved during evolution form Drosophila to vertebrates although dorso-ventral axis in Drosophila is inverted relative to that of vertebrate (De Robertis et al., 2001; Holley and Ferguson, 1997; Holley et al., 1995; Shimmi and O'Connor, 2003) (Figure 1.6)

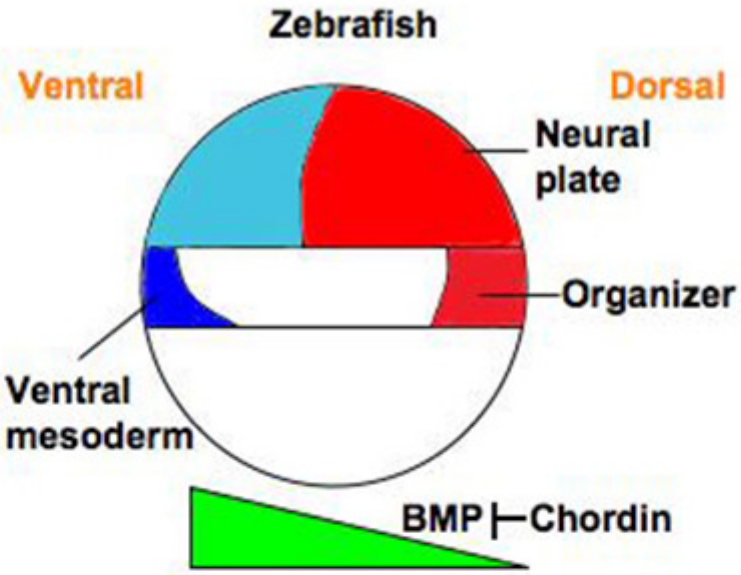
Zebrafish
Ventral
Dorsal
Neural plate
Organizer
Ventral mesoderm
BMP
Chordin

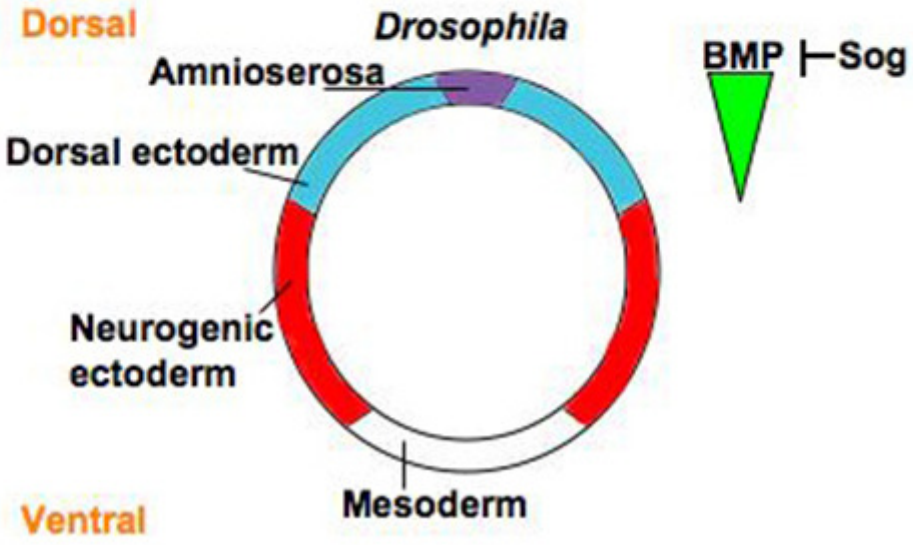
Dorsal
Drosophila
BMP
Sog
Amnioserosa
Dorsal ectoderm
Neurogenic ectoderm
Mesoderm
Ventral

Figure 1.6 The dorsoventral polarity in zebrafish and *Drosophila*.
Dorsal–ventral polarity in arthropods has been inverted with respect to that of vertebrates in the course of evolution. In zebrafish, maternally deposited factors determine the establishment of dorsal organizer. During gastrulation, the organizer induces dorsal fates by opposing BMP activities from the ventral–lateral regions of the embryo. The graded BMP activity confers positional values along the dorsoventral axis for both mesoderm and ectoderm. This morphogenetic activity of BMPs could be established via an inhibitory gradient set up by secreted BMP antagonists from the dorsal organizer, such as Cerebrus, Chordin, Follistatin and Noggin. In Drosophila, BMP/DPP signaling induces formation of the dorsal ectoderm and amnioserosa, an extra-embryonic membrane that has the dorsal-most fate in the fly embryo. In contrast, the ventral ectoderm fate, neurogenic ectoderm, requires the absence of DPP signaling. Similarly, DPP activity is negatively regulated by the fly homologue of Chordin, Sog. (Adapted from De Robertis *et al*., 2000.)

Early in Drosophila development, cells acquire distinct fates along the dorso–ventral axis. In syncytial blastoderm, graded levels of nuclear Dorsal (DL) sub-divide the embryo into mesoderm and ectoderm. The DL gradient sets the stage for further patterning of the ectoderm by BMP signaling. Normal dorso–ventral patterning requires two BMP ligands, Decapentaplegic (DPP), a BMP2/4 homologue and Screw, a BMP7 homologue. They induce formation of the dorsal ectoderm and amnioserosa, an extra-embryonic membrane that has the dorsal-most fate in the fly embryo. In contrast, the ventral ectoderm fate, neurogenic ectoderm, requires the absence of DPP signaling (Raftery and Sutherland, 2003) (Figure 1.6). Intriguing, in Drosophila, Screw and another BMP family member Gbb-60A, have been shown to synergize with Dpp to regulate growth and patterning in wing imaginal discs (Chen and Struhl, 1998; Haerry et al., 1998; Khalsa et al., 1998; Neul and Ferguson, 1998; Nguyen et al., 1998). It is possible that the BMP ligand heterodimers are important for dorso-ventral patterning as well.

In Xenopus, expression of BMP-4 is restricted to cells on the ventral side of gastrula stage embryos, where it plays a central role in specifying ventral mesodermal and ectodermal fates. When BMP-4 is mis-expressed in the organizer, the cells in the dorsal side differentiate into blood rather than notochord and muscle, or into epidermis rather than neural tissues. Conversely, when endogenous BMP signaling is blocked by introducing dominant negative forms of BMP ligands or receptors, blood fate is eliminated in ventral cells and they become muscle instead. Furthermore, blocking BMP signaling pathway in the animal caps of embryos (ectoderm explants) causes these cells to differentiate into neural tissues. Thus, BMP-4 is required for ventral mesoderm formation and for the induction of epidermal fate at the expense of neural tissues (Dale

and Jones, 1999; Fainsod et al., 1994).

It has been proposed that graded BMP activity confers positional values along the dorso-ventral axis for both mesoderm and ectoderm (Figure 1.6). This morphogenetic activity of BMPs could be established via an inhibitory gradient set up by secreted BMP antagonists from the dorsal organizer, such as Cerebrus, Chordin, Follistatin and Noggin (Dale and Wardle, 1999; De Robertis et al., 2001). Thus, according to current model, high BMP activity or low BMP antagonism induces blood in mesoderm and epidermis in ectoderm, intermediate BMP activity or intermediate BMP antagonism induces lateral plate mesoderm (heart, kidney) and neural crest in ectoderm, and low BMP activity or high BMP antagonism induces somites and notochord in mesoderm and neural plate in ectoderm (Dale and Wardle, 1999).

This morphogen model is further confirmed by phenotypic analyses of zebrafish mutants. Dorsalized mutants swirl (swr, bmp2b), snailhouse (snh, bmp7), somitabun (sbn, smad5), piggytail (pgy, smad5), mini-fin (mfn, tolloid) and lost-a-fin (laf, alk8) exhibit expansion of dorso-lateral mesoderm at the expense of ventral mesodermal derivatives, as well as expansion of presumptive neural tissue at the expense of epidermal precursors (Bauer et al., 2001; Connors et al., 1999; Kishimoto et al., 1997; Mullins et al., 1996). Conversely, the ventralized mutant chordino (din, chordin), mercedes (mes, sizzled), and ogon (ogo, sizzled) shows reduction of dorsal derivatives such as somitic mesoderm and neurectoderm, together with expansion of ventral mesoderm and epidermis (Hammerschmidt et al., 1996; Kodjabachian et al., 1999; Solnica-Krezel et al., 1996).

1.3 HEMATOLOGY IN ZEBRAFISH

When I studied the function of Ints5, I found that knocking-down Ints5 causes a lack of blood circulation, reduced expression of hematopoietic genes and arrested red blood cell differentiation in early zebrafish embryos. Therefore, here, I mainly studied the role of Integrator subunits in hematopoiesis, using zebrafish as a model system.

1.3.1 Zebrafish As A Model For Hematopoiesis

Zebrafish is an ideal organism to analyze the molecular mechanisms underlying developmental hematopoiesis. Fish represents the largest group of vertebrates, with more than 20,000 known species. Fish embryos are often externally fertilized and are optically transparent, allowing observation of blood cell formation, differentiation and migration. Usually, the circulation of blood cells can be observed from 24 hours post-fertilization in zebrafish and embryos can survive for several days without any circulating blood cells. One can screen for hematopoietic defects at different developmental stages by simple observation under a dissecting microscope. Besides, the generation time of zebrafish is short, females typically lay up to hundreds of eggs per crossing and adults are small and easy to maintain (Shafizadeh and Paw, 2004; Westerfield, 2000).

Recently, modern reverse genetic techniques have been used for zebrafish hematology research, including transient gene over-expression and knockdown (eg. anti-sense morpholinos, RNAi), stable transgenesis, and recovering stable mutated alleles by TILLING (Targeting Induced Local Lesions In Genomes) or from catalogued libraries of insertional mutant lines (Carradice and Lieschke, 2008). Furthermore, a number of hematopoietic molecular markers have been characterized, also several groups have completed large-scale forward genetic screens for chemically induced mutations, from

which, many mutants with defects in the embryonic hematopoiesis have been identified (Driever et al., 1996; Haffter et al., 1996). In addition, cell biology techniques, such as flow cytometry and transplantation, are also available for in vivo functional studies of specific cell types. So far, a dramatic progress in hematopoiesis study has been made in zebrafish. It is obvious that zebrfish has already become a popular organism for studying the hematopoiesis (Berman et al., 2005; Shafizadeh and Paw, 2004; Traver, 2004).

1.3.2 Zebrafish Primitive Hematopoiesis

All vertebrate have two waves of hematopoieis. The earlier one is known as primitive or embryonic hematopoietic wave and predominantly produces erythrocytes and primitive macrophages but not lymphoid cells. In mammals and birds, the first hematopoietic wave originates from the extraembryonic tissue-yolk sac (Galloway and Zon, 2003; Zon, 1995). In zebrafish, primitive hematopoiesis occurs at two mesodermal sites, the intermediate cell mass (ICM) located in the trunk ventral to the notochord, developing from the ventral lateral plate mesoderm (LPM), and the rostral blood island (RBI) arising from the cephalic/anterior LPM (Carradice and Lieschke, 2008; de Jong and Zon, 2005) (Figure 1.7). In zebrafish and *Xenopus*, dorso-ventral patterning depends on the presence of transforming growth factor β (TGF-β) superfamily members, especially nodal related proteins and a gradient of bone morphogenetic proteins (BMPs) (De Robertis et al., 2000; He and Chen, 2005). Establishment of the ventral mesoderm eventually leads to formation of hemangioblast progenitors (common progenitors for both hematopoietic and endothelial lineages), marked by the co-expression of transcription factor genes *stem cell leukemia* (*scl*), *lmo2* and *gata2* in both the ICM and RBI from 2-somite stage (Davidson and Zon, 2004). Cells in the ICM (analogous to mammalian yolk sac blood island)

differentiate into the endothelia cells of the trunk vasculature and proerythroblasts, which enter the circulation at around 24 hpf, whereas cells in the RBI generate endothelia cells and macrophages (de Jong and Zon, 2005; Larsson and Karlsson, 2005).

1.3.3 Zebrafish Definitive Hematopoiesis

The second hematopoietic wave is known as definitive or adult hematopoiesis, and produces all the blood lineages. Zebrafish definitive hematopoiesis starts at 48 hpf in the ventral wall of the dorsal aorta, equivalent to the aorta-gonad-mesonephros (AGM) in mammals. Mammalian hematopoiesis later transitions from the AGM to the fetal liver and bone marrow (Galloway and Zon, 2003; Zon, 1995) (Figure 1.7). In zebrafish, definitive hematopoiesis is initiated by Hedgehog, vascular endothelial growth factors (Vegfs), and Notch signalings (Gering and Patient, 2005). At 31 hpf, *c-myb* and *runx1* start to express in the dorsal aorta, predicting the formation of the definitive hematopoietic stem cells (HSCs), which can give rise to all different types of blood cells (Burns et al., 2002; Kalev-Zylinska et al., 2002; Mucenski et al., 1991). Subsequently, HSCs are colonized in the kidney, thymus and pancreas. The kidney becomes the primary hematopoietic organ from the larval stage and throughout the lifespan of zebrafish (Galloway and Zon, 2003; Willett et al., 1999) (Figure 1.7).

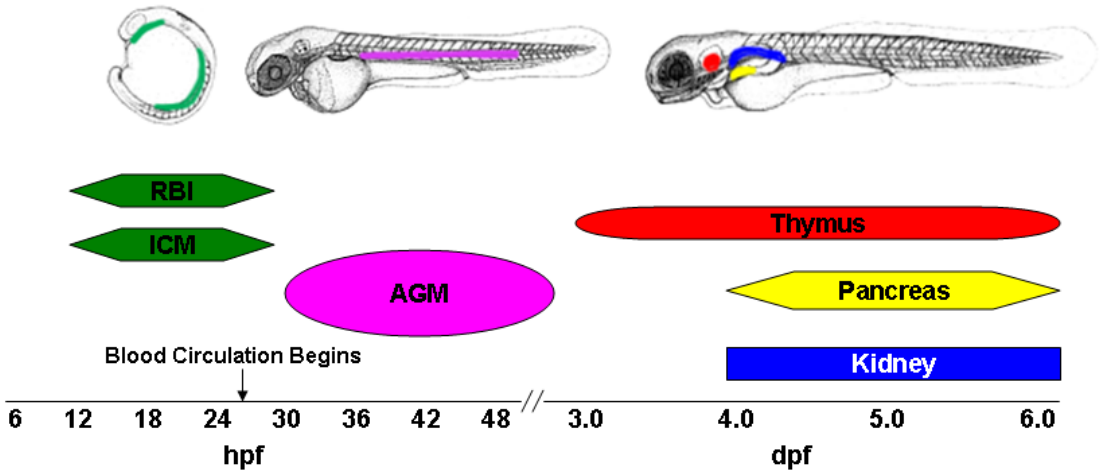
RBI
ICM
AGM
Thymus
Pancreas
Kidney
Blood Circulation Begins
6 12 18 24 30 36 42 48
3.0 4.0 5.0 6.0
hpf
dpf

Figure 1.7 Approximate duration and location of hematopoietic activity in different tissues during zebrsfish embryogenesis. (Modified from Davidson and Zon, 2004 and Hsia and Zon, 2005)

1.3.4 Transcriptional Regulation Of Primitive Hematopoiesis

In zebrafish, hemangioblasts originate from the ventral margin of the embryo (Vogeli et al., 2006). Similarly, in mouse, the hemangioblast progenitors arise from a mesodermal population of cells positive for Brachyury (T) expression (Fehling et al., 2003). Although it is not very clear how the ventral mesodermal cells are specified into hemangioblasts, BMPs, FGF and Wnt families have been implicated to induce and pattern the ventral mesoderm (Munoz-Sanjuan and A, 2001). It is also widely believed that a morphogenic gradient of BMP signaling across the dorso-ventral axis during gastrulation is primarily responsible for patterning mesoderm into distinct cell fates (Dale and Wardle, 1999) (Figures 1.6 and 1.8).

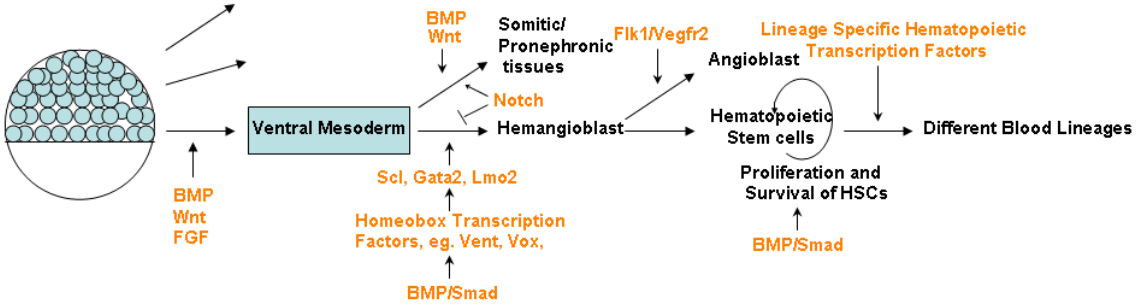
BMP
Wnt
FGF
Ventral Mesoderm
BMP
Wnt
Somitic/
Pronephronic
tissues
Notch
Hemangioblast
Scl, Gata2, Lmo2
Homeobox Transcription
Factors, eg. Vent, Vox,
BMP/Smad
Flk1/Vegfr2
Angioblast
Hematopoietic
Stem cells
Proliferation and
Survival of HSCs
BMP/Smad
Lineage Specific Hematopoietic
Transcription Factors
Different Blood Lineages

Figure 1.8 A model for the events and molecules involved in hematopoiesis.
Hematopoietic stem cells (HSCs) arise from the ventral mesoderm through an intermediate precursor with both endothelial and hematopoietic potential, the hemangioblast. BMP signaling pathway plays critical roles in regulating several aspects of specification and proliferation of HSCs. (Modified from Larsson and Karlsson, 2005)

During the segmentation period at 10 to 12 hours post fertilization (hpf), both ICM and RBI express *scl*, *lmo2* and *gata2*, together with the vascular markers, such as *flk1*(Carradice and Lieschke, 2008; Liao et al., 1997). As in mammals, the basic helix-loop-helix transcription factor Scl (Tal1) and its partner Lmo2, which is a LIM domain transcriptional factor and functions as a bridging molecule, sit at the apex of hematopoietic and endothelial development (Carradice and Lieschke, 2008; Robb et al., 1995; Shivdasani et al., 1995). In zebrafish, *scl* expression marks the formation of primitive HSCs and also vascular precursors, known as angioblasts. Knockdown of *scl* by antisense mropholinos results in the loss of primitive and definitive hematopoietic cell lineages without loss of *lmo2* and *gata2* expression, while ectopic *scl* expression leads to induction of *lmo2* and expansion of both blood and endothelial precursors at the expense of somatic and pronephronic tissues (Dooley et al., 2005; Gering et al., 1998; Gering et al., 2003). Gata2 is a member of the zinc-finger family of transcription factors that bind to the consensus core sequence WGATAR (Orkin, 1992). Gata2 is expressed in hematopoietic and endothelial lineages and is required for the proliferation of hematopoietic progenitor cells. Gata2-deficient mouse embryos are anemic and die before HSC induction and expansion (Tsai et al., 1994). The co-expression of *scl*, *lmo2* and *gata2* in ICM and RBI presumably represents the formation of the hemangioblast population (Hsia and Zon, 2005) (Figure 1.8).

In the ICM, initial erythropoietic events begin at the 5-somite stage (approximately 12 hpf) with expression of *gata1* in a subset of scl^+ cells (Detrich et al., 1995). Gata1 is another zinc-finger transcription factor. These $scl^+/gata1^+$ cells will eventually give rise to the first circulating blood cells, whereas the $scl^+/gata1^-$ cells are believed to be

angioblasts, as they differentiate into endothelial cells that specifically express the vascular endothelial growth factor receptor *flk1*/*vegfr2* (Davidson et al., 2003; Liao et al., 1997; Sumoy et al., 1997). This suggests that ICM precursors adopt either HSC or vascular fate by 5-somite stage. Following the formation of presumptive HSCs, there is a sequential activation of transcription factors critical for erythroid development, such as Tif1γ (*moonshine*), and Biklf (Davidson and Zon, 2004; Ransom et al., 2004).

The erythroid precursors-proerythroblasts undergo extensive proliferation. By the time blood circulation begins around 24 hpf, there are at least 300 proerythroblasts in the ICM (Long et al., 1997). The circulating proerythroblasts expressing embryonic globins synchronously mature into flattened erythrocytes with elliptical shape over the next 4 days and are later gradually replaced by erythrocytes originated from definitive HSCs resident in the pronephros. Unlike red blood cells in mammal, teleost erythrocytes remain nucleated for the lifespan of the fish (Davidson and Zon, 2004; de Jong and Zon, 2005).

Unlike the ICM, the RBI region does not express *gata1* and is devoid of erythropoietic activity, but instead undergoes myelopoiesis and granulopoiesis (Bennett et al., 2001). This is evidenced by expression of the myeloid-specific transcription factor gene *pu.1* (or *spi1*, a member of the ets family of transcription factors) in a subpopulation of scl^+ cells. Subsequently, more myeloid-specific markers, such as *fms* and *l-plastin*, start to express in the same cells (Bennett et al., 2001; Lieschke et al., 2002). These $pu.1^+$ cells eventually develop into mature macrophages. It is reported that they are able to migrate to sites of infection and remove bacteria, such as *Escherichia coli* or *Bacillus subtilis*, by phagocytosis at 30 hpf (Herbomel et al., 1999). It is not known whether these macrophages from RBI present transiently as primitive macrophages, which are later

replaced by definitive HSCs derived macrophages, or they are retained permanently into adulthood (Davidson and Zon, 2004).

Interesting, vascular cells are also derived from RBI. Thus, the two sites of primitive hematopoiesis show contrasting potentials to differentiate into erythroid (ICM) or myeloid (RBI) cells, and share the similar ability to generate vascular cells (Davidson and Zon, 2004).

In fact, *pu.1* expression is also found at a low level in ICM, between 10 to 19-somite stages (Bennett et al., 2001; Lieschke et al., 2002). The equilibrium of *gata-1* and *pu.1* expression controls the balance between primitive erythroid and myeloid cell production within the ICM. In *gata1*$^{-/-}$ zebrafish embryos, *pu.1* expression persists longer in the ICM than in wild-type embryos. In contrast, other early hematopoietic markers, including *scl*, *lmo2* and *gata2*, all have normal expression in the *gata1*$^{-/-}$ embryos. The early ICM blood precursors in the *gata1*$^{-/-}$ embryos are mostly converted into myeloid cells, suggesting that Gata1 not only acts to promote erythroid development but also to suppress myeloid cell fate (Galloway et al., 2005). Work from several groups has suggested that PU.1 and GATA-1 antagonize one another through direct physical interaction (Nerlov et al., 2000; Rekhtman et al., 1999; Zhang et al., 1999; Zhang et al., 2000).

In addition, around 18-20 hpf, first granulocytes (similar to mammalian neutrophils and eosinophols) expressing specific marker *myeloperoxidase* (Mpo, an enzyme that is a major component of neutrophil and eosinophil granules) are identified in the posterior ICM and later migrate to a site of injury, such as tail clipping (Bennett et al., 2001; Lieschke et al., 2001).

1.3.5 Tanscriptional Regulation Of Definitive Hematopoiesis

At approximately 24 hpf, levels of hematopoietic transcription factors begin to diminish in the primitive sites, as hematopoiesis shifts to the definitive wave. Definitive HSCs, which are capable of unlimited self-renewal and able to generate all mature hematopoietic lineages, are found in the ventral wall of the dorsal aorta in zebrafish (equivalent to mammalian AGM), where expression of definitive HSC markers *c-myb* and *runx1* are detected between 24-48 hpf. Around 4-5 dpf, HSCs aggregate in the kidney, thymus and pancreas. The kidney becomes the main lifelong location of zebrafish hematopoiesis (de Jong and Zon, 2005) (Figure 1.7).

c-myb gene encoded protein contains an N terminal DNA-binding domain, a central transactivation domain and C-termianl negative regulatory domain (Vandenbunder et al., 1989). The transactivation domain interacts with p300 and controls the proliferation and differentiation of HSCs (Sandberg et al., 2005). Loss of *c-myb* in mice results in severe anemia due to impaired definitive hematopoiesis without perturbation of embryonic hematopoiesis (Mucenski et al., 1991; Mukouyama et al., 1999). Runx1 contains a runt domain and is a key component of transcription complex. Knock-down of *runx1* in zebrafish embryo leads to accumulation of immature hematopoietic progenitors, loss of blood circulation and incomplete vascular development (Kalev-Zylinska et al., 2002; Levanon et al., 1994). Other transcription factor including *ikaros*, *lmo2* and *scl* are also expressed in the AGM (Thompson et al., 1998). The *Ikaros* gene product belongs to zinc finger family of transcription factors. Long form of Ikaros consists of two zinc fingers, an N-terminal finger domain mediating DNA binding and C-terminal domain mediating dimerization. Generally, Ikaros proteins modulate transcription by recruiting corepressor

complex to the promoters of target genes and/or sequestering transcriptional coactivators (Koipally et al., 1999; Sabbattini et al., 2001; Trinh et al., 2001). Intriguingly, several isoforms of Ikaros are differentially expressed at various stages of hematopoiesis, suggesting that regulated expression of Ikaros isoforms could provide fine regulation for hematopoiesis (Klug et al., 1998).

At 48 hpf, a subset of the *ikaros*$^{+}$ cells in the AGM are likely candidates for lymphoid progenitors that eventually seed the thymus (Willett et al., 2001). As the thymus continues to grow over the next a few days, a number of small mature lymphocytes aggregate in the thymic epithelium, expressing characteristic T cell genes, including *gata3*, *ikaros*, T cell receptor kinase *lck*, and the recombination activating genes *rag-1* and *rag-2* (Willett et al., 1997). Zebrafish adaptive immune system is composed of T cells expressing rearranged antigen-specific T cell receptors and B cells expressing immunoglobulins. In contrast to T cell development in the thymus, B cell development is established in the kidney marrow by 19 dpf (Davidson and Zon, 2004; de Jong and Zon, 2005).

In addition, definitive hematopoiesis produces nucleated blood cells-zebrafish thrombocytes. Thrombocytes function similarly as mammalian platelets to maintain hemostasis by facilitating clot formation (Jagadeeswaran et al., 1999). In mammal, multinucleated giant megakaryocytes in the bone marrow are known as precursors of platelets. However, no similar precursors have been identified, although transcription factors important for megakaryocyte development are present in zebrafish, including *gata1*, *fli1*, *fog1*, *nfe2* and *runx1* (Burns et al., 2002; Pratt et al., 2002; Schulze and Shivdasani, 2004).

In summary, the transcriptional regulation of zebrafish hematopoiesis is highly conserved compared to mammalian system. The high degree of conservation refers to the factors themselves and also the sequence of their action. The conserved regulatory hierarchy makes zebrafish mutants useful tools to study related human diseases (Table 1.1).

Table 1.1 Zebrafish models of human hematopoitic diseases

Mutant	Abbreviation	Gene	Human disease	Reference
chardonnay	*cdy*	Divalent mental transporter 1	Microcytic anemia	(Donovan et al., 2002)
chablis	*cha*	Protein 4.1 r	Hereditary elliptocytosis	(Shafizadeh et al., 2002)
chianti	*cia*	Transferrin receptor 1	—	(Wingert et al., 2004)
dracla	*dra*	Ferrochelatase	Erythropoietic protoporphyria	(Childs et al., 2000)
merlot	*mot*	Protein 4.1r	Hemolytic anemia	(Shafizadeh et al., 2002)
moonshine	*mon*	TIF1γ	—	(Ransom et al., 2004)
retsina	*ret*	Solute carrier family 4, anion exchanger 1	Congenital dyserythropoietic anemia type II	(Paw et al., 2003)
riesling	*ris*	β-spectrin	Hereditary spherocytosis	(Liao et al., 2000)
sauternes	*sau*	δ-aminolevulinate synthase	Congenital sideroblastic anemia	(Brownlie et al., 1998)
vampire	*vmp*	TIF1γ	—	(Weinstein et al., 1996)
vlad tepes	*vlt*	Gata 1	Familial dyserythropoietic anemia and thrombocytopenia	(Lyons et al., 2002)
weissherbst	*weh*	Ferroportin 1	Hemochromatosis type 4	(Donovan et al., 2000)
yquem	*yqe*	Uroporphyrinogen	Porphyria	(Wang et al., 1998)

		decarboxylase	tarda and hepatoerythropoietic porphyria	
zinfandel	*zin*	Globin locus	Similar to thalassemia	(Brownlie et al., 2003)

Adapted from de Jong and Zon, 2005, with slight modification.

1.3.6 Regulation Of Hematopiesis By Cytokines and Growth factors

The process of blood cell formation is not only regulated by a variety of intrinsic transcription factors, multiple intracellular and extracellular signaling molecules are also involved in hematopoietic regulation, such as type III receptor tyrosine kinase receptors (RTK), interleukin-3/5 (IL-3/5), erythropoietin (EPO) and its receptor. Furthermore, Hedgehog, Vegf, Notch, TGF-β and BMP signaling pathways are also shown to play essential roles in both primitive and definitive hematopoiesis (Carradice and Lieschke, 2008).

Type III receptor tyrosine kinase

The hematopoietic receptor of type III RTK Flt3 (fms-like tyrosine kinase 3) is characterized by five immunoglobulin-like domains in the extracellular (EC) region of the receptor, followed by a transmembrane (TM) and juxtamembrane (JM) domain, a split kinase domain (KD) containing a kinase insert (KI) region, and a C-terminal (CT) tail (Rosnet and Birnbaum, 1993; Rosnet et al., 1993). Type III RTKs are normally involved in the regulation of hematopoiesis or hematopoietic cell function (Reilly, 2003a; Reilly, 2003b; Rosnet and Birnbaum, 1993). Despite differences in structure, normal function, and subcellular location, many of them signal through the phosphorylation of STATs (signal transducers and activators of transcription), and typically enhance

proliferation and prolong viability (Spiekermann et al., 2003). RTKs are known as oncogenes when mutations induce their constitutive kinase activities (Porter and Vaillancourt, 1998).

Interleukin-3/5 signaling

Interleukin 3 promotes development of hematopoietic cells through activation of the IL-3 receptor (IL-3R) complex consisting of α and β subunits. The α subunit provides the specificity to cytokines and β plays a major role in signal transduction (Hara and Miyajima, 1996). IL-3, GM-CSF (granulocyte-macrophage colony-stimulating-factor) and IL-5 exhibit similar functions (Warren and Moore, 1988). However no apparent hematological defect other than a reduced number of eosinophils was found in knock-out mice lacking an entire function of IL-3, GM-CSF and IL-5, indicating a remarkable functional overlap with other cytokine systems for hematopoiesis (Hara and Miyajima, 1996; Nishinakamura et al., 1996; Warren and Moore, 1988). Binding of these cytokines to the receptor leads to activation of the Janus family tyrosine protein kinase 2 (JAK2) and STAT5, as well as induction of c-*myc.* (Hara and Miyajima, 1996).

Erythropoietin signaling

Erythropoietin, which is produced by the kidney and liver in response to hypoxia or anemia, is the primary regulator of red blood cell production. It controls proliferation, maturation and also survival of erythroid progenitor cells (Spivak, 1986). The binding of EPO to its dimer receptor induces a conformational change that brings JAK2 molecules in close proximity and stimulates their activation by transphosphorylation. In turn, JAK2 molecules phosphorylate tyrosine residues in the cytoplasmic domain of the EPO receptor, which then serve as docking sites for various intracellular signaling proteins

which contain Src homology 2 (SH2) domains. For example, the transcription factor STAT5 can bind to activated EPO receptors, become phosphorylated, homodimerized and translocated into the nucleus to activate target genes. Other pathways activated by the EPO receptor through protein phosphorylation include the Ras/MAP kinase and phosphatidylinositol 3-kinase (PI3-kinase) pathways (Foley, 2008; Fried, 2009).

In addition, Epo and other cytokine-activated intracellular signal transduction cascades, such as the JAK-STAT pathway, are negatively regulated by the suppressor of cytokine signaling (SOCS) family of proteins respect to both magnitude and duration (Croker et al., 2008; Jegalian and Wu, 2002). SOCS proteins are upregulated in response to cytokine stimulation and inhibit cytokine induced signaling pathways, forming a classical negative feedback circuit. They participate in inactivation of JAKs, blocking access of the STATs to receptor binding sites, and ubiquitinating signaling proteins and subsequently targeting them to the proteasome (Kile and Alexander, 2001). The analysis of *socs1* deficient mice has revealed that SOCS1 plays a key role in T cell differentiation (Catlett and Hedrick, 2005; Tanaka et al., 2008). Additionally, the study of embryos lacking *socs3* has revealed the function of SOCS3 in fetal liver hematopoiesis (Marine et al., 1999).

Hedgehog signaling

Hedgehog signaling is essential for proper pattern formation and morphogenesis in several species (McMahon, 2000). In mouse, there are three homologs of the *Drosophila* Hedgehog (*Hh*) gene: Sonic hedgehog (*Shh*), Desert hedgehog (*Dhh*) and Indian hedgehog (*Ihh*) (Echelard et al., 1993; Hammerschmidt et al., 1997). All three hedgehogs signal through Patched (Ptch), a twelve-pass membrane receptor, and Smoothened (Smo), a seven-pass G protein like molecule. Binding of Hh to Ptch releases inhibition of Smo,

which in turn initiates the activation and nuclear translocation of the cubitus interruptus (Ci) transcription factors: Gli1, Gli2 and Gli3. Downstream target genes include *Ptch* as well as *Bmps* (Denef et al., 2000; Murone et al., 1999a; Murone et al., 1999b).

A conditional ablation strategy in adult mice shows that the development of T and B lymphoid cells is blocked at the level of the common lymphoid progenitor in the bone marrow, when Ptch is absent. In contrast, cells of the myeloid lineage develop normally in *Ptch* mutant mice (Uhmann et al., 2007). Therefore, HH/Ptch signaling is critical for the induction of lymphoid versus myeloid lineage commitment. In addition, a role for *Ihh* in yolk sac function is also suggested. 50% of $Ihh^{-/-}$ mice die at mid-gestation, potentially due to vascular defects in the yolk sac. Embryoid bodies (EB) derived from *Ihh* or *Smo* deficient embryonic stem cells are unable to form blood islands, and express reduced levels of endothelial cell markers. $Ihh^{-/-}$ lines also show a substantial decreased *scl* expression, markers for the hemangioblast (Byrd et al., 2002).

VEGF and receptors

VEGF monomers linked by disulfide bonds induce receptor dimerization, thereby triggering the activation of both the receptor itself and several cytoplasmic signal transduction molecules including VEGFR associated protein (VRAP), Ras GTPase activating protein (Ras GAP), Src family of tyrosine kinases, PI3-kinase, STAT and so on. There are also many co-receptors of VEGFR kinase, such as Cadherins, Integrin, Neuropilin 1 and 2 (Li et al., 2008).

The role of vascular endothelial growth factors (VEGF) and their receptors (VEGFR) has been studied extensively due to their important roles during blood vessel formation (Cebe-Suarez et al., 2006). Mice deficient in various VEGF ligands or receptors show

serious defects in vascular formation and maturation (Matsumura et al., 2003). Moreover, members of the VEGF family are not only involved in angiogenesis, but also in hematopoiesis. For example, decreased level of VEGF and Ihh attenuates definitive hematopoietic progenitor cell expansion in Gata4 and Gata6 null embryoid bodies. Furthermore, VEGF and Ihh can rescue definitive hematopoiesis in these Gata-4/Gata-6 deficient murine EBs (Pierre et al., 2009).

Notch/Jagged pathway

The Notch1-Jagged pathway plays an important role in integrating extracellular regulatory signals with hematopoietic stem cell cycling control (Karanu et al., 2000). Following binding of the Notch1 receptor by extracellular ligand, cleavage events release the intracellular portion of Notch1, which in turn translocates to the nucleus and acts as a transcription factor on its target genes (Kopan and Ilagan, 2009). Constitutively over-expressing the intracellular domain of Notch1 in hematopoietic cells establishes immortalized cell lines with the potential to reconstitute myeloid and lymphoid cell lineages both in vivo and in vitro (Varnum-Finney et al., 2000). Addition of Notch ligand jagged-1 can also prompt the pluripotency of the $CD34^{+}CD38^{-}Lin^{-}$ cord blood cells (Karanu et al., 2000).

TGF-βs

TGF-β molecules belong to a large superfamily of transforming growth factors that control cell growth, differentiation, and apoptosis (Massague et al., 2000). Depending on the differentiation status of target cells, the local environment and concentration and isoform of TGF-βs (Larsson and Karlsson, 2005), they are pluripotent regulators in a number of steps of hematopoiesis. For example, in myeloid and erythroid leukemic cells,

autocrine TGF-β1 and/or its Smad signals control the ability of these cells to respond to various differentiation inducers, suggesting that this pathway plays a role in determining the cell fate of leukemic cells (Kitisin et al., 2007; Lin et al., 2005; Massague et al., 2000). The mammalian TGF-β1, 2 and 3 have distinct but overlapping effects on hematopoiesis. TGF-β ligand binds to a heteromeric complex of type I (TβRI) and type II (TβRII) serine/threonine kinase receptors. Following ligand binding, TβRII recruits and activates TβRI, which in turn phosphorylates downstream targets, including the receptor activated Smad proteins (R-Smads), which are phosphorylated on their C-terminus and then translocate to the nucleus in complex with the common mediator Smad4 (Co-Smad) to regulate transcription of target genes. The principal R-Smads are Smad2 and Smad3 for TGF-β signaling. In the nucleus, Smad proteins can bind directly to their cognate DNA-binding sites and/or interact with transcriptional coactivators or repressors (Attisano and Wrana, 2002).

Recent studies have shown that there is extensive crosstalk between TGF-β/Smad signaling pathway and ERK, p38, c-Jun N-terminal kinase (JNK) and MAPK signaling cascades. For example, a novel MAPK kinase kinase (MAPKKK) termed TGF-β-activating kinase (TAK1) participates in signal transduction of TGF-β1 and has been shown to activate both the p38 and JNK pathway (Derynck and Zhang, 2003; Guo and Wang, 2009).

BMPs

BMPs also belong to the transforming growth factor-β superfamily of secreted proteins, and signal via the downstream transcription factors, Smad-1, -5, and -8 (von Bubnoff and Cho, 2001). Recently, more and more work has shown that BMP signaling is important

not only for the patterning of ventral mesoderm from where the primitive HSCs arise, but also for regulating proliferation and specification of blood progenitors (Figure 1.8). BMP/Smad signaling regulates hematopoiesis by crosstalk with other regulatory signals, so the outcome is very context dependent (Larsson and Karlsson, 2005; Winnier et al., 1995).

Work in *Xenopus* embryos suggests a model for primitive HSC formation. During gastrulation, BMP4 transcriptionally induces expression of homeobox genes such as Mix.1 and Vent-1 via xMad1. These homeobox genes directly or indirectly induce the expression of transcription factors Scl and Gata2, marking the formation of hemangioblast (common precursor for hematopoietic and endothelial cells) (Huber and Zon, 1998). In fact, a large number of studies in several other species have confirmed the key role of BMP signaling in hematopoietic commitment (Larsson and Karlsson, 2005; Snyder et al., 2004). Mice lacking BMP4 die between E7.5 and E 9.5 with severe defects in mesoderm formation. Those embryos, which survive up to E9.5 show defective blood island (Winnier et al., 1995). Similar to the studies using mouse embryonic stem (ES) cells, addition of BMP and cytokines promotes the hematopoietic differentiation of human ES cells (Chadwick et al., 2003; Johansson and Wiles, 1995; Park et al., 2004). Strikingly, studies by Jay *et al* demonstrate that BMP4, in combination with various cytokines, including erythropoietin (EPO), is able to induce several blood lineages from human skeletal or neural tissues (Jay et al., 2002). Finally, dorsalized zebrafish mutants of BMP pathway components usually have defective blood system. For example, zygotic *laf* (mutant for type I BMP receptor *alk8*) mutant embryos lack the ventral tail fin and vein at 1 dpf. They fail to develop blood circulation and die by 3 dpf (Mintzer et al.,

2001). In contrast, ventralized *din* mutant (mutant for bmp antagonist Chordin) show expanded blood island and expanded hematopoietic gene expression (Kawahara and Dawid, 2000; Leung et al., 2005; Schulte-Merker et al., 1997). Therefore, hematopoietic commitment requires intact BMP signaling.

However, it is not clear how many steps and what factors are involved between ventral mesoderm patterning and the specification of hemagioblast. In another word, it is not known what controls the separation of blood/endothelia cell (BC/EC) lineages from other ventral mesoderm cell types. Observations in chick embryo suggested some clues. During embryonic development in amniotes, the extra-embryonic mesoderm, where the earliest hematopoiesis and vasculogenesis take place, also generates smooth muscle cells (SMCs). Chick extraembryonic SMC and blood/endothelia cell (BC/EC) lineages are segregated early, and are marked by dHAND and Scl, respectively. It is proposed that once ventral mesoderm is specified by active BMP signaling, blood/endothelia cell (BC/EC) specification takes place as a default choice. SMC differentiation is promoted by canonical Wnt signaling and the balance between SMCs and BC/ECs is mediated by Notch signaling. Another possibility is that graded levels of BMP activity have discernable effect on *Scl* or *dHand* expression, resulting in qualitative differences in SMCs or BC/ECs induction (Shin et al., 2009) (Figure 1.8).

Apart from important function in specification of primitive HSCs, described above, BMP signals have been shown to regulate definitive hematopoiesis as well. BMP4 signaling is important in mediating shh-induced proliferation (Bhardwaj et al., 2001). BMP4 is shown to positively regulate both proliferation and survival of human blood progenitors (Larsson and Karlsson, 2005). Work by McReynolds show that zebrafish embryos

depleted for Smad1 fail to produce mature embryonic macrophages, where Smad5 depleted embryos are defective in primitive erythropoiesis. Loss of either Smad1 or Smad5 causes a failure in the generation of definitive hematopoietic progenitors (McReynolds et al., 2007). Furthermore, as I mentioned in chapter 1.3.1.4, the Smad5 C terminal truncated isoform *smad5β* is expressed higher in CD34+ hematopoietic stem cells than in terminally differentiated peripheral blood leukocytes, implicating the function of β form in hematopoietic stem cell homeostasis. It is also indicated that the proper splicing of *smad5* is important for normal adult hematopoietic development (Jiang et al., 2000). However, conditional knock-out mice for BMP type I receptor, BMPRIA, have increased numbers of spindle-shaped N-cadherin^{+}CD45^{-} osteoblastic (SNO) cells in the stem cell niche, leading to an increase in the number of definitive HSCs in these mice. It is postulated that SNO cells lining the bone surface function as a key component of the niche to support HSCs, and that BMP signalling through BMPRIA controls the number of HSCs by regulating niche size (Zhang et al., 2003).

In summary, BMP signaling activity plays essential role in both primitive (embryonic) and definitive (adult) hematopoiesis in a context dependent manner.

1.4 RESEARCH OBJECTIVE

The Integrator complex proteins are identified to directly interact with RNA polymerase II to mediate 3'end processing of U1 and U2 snRNAs. Integrator subunit 5 (Ints5) is picked up in a screen searching for genes acting in *Drosophila* oogenesis. It is found that the BMP homologue, DPP signaling is affected in *ints5* depleted germarial cells, leading to production of immature oocytes (Cai et al., unpublished data). This work indicates the role of Ints5 in regulating BMP signaling during vertebrate development. More improtantly, I found that knock-down of *ints5* in early zebrafish embryo leads to a lack of blood circulation, reduced expression of the hematopoietic genes and arrested red blood cell differentiation. It is long known that hematopoiesis, the dynamic process of blood cell development, is regulated by the activity of the Bone Morphogenetic Protein (BMP) signaling pathway and many transcription factors. Therefore, my research focused on studying the function of Integrator subunits in hematopoiesis. The detailed analysis of Ints5 function will reveal the link between the housekeeping snRNA processing machinery and the downstream effectors of BMP signaling during hematopoiesis development.

Chapter II

MATERIALS AND METHODS

2.1 ZEBRAFISH MAINTENANCE AND STRAINS

2.1.1 Fish Maintenance And Embryos Culture

Zebrafish were maintained under standard conditions at 28.5°C and embryos were obtained by standard breeding methods. All experimental procedures were carried out according to the guidelines of the Institutional Animal Care Use Committee at Temasek Life Sciences Laboratory as described in the Zebrafsih book (Westerfield, 2000). Embryos were collected after natural mating and raised in egg water (0.03% sea salt) at 28.5°C. Embryos were staged by hours post fertilization (hpf) and according to standard staging criteria according to Kimmel (Kimmel et al., 1995).

2.1.2 Fish Strains Used For The Studies

The zebrafish wild type (WT) strain AB (Johnson et al., 1994) was used for embryo injection and protein extraction.

2.2 CLONING OF INTEGRATOR SUBUNITS

2.2.1 5’ and 3’ Rapid Amplification Of cDNA Ends (RACE)-Ints5 Cloning

Total RNA was extracted from wild-type embryos and subjected to 5’and 3’RACE using the FirstChoice RLM-RACE Kit (Ambion #AM1700) according to manufacturer’s instructions. The following primers were used:

Ints5 5’Race 1: 5’ TCACCCTATGCAGGCCTTGTAGA 3’

Ints5 5’Race 2: 5’ GGGAGTAGCACTCCATTAGTGA 3’

Ints5 3'Race 1: 5' GCTACTTCCTCCAGTCTTGAGT 3'

Ints5 3'Race 2: 5' CGCTGTGCTATTGCTCTGTCAT 3'

The RACE products were cloned with *BamHI* and *XhoI* into the plasmid pCS2+ and sequenced.

2.2.2 Cloning Of Ints3, Ints6, Ints7, Ints9, Ints10, Ints11 and Ints12

ints3 was amplified from cDNA template with primer pair:

Ints3 F 5'CCATCGATGGTGCCCTGCGGAAGTTGAAT 3'

Ints3 R 5'AACCAAACATTTCCGCCCTT 3'

PCR product was cloned with *ClaI* and *EcoRI* into pCS2+ and sequenced.

ints6 was amplified from cDNA template with primer pair:

Ints6 F 5' CCGCTCGAGCGGCCGATTGTAGCTATTTTAGAC 3'

Ints6 R 5' CCGCTCGAGCGGAACCCCTATCGAACCTGGAA 3'

PCR product was cloned with *XhoI* into pCS2+ and sequenced.

ints7 was amplified from cDNA template with primer pair:

Ints7 F 5' GGAATTCATAAACAATGTCGCTTTCAGCAGC 3'

Ints7 R 5' GCTCTAGAATGAGGAGAGCACCACAGAAC 3'

PCR product was cloned with *EcoRI* and *XbaI* into pCS2+ and sequenced.

ints9 was amplified from cDNA template with primer pair:

Ints9 F 5' CCGGAATTCGGAGGTATCGCTAAATATGC 3'

Ints9 R 5' CCGCTCGAGGACAAGCATCAACATACACCG 3'

PCR product was cloned with *ClaI* and *XhoI* into pCS2+ and sequenced.

ints10 was amplified from cDNA template with primer pair:

Ints10 F 5' CCATCGATGGAAGAAAACAGAGCAGATGTCCG 3'

Ints10 R 5' GCTCTAGAGACACACACACAGCTTATGAGG 3'

PCR product was cloned with *ClaI* and *XbaI* into pCS2+ and sequenced.

ints11 was amplified from cDNA template with primer pair:

Ints11 F 5' CGCGGATCCGCGCTGTGTTGGAGTTGACATATC 3'

Ints11 R 5' CCGCTCGAGGTTTCAGCAGTCAAGAAGGCAGACC 3'

PCR product was cloned with *BamHI* and *XhoI* into pCS2+ and sequenced.

ints12 was amplified from cDNA template with primer pair:

Ints12 F 5' CCATCGATCGCTAAACAATGGCTGGGACAG 3'

Ints12 R 5' CCGCTCGAGGACATTCTGCCTACTTCCTCC 3'

PCR product was cloned with *ClaI* and *XhoI* into pCS2+ and sequenced.

2.3 SMAD CONSTRUCTS

pCS*smad5ΔExon4* and pCS*smad5ΔExon4, 5* were generated by over-lapping PCR amplification from cDNA templates (Dick et al., 1999) using the following primers:

smad5 5' F: 5'CGGGATCCTCCTGTCCTTGGTCCTGCAA3'

smad5 3'UTR R: 5'CGGAATTCCCTATGCTAGATGTGCTTGT3'

smad5Δexon4F:

5'CACTACAAACGAGTTGAAAGTCCAGCTGATACTCCTCCTCCTGCCTACAT 3'

smad5Δexon4R:

5'ATGTAGGCAGGAGGAGGAGTATCAGCTGGACTTTCAACTCGTTTGTAGTG3'

smad5Δexon4, 5F:

5'CACTACAAACGAGTTGAAAGTCCAGATGTGCAGCCAGTGGAGTATCAGG3'

smad5Δexon4,5R:

5'TCCTGATACTCCACTGGCTGCACATCTGGACTTTCAACTCGTTTGTAGTG3'

PCR products were cloned into pCS2+ with *BamHI* and *EcoRI*.

2.4 RNA AND MORPHOLINOS INJECTIONS

2.4.1 mRNA Synthesis

For injection, constructs were digested with *NotI* and the capped mRNA was synthesized with the mMessage mMachine SP6 kit (Ambion # 1340) according to manufacturer's instructions.

Linearized DNA	1-2 µg
10 x Reaction Buffer	2 µl
2 x NTP/cap	10 µl
SP6 Enzyme Mix	2 µl

DEPC treated water was added to a final volume of 20 µl. Then, the reaction was incubated at 37°C for 2 h. Following this, 1 µl of DNase I was added and the reaction was incubated further at 37°C for 30 min.

The reaction was stopped by adding 15 µl of ammonium acetate. Then, 115 µl of distilled sterile DEPC (Diethylpyrocarbonate) treated water and 150 µl of phenol/chloroform/isoamyl alcohol (Sigma #P3803) were added into the tube. After mixing and centrifugation, the aqueous phase was transferred to a fresh tube. To precipitate the capped mRNA, 150 µl of isoproponal was added to the tube and it was kept at -80°C for half an hour or -20°C overnight. After centrifugation, the RNA pellet was washed with 1 ml of 75% ethanol, air-dried and dissolved in 20 µl of distilled sterile DEPC treated water. The quality and quantity of the capped mRNA was determined by measuring the optical density (OD).

2.4.2 Injection Of Morpholinos

All morpholinos were obtained from GeneTools company (www.gene-tools.com). The *ints5* donor and acceptor morpholinos were designed to target the splice sites. Co-injection of two *ints5* morpholinos (donor + acceptor MO) at an optimal dose of 2.5 ng+ 2.5 ng/embryo was found to be more efficient, therefore all injections, unless otherwise specified, were performed using this combination. The *ints9* splice morpholino (*ints9* SMO) targeting the intron2-exon3 boundary of *ints9* was used at a dose of 12.5 ng/embryo. The *ints11* ATG morpholino (*ints11* ATG MO) were injected at a dose of 25 ng/embryo. The *ints11* splice morpholino (*ints11* SMO) targeting the intron4-exon5 boundary was injected at a dose of 2.5 ng/embryo. The morpholino sequences are listed:

ints5 donor MO: 5 CTTGTATTGCTCACCTGTAA 3’

ints5 acceptor MO: 5’AGCTCTTGAGGACTGATGGA 3’

ints9 SMO: 5’GATAATCGTGGACTGTAAATCCAAC3’

ints11 ATG MO: 5’ AAGGCGTAACTTTGATATCAGGCAT3’

ints11 SMO: 5'AGATGGAAATGACTGAGAGGAAGAG3'

For rescue experiments, 50 pg of *ints5 RNA* and 10 pg of *smad1* or *smad5* RNA was co-injected with *ints5* morpholinos.

2.4.3 Embryo Injection And Fixation

Different doses of mRNA and morpholinos were injected into one-cell stage embryos and embryos were either fixed at different stages using 4% paraformaldehyde (PFA) (Sigma #P-6148) or were raised until 24 hours for phenotypic observation.

2.5 WHOLE MOUNT RNA IN SITU HYBRIDIZATION ANALYSES

2.5.1 Digoxigenin (DIG) Or Fluorescein (FLU)-Labeled RNA Probe Synthesis

Linearization of plasmids

Plasmids were linearized by the restriction enzyme near the 5' cloning site and purified from gel by using a QIAquick Gel Extraction Kit (Qiagen #28706).

The following plasmids were linearized and antisense probes were synthesized by *in vitro* transcription:

pBS*ints5: BamHI*/T3 RNA Polymerase (Baillat et al., 2005)

pGEMT-Easy*scl: NcoI*/SP6 RNA Polymerase (Gering et al., 1998)

pBS*gata1: XbaI*/T7 RNA Polymerase (Detrich et al., 1995)

pBS*flk1*: *SmaI*/T7 RNA Polymerase (Liao et al., 1997)

pKS*pax2a*: *BamHI*/T7 RNA Polymerase (Majumdar et al., 2000)

pBS*hgg1*: *XbaI*/T7 RNA Polymerase (Thisse et al., 1994)

pBS*gsc*: *EcoRI*/T7 RNA Polymerase (Thisse et al., 1994)

pBS*ntl*: *XhoI*/T7 RNA Polymerase (Schulte-Merker et al., 1994)

pBS*spt*: *EcoRI*/T7 RNA Polymerase (Griffin et al., 1998)

pBS*sox17*: *EcoRI*/T7 RNA Polymerase (Alexander and Stainier, 1999)

pBS*myoD: BamHI*/T7 RNA Polymerase (Weinberg et al., 1996)

pBS*dlx3*: *SalI*/T7 RNA Polymerase (Akimenko et al., 1994).

The *in vitro* transcription reaction:

5 X transcription buffer (Promega #P118B)	10 µl
RNA polymerase (SP6 polymerase, Promega #P108B;	2 µl
T7 RNA polymerase, Promega #P2075 and T3 RNA	
polymerase, Promege #P2083.)	
10 X DIG RNA labeling mix (Roche #1277073910)	5 µl
or 10 X Fluorescein RNA labeling mix (Roche #1685619)	
RNase inhibitor (Roche #03335399001)	1 µl
100 mM DTT (Promega #117B)	1 µl
linearized DNA template	1-2 µg

Distilled, sterile DEPC treated H_2O was added to a final volume of 50 µl, and incubated at 37°C for 2 h.

Then, 1 µl of DNase I recombinant, RNase-free (Roche # 04 716 728 001) was added to the above reaction, incubated at 37°C for 30 min.

The reaction was stopped by adding 1 µl of 0.5 M EDTA (pH 8.0). Labelled RNA was precipitated by adding 5 µl LiCl (4 M), 100 µl cold isopropanol, and incubated at –20°C overnight. After centrifuging, the RNA pellet was washed with 75% cold ethanol and then air dried and dissolved in 50 µl DEPC treated sterile H_2O. The quality and quantity

of the RNA was determined by measuring its OD. The probe stocks were stored at –80°C.

For *in situ* hybridization, the DIG-labeled or Flu-labeled probe was diluted in 60% hybridization buffer (hyb) to a final concentration of 100 ng probe/200 µl hyb and stored at –20°C.

The components of 60% hybridization buffer are as follows:

5 x Standard Sodium Citrate (SSC)

60% Formamide

0.1% Tween 20 (SIGMA-ALDRICH #P9416)

1 mg/ml tRNA (Roche #109 509)

100 µg/ml heparin (SIGMA-ALDRICH #A6039)

1 x Denhardt's solution

0.1% CHAPS

10 mM EDTA

2.5.2 In Situ Hybridization Procedure

Embryos were fixed in 4% PFA, incubated at room temperature (RT) or 4°C overnight. Embryos were washed with PBST (0.1% Tween 20 in phosphate buffered saline, PBS) three times, followed by dechorionation using forceps under the dissecting microscope. Dechorionated embryos were gradually dehydrated in 25%, 50%, 75% and 100% methanol, and stored at –20°C for later use. The whole-mount *in situ* hybridization analysis was performed according to Tian Jing (Tian et al., 2003).

Day I: Pre-hybridization and hybridization

Embryos were rehydrated gradually from methanol to PBST. Embryos older than 24 hpf

need proteinase K treatment (3 μg/ml for 24 h embryos, 100 ng/ml for 50% to 100% epiboly embryos) for better probe penetration. After proteinase K treatment for 1 min, embryos were post-fixed in 4% PFA for 20 min. Then, embryos were washed with PBST three times before incubation with 60% hyb buffer for at least 4 h at 65°C. Then the diluted probes were added to embryos and incubated in the 65 °C water bath overnight.

Day II: Post-hybridization washes and antibody incubation

The non-hybridized RNA probes were washed away by the following buffers in sequence:

50% formamide/5 x SSC (FS), 65 °C 10 min

75% FS/25% 2 x SSC (0.1% Tween 20 in 2xSSC), 65°C 10 min

50% FS/50% 2 x SSC, 65 °C 10 min

25% FS/75% 2 x SSC, 65 °C 10 min

2 x SSC, 65 °C 15 min for 2 times

0.2 x SSC (0.1% Tween 20 in 0.2xSSC), 65°C 15 min for 2 times

75% 0.2 x SSC/25% Maleic acid buffer (MAB) (0.1% Tween 20 in MAB), RT 10 min

50% 0.2 x SSC/50% MAB, RT 10 min

25% 0.2 x SSC/75% MAB, RT 10 min

MAB, RT 10 min

Embryos were incubated in 0.5% blocking reagent (Roche #11 096 176 001) in MAB at RT for at least half an hour, and then incubated with 1:2000 anti-Digoxigenin alkaline phosphatase (AP) antibody (for detecting DIG-labeled probe) (Roche #11093274910) or 1:500 anti-Fluorescein-AP antibody (for detecting FLU-labeled probe) (Roche #11426338910) in blocking buffer at 4°C overnight.

Day III: Post-antibody washes and signal detection

To wash out the unbound antibody, embryos were washed with MAB at room temperature, 15 min x 5 times. Embryos were then washed in Buffer 9.5 at RT 5 min x 3 times.

Then, the reaction was developed with the BM Purple AP substrate (Roche #11442074001). Embryos were stained with purple in color.

Buffer 9.5:

0.1 M Tris-HCl pH9.5

0.1 M NaCl

0.05 M $MgCl_2$

0.1% Tween 20

Alternatively, embryos were washed in Buffer 8.2 at RT 5 min x 3 times. The reaction was developed with Fast Red substrate (Sigma # F4523). Embryos were stained with red in color.

Buffer 8.2:

0.1 M Tris-HCl pH8.2

0.1 M NaCl

0.05 M $MgCl_2$

0.1% Tween 20

The excess substrate was washed away using PBST for two times and embryos were post-fixed in 4% PFA at 4°C overnight. For imaging, fixed embryos were washed again with PBST to remove PFA, and stored in 50%/50% glycerol/PBST at 4 °C.

For two-color *in situ* hybridization, the embryos were washed in PBST for three times

and then in MAB buffer after the completion of the first staining. Then the embryos were re-blocked in 0.5% blocking buffer before adding the antibody for detecting the second probe, and the reaction was developed with a different substrate.

2.6 TOTAL RNA EXTRACTION AND RT-PCR

2.6.1 Total RNA Extraction

Embryos were collected in 1 ml of TRIZOL (invitrogen) in an eppendorf tube and homogenized using a syringe with a $26^1/_2$ G needle. The homogenized samples were incubated for 5 minutes at room temperature to permit the complete dissociation of nucleoprotein complexes. Then 0.2 ml of chloroform (Sigma # C0549-1PT) was added into 1 ml of TRIZOL. The securely capped tubes were then vigorously inverted back and forth for 15 seconds and incubated at room temperature for 2 to 3 minutes. The samples were centrifuged at no more than 12,000 g for 15 minutes at 4°C. Upon centrifugation, the mixture separates into a lower pink phenol-chloroform phase, a white inter-phase, and a colorless upper aqueous phase. RNA remains exclusively in the aqueous phase. The volume of the aqueous phase is about 0.6 ml.

The aqueous phase was transferred to a fresh tube and the RNA was precipitated from the aqueous phase by mixing with 0.5 ml of cold isopropyl alcohol. After incubation at room temperature for 10 minutes, the samples were centrifuged at no more than 12,000 g for 10 minutes at 4°C. The RNA precipitates and usually forms a gel-like white pellet at the bottom of the tube.

After removing the supernatant, the RNA pellet was washed with 1 ml of cold 75%

ethanol, and centrifuged at no more than 7,500 g for 5 minutes at 4°C. At the end of the procedure, the RNA pellet was air-dried for 5-10 minutes. RNA was dissolved in RNase-free water and incubated for 10 minutes at 55 to 60°C. RNA can be stored at -80°C.

2.6.2 DNase Treatment Of Total RNA

The DNase treatment reaction was set as below:

Total RNA	x µl
10x DNase I buffer (Roche # 04 716 728 001)	5 µl
RNAse inhibitor (Promega # N211A)	1 µl
100 mM DTT (Promega # P117B)	1 µl
DNase I (Roche # 04 716 728 001)	1 µl

Distilled, sterile DEPC treated H_2O was added to a final volume of 50 µl, and the reaction was incubated at 37°C for 1 hour.

Mix 50 µl of the above reaction with 100 µl of sterile DEPC treated H_2O to make it up to 150 µl and mix it well with 150 µl of phenol: chloroform: isoamyl alcohol (25:24:1, Sigma # P3803-100 ml). Following centrifugation at 12,000 g for 15 minutes at 4°C, the upper aqueous phase containing RNA was transferred to a new tube and mixed with 150 µl of chloroform (Sigma # C0549-1PT). Following this, the phase separation, RNA precipitation, RNA washing and re-dissolving steps were repeated as described earlier. The RNA can be stored at -80°C, and is ready for reverse transcription (RT).

2.6.3 Reverse Transcription (RT)

1-2 µg of total RNA from injected embryos was used to generate cDNA with Superscript II Reverse Transcriptase (Invitrogen # 18064-022) and primer $p(dT)_{15}$ (Roche # 10 814 270 001) or primer random $p(dN)_6$ (Roche #1 034 731).

First-Strand cDNA Synthesis

1. The following components were added to a clean tube:

$p(dT)_{15}$ (500 µg/ml) or	1 µl
50–250 ng random primers or	
1 to 2 µg total RNA	x µl
1 µl dNTP Mix (100 mM)	1 µl
Sterile, distilled water	to 12 µl

2. The mixture was heated to 65°C for 5 min and quickly chilled on ice. Following brief centrifugation, add:

5X First-Strand Buffer	4 µl
100 mM DTT (Promega # P117B)	2 µl
RNase inhibitor (Promega # N211A)	1 µl

3. The contents were gently mixed. If $p(dT)_{15}$ primer was used, incubate at 42°C for 2-3 min. If random primer was used, incubate at 25°C for 5 min.

4. 1 µl (200 units) of SuperScriptTM II RT was added and mixed by pipetting gently up and down. When using random primers, incubate tubes at 25°C for 10 min.

5. Incubate at 42°C for 90 min.

6. Inactivate the reaction by heating at 70°C for 15 min.

Amplification of PCR targets (>1 kb) requires the removal of RNA complementary to the

cDNA. To remove RNA complementary to the cDNA, 1 µl (2 units) of E. coli RNase H was added and incubated at 37°C for 20 min. The cDNA was then used as template for PCR (Tables 2.1, 2.2, 2.3, 2.4, 2.5, 2.6) or Real-Time PCR reactions (Table 2.7).

Table 2.1 Primers for checking efficiency of *ints5*, *ints9*, and *ints11* splice junction morpholinos (Figures 3.3 and 5.3)

Primer	Sequence
Ints5 exon1 F	5' GAGCTTCCGGTGTCTGGTGCA 3'
Ints5 exon1 R	5' GCAGCAATGCAAACTAGAACT 3'
Ints5 exon2 F	5' CCCCCCCCTGCTGTATGTTTCCT 3'
ints5 exon2 R	5' CGCTGGCTCCTCCACTTGCACT 3'
ints9 exon2 F	5' CTGTCTGTCAGGTCATCCCA 3'
ints9 exon5 R	5' CCTGTAAAGCCTGTGTGTTC 3'
ints11 exon9 R	5' CTGCAGCGTTTGGAGTCTCT 3'
ints11 exon3 F	5' GACTGCGGGATGCACATGGG 3'

Table 2.2 Primers to detect splicing of *smad1* RNA (Figure 4.4)

Primer	Sequence
smad1 Exon1 F1	5' AATCTGACGGAGTAACTGAG 3'
smad1 Exon1 F2	5' GCATCAACCCTTACCACTAC 3'
smad1 Intron1 F	5' GAAGCATAAAGGAGGCGACT 3'
smad1 Intron1 R	5' GATAGTCTACAGAACAAACC 3'

smad1 intron1 R2	5’ CAATCTATGATGCCTTCAAG 3’
smad1 Exon2 F	5’ ACGCTAAACTCTCCATGCTG 3’
smad1 Exon2 R	5’ CAGCATGGAGAGTTTAGCGT 3’
smad1 intron2 F	5’ GGAGTTCACCTACAGTATGT 3’
smad1 intron2 R	5’ CATACTGTAGGTGAACTCCT 3’
smad1 Exon3 R	5’ CAGTCCTGTGTCATTGGCTC 3’
smad1 Exon3 F1	5’ CCAGAGGAGCCAATGACACA 3’
smad1 Intron3 R	5’ TCAGACTGTAAGGAAGGAGC 3’
smad1 Exon3 F2	5’ ACTTGCCATTGGAGATCAGC 3’
smad1 Exon5 R1	5’ CTCAAACATTCGGCATACAC 3’
smad1 Intron3 F	5’ GCGTATGTGCTCTTGTGCTT 3’
smad1 Exon4 F1	5’ TGTTCATCCTGTGGCCTATC 3’
smad1 Exon5 F1	5’ GTGTATGCCGAATGTTTGAG 3’
smad1 Exon6 R	5’ CCTCCCTTCAACCAATCAGC 3’
smad1 Intron5 R1	5’ ACCTTGTGTTCATCTTGTGT 3’
smad1 Intron5 F1	5’ AACCATTAGACGCTGAAGTA 3’
smad1 Intron3 R2	5’ CAGACTGTAAGGAAGGAGCA 3’
smad1 Intron4 R	5’ CAGACGCGATCAATCATCAG 3’
smad1 Intron4 F	5’ CTGATGATTGATCGCGTCTG 3’
smad1 Intron5 R2	5’ CCTTGTGTTCATCTTGTGTA 3’
smad1 Intron5 F2	5’ CCATTAGACGCTGAAGTAAA 3’
smad1 Exon4 R1	5’ CGATGGTTGAGTTCCGGTTG 3’

Table 2.3 Primers to detect splicing of *smad5* RNA (Figure 4.1)

Primer	Sequence
smad5 Exon1 F	5’ CTCCTTCATGTCGGTGTCTG 3’
smad5 Exon2 R	5’ CACTTCTCAACACCTCCCTG 3’
smad5 Exon2 F	5’ CAGGGAGGTGTTGAGAAGTG 3’
smad5 Exon3 R	5’ GGACAGGAAGTGGAAAGCAG 3’
smad5 Intron2-3 R	5’ GGTGCTACATAGCCAGTTAG 3’
smad5 Intron2-3 F	5’ GGAAAATCTATTCAACTCCC 3’
smad5 Exon4 R	5’ GGGTGAGTTTGGAGAGATGG 3’
smad5 Intron3-4 R	5’ CTGTGCACGATATGTCAGCG 3’
smad5 Intron3-4 F	5’ GATGTCAAGGATGCTGGATA 3’
smad5 Exon4 F	5’ CCATCTCTCCAAACTCACCC 3’
smad5 Eoxn5 R	5’ GTTCTGAGGAGCCAGGCTGC 3’
smad5 Intron4-5 R	5’ CTATAAGTGGTGCCTACAAG 3’
smad5 Intron4-5 F	5’ GGAGTTGTGAAATCTGACAC 3’
smad5 Eoxn5 F	5’ GCAGCCTGGCTCCTCAGAAC 3’
smad5 Eoxn6 R	5’ GGAGTTGCGATTGACATTAG 3’
smad5 Intron5-6 R	5’ CTCAACAGAGCGTGTAGGTG 3’
smad5 Intron5-6 F	5’ CGCTAACACCATTTGCTTGC 3’
smad5 Exon6 F	5’ CTAATGTCAATCGCAACTCC 3’
smad5 Intron6-7 R	5’ GAACACCTGTGCAACCAAGA 3’
smad5 Intron6-7 F	5’ CATTGGATCACAGATTAGCC 3’

smad5 Eoxn7 F	5’ GTCCAGAGTCGAAACTGCAAC 3’
smad5 Exon8 R	5’ CAGGTCAGCCCATCATTACG 3’
smad5 Intron7-8 R	5’ GCTACTTTCAGCTACAAATG 3’
smad5 Intron7-8 F	5’ CAAGAACCAAGTGATATGAA 3’

Table 2.4 Primers to detect splicing of *smad2* RNA (Figure 4.5)

Primer	**Sequence**
smad2 Exon1 F	5’ CATGTCGTCCATCTTGCCATTC 3’
smad2 Exon2 F	5’ CCAGAGACCCAGTTAGGAAC 3’
smad2 Exon5 F	5’ GTTGCCACCTTTGGACGACT 3’
smad2 Exon5-6 R	5’ GTGGAGGAGTTTCTGGTATG 3’
smad2 Exon11 R	5’ CGAGTTGTCGCTTGATGTGA 3’
smad2 Exon3 R	5’ GGTATCCCACTGTTCTATCG 3’
smad2 Exon4 R	5’ CAGACCTTTACGGTGAGACA 3’
smad2 Exon5 R	5’ GGAGTTGGTGTAGTCGTCCA 3’
smad2 Exon6 F	5’ GCCAGTGACCAGCAAATGAA 3’
smad2 Exon7 F	5’ GTCACCAAGCACACTCTCGC 3’
smad2 Exon8 F	5’ CGTGGACGGCTTCACAGACC 3’
smad2 Exon9 F	5’ CAGAGGTATGGCTGGCATCC 3’
smad2 Exon10 F	5’ CAACCAGGAGTTTGCAGCAT 3’

Table 2.5 Primers to detect splicing of *smad3a and smad3b* RNA (Figure 4.5)

Primer	Sequence
smad3a Exon1F	5’ CACAACTCAGGATGTCAACA 3’
smad3a Exon2R	5’ GCTGATAGTGGTAGGGATTG 3’
smad3a Exon2F	5’ CAATCCCTACCACTATCAGC 3’
smad3a Exon3F	5’ CTGGTGCCTCGACACACTGA 3’
smad3a Exon3R	5’ TCAGTGTGTCGAGGCACCAG 3’
smad3a Exon4F	5’ CAGATGAACCGGAGCATGGA 3’
smad3a Exon4R	5’ TCCATGCTCCGGTTCATCTG 3’
smad3a Exon6F	5’ CAGACCCGTCCAACTCAGAG 3’
smad3a Exon6R	5’ CTCTGAGTTGGACGGGTCTG 3’
smad3a Exon7F	5’ CGGCTGGCACCCTGCTACTG 3’
smad3a Exon7R	5’ CAGTAGCAGGGTGCCAGCCG 3’
smad3a Exon8F	5’ GTTGGCCCAGTCTGTGAATC 3’
smad3a Exon8R	5’ GATTCACAGACTGGGCCAAC 3’
smad3a Exon9R	5’ CTCTATCCAGCAGGGGGTGC 3’
smad3b Exon1F	5’ GAGCAGAACGGACAGGAGGA 3’
smad3b Exon2R	5’ CACGCTGGTAGTGATAAGGG 3’
smad3b Exon2F	5’ CCCTTATCACTACCAGCGTG 3’
smad3b Exon3F	5’ CATCCCCACAGACTTCCCTC 3’
smad3b Exon3R	5’ GAGGGAAGTCTGTGGGGATG 3’
smad3b Exon5F	5’ GTTCTCCAACGCTTTCGCCT 3’
smad3b Exon5R	5’ AGGCGAAAGCGTTGGAGAAC 3’

smad3b Exon6F	5’ CTGCTCTCCAATGTCAACCG 3’
smad3b Exon6R	5’ CGGTTGACATTGGAGAGCAG 3’
smad3b Exon7F	5’ CTGTGTGTAAGATTCCTCCA 3’
smad3b Exon7R	5’ TGGAGGAATCTTACACACAG 3’
smad3b Exon8F	5’ CCCAATCAGTGAATCAGGGA 3’
smad3b Exon8R	5’ TCCCTGATTCACTGATTGGG 3’
smad3b Exon9R	5’ GAGCCCATCTGAGTGAGCAC 3’

Table 2.6 Primers to detect splicing of *cyclops* and *squint* RNA (Figure 4.6)

Primer	**Sequence**
cyc Exon1 F	5’ GCACGAGCACGCAGACACAA 3’
cyc Exon2 F	5’ CCAGTCTCCTACACACCGCC 3’
cyc Exon2 F2	5’ GAAGGAATTCGGTGCGAGGGGGCCTGCCCG 3’
cyc Exon2 R	5’ CTCCGCTGCCTGAATCTGAC 3’
cyc Exon3 R	5’ GGAACACGACTGGGGTGATG 3’
cyc Exon3 R2	5’CAAGGAGCTCACAGGCATCCGCACTCCTCC AC 3’
cyc Intron1 F1	5’ GTTCGCTCTCATAATCACAA 3’
cyc Intron1 F2	5’ GACTGTTTGGTCACAATCAC 3’
cyc Intron1 R1	5’ GTACCGTCAATCACTCTAAT 3’
cyc Intron1 R2	5’ GCGAATCCACATCGGCTTCA 3’

sqt Exon1 F1	5’ CCGCTGTATATGATGCACCTC 3’
sqt Exon1 F2	5’ ATGATGCACCTCTACCGGACACTT 3’
sqt Exon2 F	5’ TGCCGAGCACTCCAAGTATG 3’
sqt Exon2 R1	5’ ATCCACCTCCAACTCAGACC 3’
sqt Exon2 R2	5’ TGAGGAGCGCAGTGATGTTGAAGA 3’
sqt Exon3 R	5’ CATCAAGTTATCCAGGTGCC 3’
sqt Intron1 F	5’ TTAATTGCTTGTCCCGAACGTGGC 3’
sqt Intron1 R	5’ TTGATGCCCAGGCCACTTTGAAAC 3’

2.6.4 Quantitative Real-Time PCR

First-strand cDNA was synthesized by using Superscript II Reverse Transcriptase (Invitrogen # 18064-022). Semi-quantitative Real-Time PCR was performed with the Power SYBR Green PCR mix (Applied Biosystems # 4367659) on the 7900HT Fast Real-Time PCR system (Applied Biosystems http://www.appliedbiosystems.com.sg/).

A real-time PCR reaction was set as below:

Power SYBR Green PCR Master Mix (2X)	25 µl
Forward Primer (10 µM)	2.5 µl
Reverse Primer (10 µM)	2.5 µl
Template (<100ng)	1 µl
Distilled, sterile H_2O	up to 50 µl

Each PCR reaction was performed in triplicate, and each experiment was repeated three times. The PCR cycle conditions were: 95°C, 10 min, 94°C, 15sec, 60°C, 1 min, 45

cycles. The CT values were analyzed using the $2^{-\Delta\Delta T}$ method. The primers used for real-time PCRs are listed in Table 2.7.

Table 2.7 Primers used in Real-Time PCRs

Primer	Sequence
scl F	5’ GCTGGAGATGCGGAACAGTA 3’
scl R	5’ GAAGGCACCGTTCACATTCT 3’
gata1 F	5’ CTGACCTACTGCCATCGTAT 3’
gata1 R	5’ GACTGAGATGAGTAGACTTG 3’
flk1 F	5’ CCTGGAGAACGGAACCAACA 3’
flk1 R	5’ CAGCCGCTTCAGCGTCTTCA 3’
actin F	5’ GGCTACAGCTTCACCACCA 3’
actin R	5’ TGCTGATCCACATCTGCTG 3’
U1 mature F	5’ CTTACCTGGCAGGGGAGACA 3’
U1 mature R	5’ GCAGTCGAGATTCCCACATT3’
U1 primary F	5’ GACACCATGATCAGGAAGGT 3’
U1 primary R	5’ CTATTTTGACCATGTGATC 3’
U2 mature F	5’ GGCTAAGATCAAGTGTAGTATC 3’
U2 mature R	5’ AGCAAGCTCCTATTCCAACTCC 3’
U2 primary F	5’ CAAGTGTAGTATCTGTTCTTATC 3’
U2 primary R	5’ TTTACCAGGTTAGGGGGTGCAC 3’
18s rRNA F	5’ GAGAAACGGCTACCACATCC 3’
18s rRNA R	5’ GGACACTCAGCTAAGAGCATCG 3’

2.7 MAY-GRUNWALD GIEMSA STAINING

2.7.1 Cytospin

200 µl of blood cells were extracted in Tricaine buffer (0.02% Tricaine/PBS with 1% BSA) from approximately 20 fishes by clipping their tails.

Before cytospining, 200 µl of Tricaine buffer was loaded into the cytofunnel for normalization. After loading, the samples were spun at 400 rpm for 3 min (Shandon Cytospin 4). The blood cells will be concentrated in the circular area of the cytospin glass slides. The slides were air-dried and subjected to May-Grunwald Giemsa staining (Qian et al., 2007).

2.7.2 Giemsa Staining

After cytospining, 1 ml of May-Grunwald eosin methylene blue stain solution (May-Grunwald solution:methanol = 1:3, Merck # 1.01424.0100) was gently added to cover the cytospin area and leave for 1min before running off the solution completely. Then 1 ml of Giemasa stain solution (freshly prepared; Giemsa solution:Phosphate buffer = 1:20, Merck #1.09204.0500) was added onto the cytospin area and rocked gently for 15-30 min. After runing off the solution with slow running water, slides were left at room temperature to air-dry (Qian et al., 2007).

Phosphate buffer (every 1000 ml):

KH_2PO_4 6.63 g

Na_2HPO_4 2.56 g

Adjust the pH value to 6.4 and filter before use.

2.8 WESTERN BLOTTING

To reduce the background, the yolk of embryos was removed using needles under a dissecting microscope. Cells from 20 embryos were collected into a tube and excess egg water was removed by pipetting. 20 µl of 1 x SDS loading buffer was added to the embryos and the mixture was vortexed vigorously, and boiled for 5 min. Then the sample was analyzed on a protein electrophoresis gel in 1 x SDS running buffer. Protein was transferred to a nitrocellulose membrane (Amersham Biosciences #RPN203E). The membrane was blocked in 5% milk blocking buffer for 2 h at RT or at 4°C overnight with slight rocking.

Ints5 protein was detected using rabbit anti-Ints5 antibody (1:500, Bethyl Laboratories A301-268A). Smad5 protein was detected using rabbit anti-Smad5 polyclonal antibody (1:500, Abcam ab13724). The expression of α-tubulin control was detected using mouse anti-α-tubulin monoclonal antibodies (1:1000, Sigma #T5293). Anti-mouse immunoglobulins (1:5000, DAKO #P0260) or anti-rabbit immunoglobulin (1:5000, DAKO #P0448) were used as secondary antibodies and detected by SuperSignal West Femto Maximum Sensitivity Substrate (Pierce #34095) or by SuperSignal West Pico Chemiluminescent Substrate (Pierce #34077).

2.9 MICROSCOPY

All the images were taken under the Zeiss Axioplan 2 Imaging System.

The DIC images for live embryos were taken under 10X/0.3 objective, using Photometrics Coolsnap HQ monochrome camera and MetaMorph software (Universal Imaging Corporation).

The bright-field images for red blood cells with Giemsa staining and *in situ* embryos were taken under 63X/1.4 oil and 10X/0.3 objectives, respectively, using Nikon DXM 1200F digital camera and ACT-1 software (Nikon).

CHAPTER III

THE FUNCTIONAL ANALYSIS OF INTS5

3.1 BACKGROUND

The C-terminal domain (CTD) of RNA polymerase II (RNAPII) is not only essential for transcription of protein-coding genes. A large body of data also implicates CTD in the transcription and processing of RNAPII-mediated small nuclear RNAs (snRNAs) (Egloff and Murphy, 2008; Egloff et al., 2007; Egloff et al., 2008; Uguen and Murphy, 2003). However, the identity of the protein (or complex) that associates with the CTD and mediates specific processing of snRNAs has remained elusive. Baillat *et al*. described an RNA polymerase II associated complex that contains at least 12 novel subunits, termed the Integrator (Int). Two of the Integrator subunits (Ints), Ints9 and Ints11 display similarities to the subunits of the cleavage and polyadenylation specificity factor (CPSF) complex (Baillat et al., 2005).

Baillat *et al*. also showed that the Integrator complex directly interacts with the C-terminal domain of the RNA polymerase II largest subunit and is recruited to the U1 and U2 snRNA genes where it mediates 3'end processing of the snRNA (Baillat et al., 2005).

3.2 IDENTIFICATION OF INTEGRATOR SUBUNITS

The Integrator complex is conserved in metazoans (Baillat et al., 2005). To study the function of these novel genes during embryogenesis, we have cloned several subunits of Integrator complex in zebrafish: Ints3, Ints5, Ints6, Ints7, Ints9, Ints10, Ints11, Ints12 (Table 3.1, Figure 3.1). The genomic locus of *ints5* has several gaps in the sequence assembly, so RACE (Rapid Amplification of cDNA Ends) was performed for cloning of *ints5*, whereas other genes were cloned into pCS2+ vector by PCR with primers designed

according to Ensembl sequence (Table 3.1, Section 2.2.1). It has been recently found that depletion of Integrator subunit 5 (Ints5) in the *Drosophila* germarium affects Decapentaplegic (Dpp, the homologue of vertebrate BMP) signaling activities, which in turn leads to failure in oogenesis (Cai et al., unpublished data). It is possible that the Integrator complex is required for proper BMP function during vertebrate development as well, so I got interested in studying the function of Integrator subunits, especially Ints5, and elucidating the link between Ints5 and BMP signaling during early development of zebrafish. Therefore, I focused on the function of Ints5 in zebrafish.

Zebrafish Ints5 shares about 53% similarity with its human orthologue and there is no known functional domain in the peptide sequence (Figure 3.1).

Table 3.1. The integrator complex is evolutionarily conserved

Protein name	**Synonyms**	***Similarity %**	**Ensembl accession number**
Ints1	DKFZp586J0619, KIAA1440, INT1	73%	ENSDARG00000059631
Ints2	KIAA1287, INT2	81%	ENSDARG00000076823
Ints3	si:dkey-27c15.2, INT3	83%	ENSDARG00000016811
Ints4	MGC16733, MST093, LOC564681, INT4	77%	ENSDARG00000063610
Ints5	KIAA1698, LOC564642, INT5	53%	ENSDARG00000077189

Ints6	ddx26b, INT6	67%	ENSDARG00000017931
Ints7	chunp6916, dkfzp434b168, hi1548, INT7	76%	ENSDARG00000019300
Ints8	C8orf52, FLJ20530, MGC131633, Kaonashi-1, zgc:111823, INT8	69%	ENSDARG00000057986
Ints9	cpsf3, INT9	87%	ENSDARG00000027649
Ints10	wu:fb96d03, wu:fi39h05, zgc:111853, zgc:136485, INT10	67%	ENSDARG00000043031
Ints11	zgc:110671, INT11	81%	ENSDARG00000025212
Ints12	zgc:86602, PHD finger protein 22, INT12	56%	ENSDARG00000009380

*** The percentage similarity of zebrafish Integrator subunits compared to human proteins.**

A

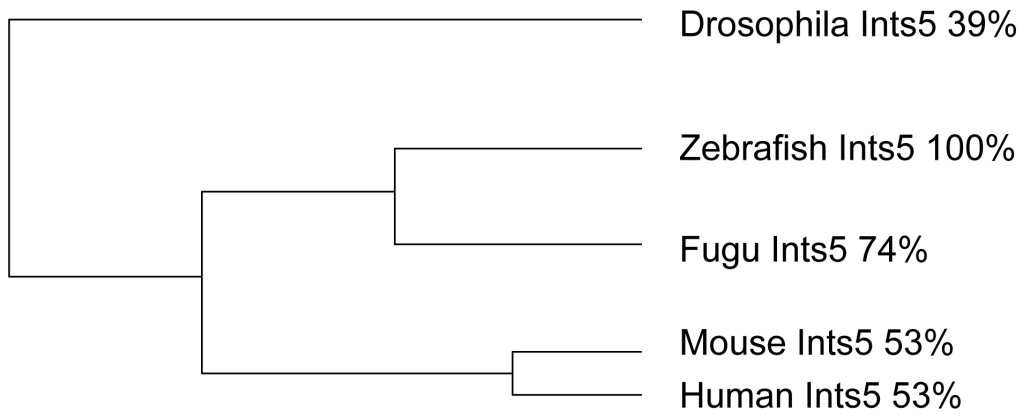

B

ACGAGAGCTTCCGGTGTCTGGTGCATCGTTCAATGAAACGGGGCTGAAACTGGTATAAGTTGTAAATAGTCAACTTTCCT
ATCATAAATCGACGTTGTTGTTGTTATTATTTATGGCAATATAATACTCTGCATGGAATATTTAGCGTAAGCTCATTAAA
GATGTCTGGGATGTTCGAGGGGAATGCCTTACCAGGCATACAAACTCATAGCCACACTCCAAACAATTACAGTCCTCAAG
AGCTGTCATTAGAAATCAAGGCTTTCATCAGTGGAGTCGACCAGACACAAGGACGTAAACTCAGTGTTCGGGATCATGCT
CGCTGTGCAATACGCCTCCTTCGAACTGTCCCAGCCTGCCGCGAAGCCGTCTTGGAGCATTTAAGGGGAGTGTATGATGA
ATACGTTGCTTCCTTTCTACAGGACCTGGAGGCAGAGGGTGAAAATGGTGGTAACAGTGCAAGTGGAGGAGCCAGCGTCA
GCATATCAAATTTAGAGGATGTTATTAAAGAAGTCCACGCAGTCCTCTCTGAATTTATCAAGCTGAGTCCGAAAGCTTGG
GCTCCCCTTGTGTCTAGCTGGGCTGTAGACCTCCTTGGTCAGCTTAGCAGCAAGCATGCAGGACGACGGGCTGCTCCTCA
CTCCTCCAGCCTGAATGAGCTGCTGCAGCTTTGGATGTCATGTGCAGCCACTCGCTCACTAATGGAGTGCTACTCCCAGT
GTCTAGCGGCCATGTTGGCCTGGTGTCCCGATGCATGTGTGGATGCCTTGTTGGACACCTCAGTCCAGCATTCTCCTCAT
TTTGACTGGGTCGTCGCCCATATTGGTTCTGCTTTTCCTGGTACTATCATTAGCAGGGTTTTAGCTTGTGGTCTCAAAGA
CTTCTATGCACACGGATATTCCTCTGCTGAGAAGATCAGCCAACAGCAGGCAATAGACAAGAGTAGCAGAGTCCCTAAAA
TTGGCTCAGTAGTTGGTATCCTTGGACACCTGGCCTCCAGACATTCAGATAGCATCAAGAAAGAGCTTCTCAGGATGTTT
CAGGACAGTCTGTCTGTGCCTCCACAAAATGTACCTCAGCTTACATCTGGAGCAGGTGGATGGGAAAATTCCCCTCATCT
CCGTAGGGCAACTGTACCATTCCTTCTTCAACTCGCTGCTCTTTCCCCAACTCTCCTTGGTGCCGTTTCTACAGAGCTTG
TTGAGTTTCTCAGACCACCTGTCCTAATTCAATTACAAGCCCAATTCCAGGCTTTGCCTCGGGAGGAGCTTGAGAATATG
CTGGGTCTAGCCGTGCACCTCATAAGCCAAAGCCCTTCAGGTGGAGCAAGAGTGCTGAAGTTTCTTGCAGACACGGCCAC
ACCCTCTTCAGTGATCATATCAGGTCCTACACCCTCTCCCCATGATGGTATTCGAGAGGCCTGTGACCGATTACTGCAAA
TGCTTCTGCTGCATCTTCACAAACTGGTGCACAACCGACCGGACGGTGATGAACCTTTTCCACAGTCCTCTACTTCTCCG
GCAATGCCCCAAGTGATCCCATTTCTTGAGGAGCTCCAGGCACACATTGCTGATCTGTGTGCTGAAACTCTTCGACTTGA
GAGGAAGCGGCACCTTTGGTTGCACCAGCTCCTGTGTCTGCTGTCAGTCTATGGTGGCCCAAGCATAGCCACTGAAGCTT
TATGCCAGCTCTTCACTCAAGCCCGAAATCCAGAGGAGCTTGCATTGGCCTCGCAATTATACACCCAACTTTCCACTTCA
CTTTCCGGTTTGCTACCCTCAACAGTAGCCCGCTGTGTTGCTCAGATCCACACACAAACTCTTGATATCAAAGAGTTAGC
TCAGCTGCTGAATAACCTGGCTACTGCGGTACAGAGTCAAGAGGAGGATGGAAAAAATGGAGGAGGAACAACAACAACAA
CGGGTAGTTTAACACAGTCTTCAATGGCTTCAGAAGTCAGAGTTGCCGTGTCCAGCAACCTTCAGGATTTCTGTCCATTA
CTGCTTCATGGGGATTCAGGGGTATCCAAAGCGGCTGTCCGACTTCTCTCATGTAGCCAGATTCCCAGAGCGTGCTCTCC
AGCTCATCTGTTGCGGATATGTAGAGCTGCGGTGTCGCACTTCTTTGTGTGTTTACGACAACAAGGGAAGAGTCCTCAAG
CAGGCCAAGAGGAAGTAGGCTACTCCAGGCGACTCTTATCACGTCTTGCGGCTTATTCTTCTTTGTCGCAAAAAGCTGTG
CTTCAACAACTGGTGGAGGGAGCTCTACATAAAGGCAACCAAGATTTATTTGGAGGTCTGCAAGAGAACCCAAGTGATGA
CACCACACAGGCCCAAAACCTCGTCCCAGACTTGGGCATCTCCTTATTGGACGTCAACCGCAAATTTGGCACCTCAGTTA
ACTTCTCTGGAAACGTGTGGTCTGTTTTCCACGCTGGAATAATCGGAAAGGGTTTGAAGCCTCCATATACTCCCTTACAT
CCTGACCCAGATCGAGTCAGTCAGAATATGCAGACCTTGCTTGCGGTCATGGTTCAGTGCTGCAGCTCAAGTGGAGGAAA
CCCTACTGGTTCTGCTGGCAGTACTTGTAGTGAACCTAATGTTTCTGATAAACTCCCACCAATCAATGCTGAAGCTGCAA
AGGTAATTGCCGTAACTCTTGTGGAGAATATATGCCCAGATGTGGCAAACGGAGAACTTTCCTGGCCTCCAGAGGAACAT
TCAAAAACCACAGTTGAGCGAGACATACACATTCGTCGTTGCTTCGAAAAAAACCCTGTGCTATTTTACCTCCTCCATGT
GGTCGCAGCTGGACGTCCAGCGCTGTGCTATTGCTCTGTCATTTTAAGGGCTCTACTTTCCACCTTACTGGCTCACTGGG
AGTCCTCAAGGGAGCCGTCGGTGTCTGACTCCCCCTGGCACCTTCAAACTTCCTGTTGGCTTGTATCATGTATGGGTGAA
GGTCAGCTACTTCCTCCAGTCTTGAGTAATATCAATGAGGTCTTCCCTCACCTCTCGCCCTTTGAGGTTCGGCTGCTGCT
GTTGGGTGTATGGGAGTATATGCGAGGGAACAGCCCAATGCCACAGAAATTTACCTTCTGTGCAGACCAGGGACTTTTCT
TTCGGGACTTTTCACGTGATGGAGATGTTGCACGCTATATTGCGCCCATCCACAGCGTTCTGCATAAAAACATTGACCGA
TTGGGACACCTGTGCTGGAGGTTTCAAGTTTGATGACTGAAAAAATATTAGAAGATGTGTTGCAAACATGAATTTCTTTC
AGGGTCACATACCTTTTCGGATTTAGATATTTTTCTACTTTGTTGTGTGTTGTAAACTTGACATCTGAAGTTGACATTTC
TACATTTTTAAAAGTTATCAATGTTAAAAAACCTT

C

MSGMFEGNALPGIQTHSHTPNNYSPQELSLEIKAFISGVDQTQGRKLSVRDHARCAIRLLRTVPACREAVLEHLRGVYDE
YVASFLQDLEAEGENGGNSASGGASVSISNLEDVIKEVHAVLSEFIKLSPKAWAPLVSSWAVDLLGQLSSKHAGRRAAPH
SSSLNELLQLWMSCAATRSLMECYSQCLAAMLAWCPDACVDALLDTSVQHSPHFDWVVAHIGSAFPGTIISRVLACGLKD
FYAHGYSSAEKISQQQAIDKSSRVPKIGSVVGILGHLASRHSDSIKKELLRMFQDSLSVPPQNVPQLTSGAGGWENSPHL
RRATVPFLLQLAALSPTLLGAVSTELVEFLRPPVLIQLQAQFQALPREELENMLGLAVHLISQSPSGGARVLKFLADTAT
PSSVIISGPTPSPHDGIREACDRLLQMLLLHLHKLVHNRPDGDEPFPQSSTSPAMPQVIPFLEELQAHIADLCAETLRLE
RKRHLWLHQLLCLLSVYGGPSIATEALCQLFTQARNPEELALASQLYTQLSTSLSGLLPSTVARCVAQIHTQTLDIKELA
QLLNNLATAVQSQEEDGKNGGGTTTTTGSLTQSSMASEVRVAVSSNLQDFCPLLLHGDSGVSKAAVRLLSCSQIPRACSP
AHLLRICRAAVSHFFVCLRQQGKSPQAGQEEVGYSRRLLSRLAAYSSLSQKAVLQQLVEGALHKGNQDLFGGLQENPSDD
TTQAQNLVPDLGISLLDVNRKFGTSVNFSGNVWSVFHAGIIGKGLKPPYTPLHPDPDRVSQNMQTLLAVMVQCCSSSGGN
PTGSAGSTCSEPNVSDKLPPINAEAAKVIAVTLVENICPDVANGELSWPPEEHSKTTVERDIHIRRCFEKNPVLFYLLHV
VAAGRPALCYCSVILRALLSTLLAHWESSREPSVSDSPWHLQTSCWLVSCMGEGQLLPPVLSNINEVFPHLSPFEVRLLL
LGVWEYMRGNSPMPQKFTFCADQGLFFRDFSRDGDVARYIAPIHSVLHKNIDRLGHLCWRFQV.

Figure 3.1 Ints5 is evolutionarily conserved. (A) The phylogenetic tree of Ints5. (B) Full cDNA sequence of zebrafish *ints5*. The translation start site is shown in yellow, splice site in red. The sequence of 5'and 3' UTRs is in light blue. (C) Peptide sequence of zebrafish Ints5.

3.3 THE EXPRESSION OF INTS5 TRANSCRIPTS

We choose to study the function of Integrator subunit 5 during zebrafish embryogenesis. Whole Mount In Situ Hybridization (WISH) with labeled anti-sense RNA probes shows that *ints5* transcript is expressed both maternally and zygotically (Figure 3.2). As shown in figure 3.2, *ints5* transcripts can be detected immediately after fertilization, in the whole blastodisc of a one-cell stage embryo (Figure 3.2A), preceding the onset of zygotic transcription at mid-blastula transition (MBT). The distribution of *ints5* transcript is ubiquitous during cleavage and gastrulation stages (Figure 3.2B, C). During somitogenesis (Figure 3.2D), *ints5* transcripts persist, with expression noticeably stronger in the anterior region of the embryo. In contrast, WISH with control sense RNA probes does not show any staining in the embryos at comparable stages (Figure 3.2E-H). The presence of maternal and zygotic *ints5* transcripts at various stages was further confirmed by RT-PCR, using oligo dT-primed cDNA templates (indicated by 150 bp fragments in Figure 3.2I).

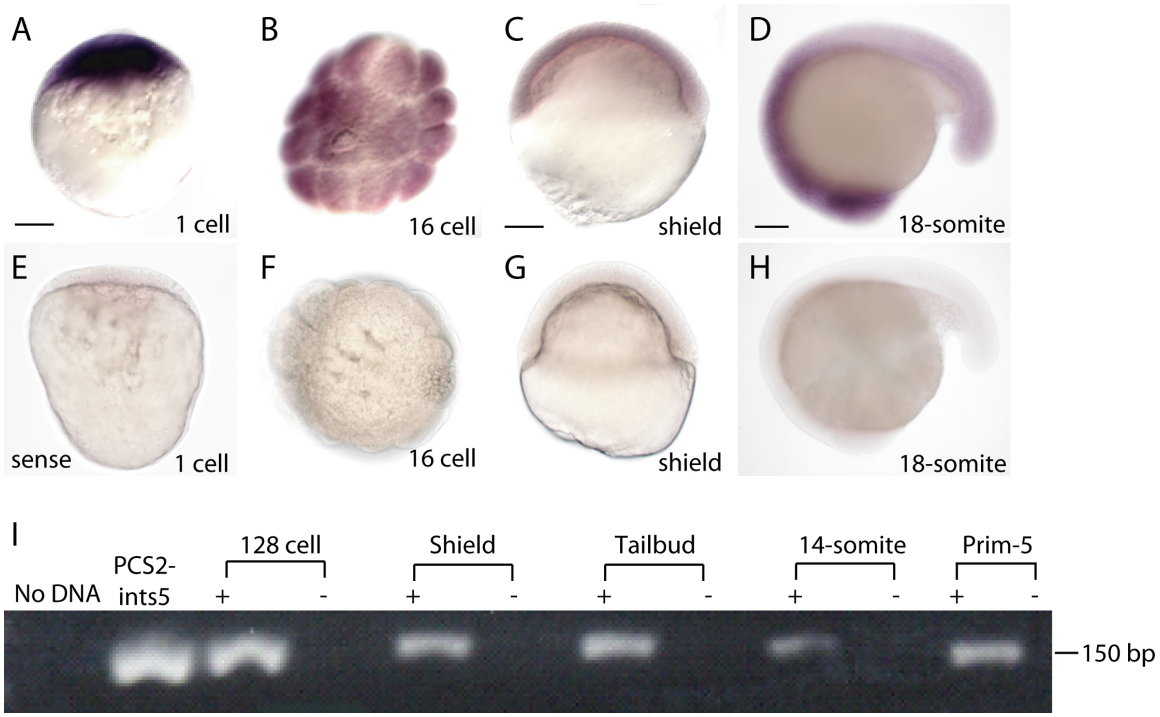
A
1 cell
B
16 cell
C
shield
D
18-somite
E
sense
1 cell
F
16 cell
G
shield
H
18-somite
I
No DNA
PCS2-ints5
128 cell
Shield
Tailbud
14-somite
Prim-5
+ - + - + - + - + -
150 bp

Figure 3.2 Ints5 is expressed both maternally and zygotically in zebrafish embryos. (A-D) Whole mount *in situ* hybridization to detect *ints5* expression in wild type (WT) embryos at various stages. (E-H) WT embryos hybridized with control *ints5* sense strand probe. (A, C-E, G, H) Lateral views of embryos. (B, F) animal pole views. (I) RT-PCR shows *ints5* RNA expression at various embryonic stages. Scale bars in (A, C) 50μm, in (D) 100μm.

3.4 KNOCK-DOWN OF INTS5 BY ANTI-SENSE MORPHOLINOS

The *ints5* locus consists of two exons and one 2.6kb intron. To investigate the function of Ints5 during early zebrafish development, I knocked down Ints5 function using anti-sense morpholinos. Two anti-sense splice-junction morpholinos were designed to target the intronic splice donor and acceptor sites of the *ints5* transcirpts (Figure 3.3A). In *ints5* morphants, reverse transcription–PCR (RT-PCR) analysis with primer pair 1 and 4 shows the presence of aberrantly spliced *ints5* transcripts (Figure 3.3B). PCR with primer pairs 1 and 3 and 2 and 4 also shows accumulation of non-spliced *ints5* transcripts in embryos injected with *ints5* splice-junction morpholinos (Figure 3.3B). Sequence analysis of the PCR products indicates that in the morphants, the correct exon/intron boundary is not chosen and instead, a cryptic site in exon1 of *ints5* transcript is used. This leads to the production of incorrectly spliced *ints5* transcripts lacking 170 bp of the coding sequence (Figure 3.3C). Therefore, the splice-junction morpholinos indeed disrupt the correct processing of *ints5* transcripts.

Western blot analysis using antibodies to detect Int5 protein (110 kDa) in embryo extracts shows that the *ints5* morpholinos abolish the synthesis of Ints5 proteins, whereas injection of *ints5* RNA leads to high Ints5 protein levels in injected embryos (Figure 3.4). The expression of control α-tubulin protein is not altered in the same embryo extracts (Figure 3.4).

By 24 hours post fertilization (hpf), embryos injected with *ints5* splice-junction morpholinos show severe defects, with a shortened anterior-posterior axis and no circulating blood cells (Figures 3.5B, 3.9J), in contrast to control morpholino injected

embryos (Figure 3.5A). These phenotypes are rescued by co-injecting *ints5* RNA with the *ints5* splice-junction morpholinos (Figure 3.5C).

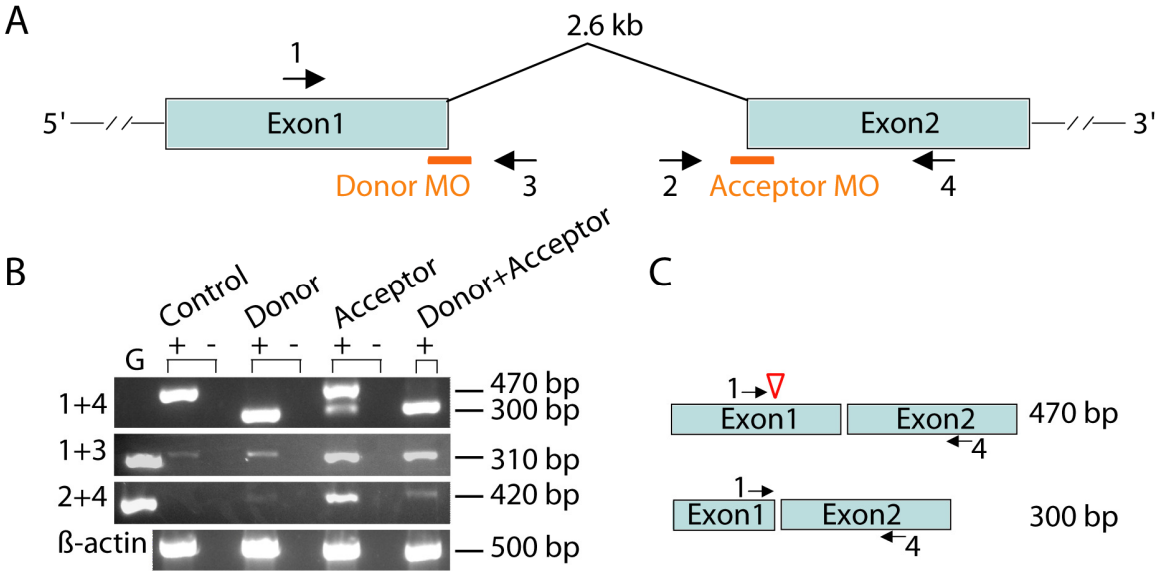
A
2.6 kb
1
5'
Exon1
Exon2
3'
Donor MO
3
2
Acceptor MO
4
B
Control
Donor
Acceptor
Donor+Acceptor
G
+ - + - + - +
1+4
1+3
2+4
ß-actin
470 bp
300 bp
310 bp
420 bp
500 bp
C
1
Exon1
Exon2
4
470 bp
1
Exon1
Exon2
4
300 bp

Figure 3.3 Knockdown of *ints5* with anti-sense splice morpholinos.

(A) Schematic representation of the *ints5* genomic locus. Two orange bars indicate target sites of the donor and acceptor morpholinos. Numbered black arrows show the position of primers used in RT-PCRs (B) to examine whether the splicing of *ints5* RNA has been disrupted. (B) RT-PCRs to detect splicing of *ints5* and control *β-actin* RNA from sphere stage (4 hours post fertilization, 4 hpf) embryos injected with control or *ints5* donor and acceptor morpholinos at one-cell stage. (C) Schematic representation of the correctly spliced (upper) and aberrantly spliced (lower) *ints5* transcripts. The sizes of the fragments amplified by primer pair 1 and 4 are indicated on the right. The red open arrowhead indicates the position of a cryptic splice site in exon1.

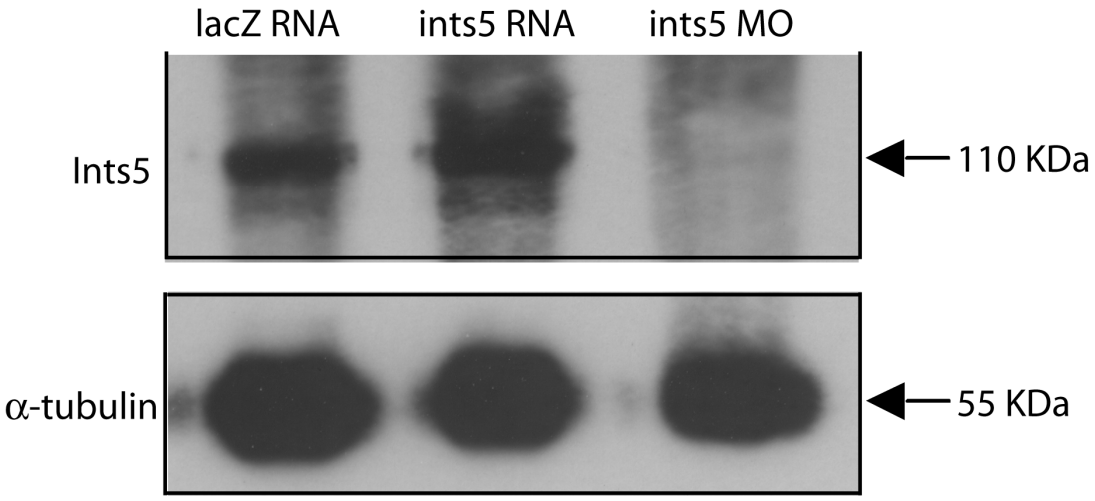
lacZ RNA
ints5 RNA
ints5 MO
Ints5
110 KDa
α-tubulin
55 KDa

Figure 3.4 Ints5 morpholinos abolish Ints5 protein in embryos.

Western blots on extracts of embryos injected with *lacZ* RNA, *ints5* RNA or *ints5* morpholinos. Proteins of each sample were harvested from 20 injected embryos at 8 hpf. Ints5 proteins were detected by using rabbit anti-Ints5 antibody (Bethyl Laboratories) (upper panel); the lower panel shows expression of α-tubulin control detected using anti-α-tubulin antibodies (Sigma). Black arrows indicate the size of each protein.

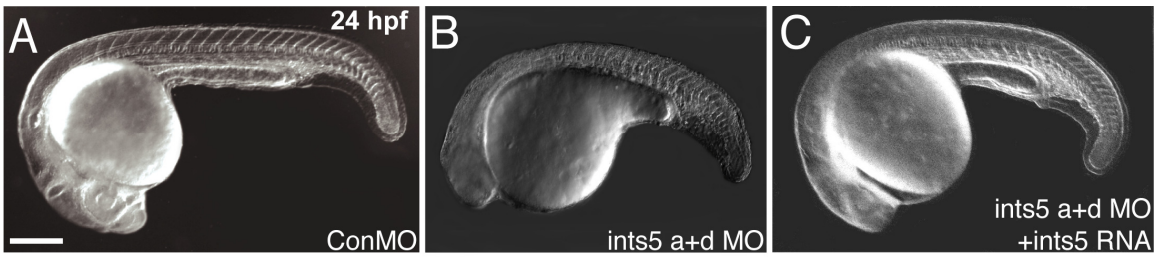
A
24 hpf
ConMO
B
ints5 a+d MO
C
ints5 a+d MO
+ints5 RNA

Figure 3.5 Knockdown of *ints5* leads to abnormal development of zebrafish embryos.

(A-C) DIC images of live embryos injected with control morpholinos (A), *ints5* acceptor and donor morpholinos (B) or co-injected with *ints5* morpholinos and *ints5* RNA (C).

3.5 ANALYSIS OF GERM LAYER GENE EXPRESSION IN INTS5 MORPHANT EMBRYOS.

Although live embryos injected with *ints5* splice-junction morpholinos look stubby (Figure 3.5B), their general dorso-ventral axis formation seems normal. To further examine the effect of knocking-down *inst5* on dorso-ventral axis and germ layer specification, we applied WISH with various markers on morpholino-injected embryos at different gastrula stages (Figures 3.6, 3.7).

3.5.1 Expression Of Dorsal-Ventral Markers In *ints5* Morphant Embryos

In lower vertebrate, maternally deposited determinants lead to the establishment of the dorsal axis and the organizer. One of the essential organizer factors is Nodal. Nodal related proteins serve as mesoderm and endoderm inducers. The organizer seems to pattern the dorsal cell fate primarily by opposing morphogenetic activities of BMPs from the ventro–lateral regions of the embryo. There are a number of molecular markers involved in this event, such as, *goosecoid* (*gsc*) and *chordin* (*chd*) on the dorsal side and *even-skipped 1*(*eve1*) on the ventral side (De Robertis et al., 2001; Joly et al., 1993; Schier and Talbot, 2005).

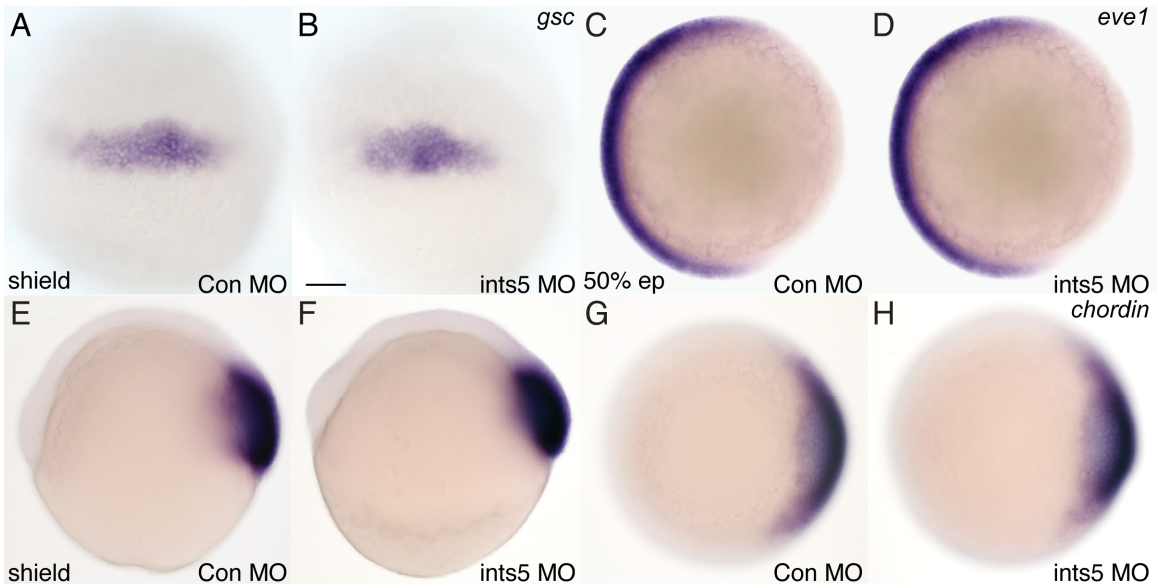
A
shield
Con MO
B
gsc
ints5 MO
C
50% ep
Con MO
D
eve1
ints5 MO
E
shield
Con MO
F
ints5 MO
G
Con MO
H
chordin
ints5 MO

Figure 3.6 Knock-down of *ints5* does not affect dorso-ventral patterning.

(A-H) Whole mount *in situ* hybridization to detect expression of *goosecoid* (*gsc*) (A, B), *even-skipped 1* (*eve1*) (C, D) *chordin* (E-H), at sheild (6 hpf) or 50% epiboly (5.3 hpf) stage. Embryos are injected with control (A, C, E, G) or *ints5* morpholinos (B, D, F, H). Scale bars in (B), 50 μm. (A, B, E, F) lateral view, (C, D, G, H) animal pole view.

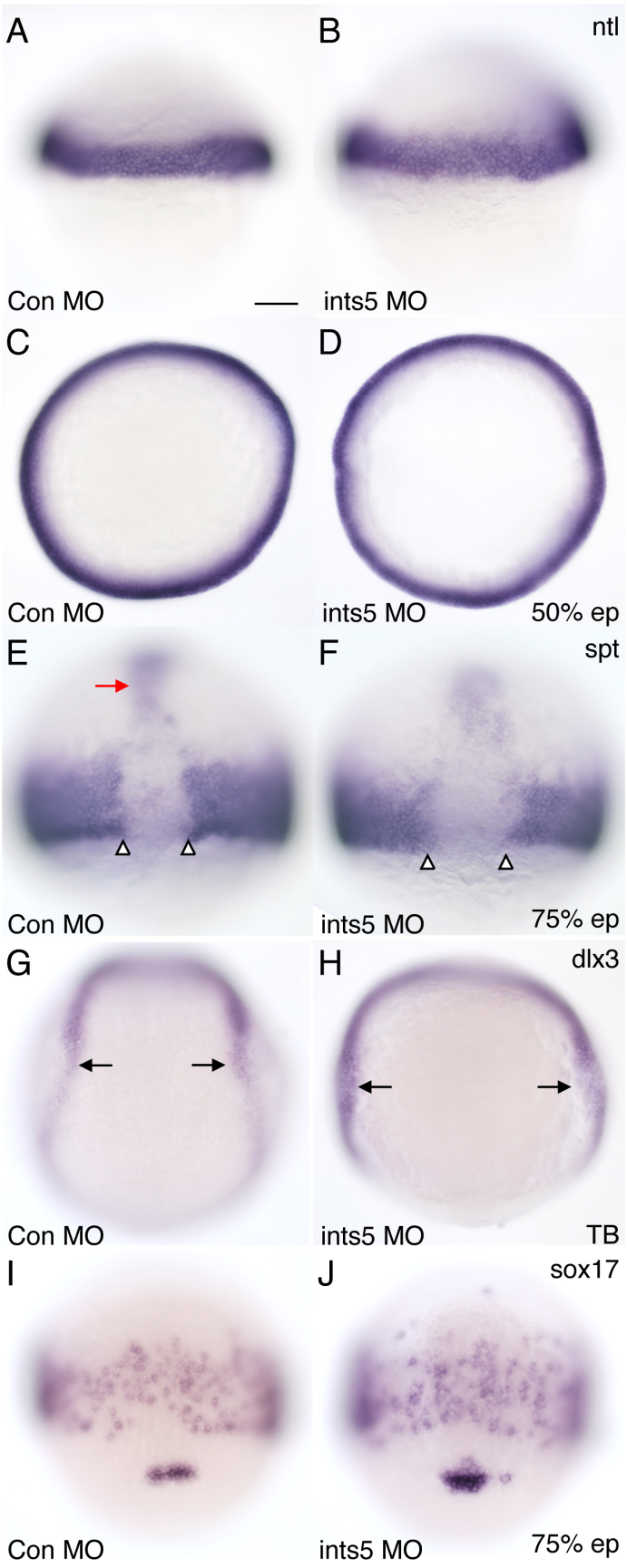
A
B
ntl
Con MO
ints5 MO
C
D
Con MO
ints5 MO
50% ep
E
F
spt
Con MO
ints5 MO
75% ep
G
H
dlx3
Con MO
ints5 MO
TB
I
J
sox17
Con MO
ints5 MO
75% ep

Figure 3.7 Knockdown of *ints5* does not affect germ-layer specification.

(A-J) Whole mount *in situ* hybridization to detect expression of *no tail* (*ntl*) (A-D) and *spadetail* (*spt*) (E, F), at 50% epiboly (5.3 hpf), and 75% epiboly (8 hpf) respectively. Embryos are injected with *ints5* morpholinos (B, D, F), or control morpholinos (A, C, E). Open arrowheads in (E, F) indicate the distance between *spt* positive cells in the midline. The red arrow indicates the head mesoderm. (G-J) Expression of *dlx3* (G, H) in the neural plate boundary at tailbud stage (TB, 10 hpf), and *sox17* (I, J) in the endoderm of 75% epiboly embryos injected with *ints5* morpholinos (H, J) or control morpholinos (G, I). Black arrows in G, H mark the distance between the boundary of *dlx3* expression. (A, B) lateral view of embryos with animal pole to the top; (C, D) animal pole view. (E-J) dorsal view of embryo with animal pole to the top. Scale bars in (A), 50 μm.

goosecoid (*gsc*), homeobox-containing gene, is a direct target of Nodal signaling pathway which induces dorsal cell fates (Toyama et al., 1995). *gsc* transcripts accumulate after the midblastula transition at the margin of the blastoderm. Its expression increases during the beginning of epiboly, and at the onset of gastrulation, *gsc* transcripts are observed in the deep cell layer of the margin. As gastrulation begins, all *gsc*-expressing cells invaginate and form the central part of the embryonic shield (Figure 3.6A). After 70% epiboly, these cells will become the leading edge of the mesendoderm, the prechordal plate (Thisse et al., 1994). Chordin is secreted by dorsal organizer and functions as a BMP antagonist, and its expression is restricted at the dorsal side of the embryo (Figure 3.6E, G) (Wagner and Mullins, 2002). The homeobox gene zebrafish *eve1* is a member of *even-skipped* (eve) gene family. During gastrulation, *eve1* transcripts are confined to ventral and lateral cells of the marginal zone of the embryo (Figure 3.6C). Later, eve1 is expressed in the most posterior part of the tail bud during somitogenesis. In LiCl-treated dorsalized embryos, eve1 transcripts are completely absent, suggesting that *eve1* marks the specification of ventral mesoderm in zebrafish gastrulae (Joly et al., 1993).

As zebrafish embryos with mutations in a number of genes that affect dorso-ventral patterning usually have altered *gsc*, *chordin*, *eve1* expression (Joly et al., 1993; Miller-Bertoglio et al., 1997; Stachel et al., 1993; Thisse et al., 1994; Wagner and Mullins, 2002), we examined expression of these genes in *ints5* morphants at mid-gastrulation stages. In *ints5* morpholino injected embryos, expression of *gsc* (Figure 3.6B), *chordin* (Figure 3.6F, H) and *eve1* (Figure 3.6D) is normal and not altered in either expression level or distribution, similar to that of control morpholino injected embryos (Figure 3.6A,

C, E, G). Thus, the early dorso-ventral patterning is not perturbed by knocking-down *ints5*.

3.5.2 Expression Of Germ Layer Markers In *ints5* Morphant Embryos

I also examined the patterning of the three germ layers by monitoring the expression of *no tail* (*ntl*) and *spadetail* (*spt*) in mesoderm, *distal less 3* (*dlx3*) in ectoderm and *sox17* in endoderm of the embryos (Figure 3.7).

For mesoderm development in the mouse, the *T* or *Brachyury* gene is crucial. Embryos homozygous for the mutation *T* fail to produce sufficient mesoderm and lack all posterior structures. Most strikingly, they lack the entire notochord (Gluecksohn-Schoenheimer, 1944; Yanagisawa et al., 1981). Similarly, in zebrafish, expression of the T-box gene *ntl* is first detected at dome stage in a restricted ring-like area, the marginal zone of the blastoderm (Schulte-Merker et al., 1992). In concert with movements of convergence and extension, *ntl* expression domain converges towards the midline and extends along the embryonic axis. By the end of gastrulation, *ntl* expression occurs in the midline axis which later will give rise to the presumptive notochord (Schulte-Merker et al., 1992).

Another T-box transcription factor gene, *spt*, is required for non-notochordal trunk mesoderm formation. Homozygous *spt* mutant embryos have major trunk mesoderm deficiencies, but relatively normal tail and notochord development. Trunk and tail development are therefore dependent upon the complementary actions of two T-box genes, *spadetail* and *no tail* (Griffin et al., 1998). Expression of *spt* is first detected between sphere and dome stages where it is initially ubiquitous. By early gastrula stage, *spt* expression becomes rapidly restricted to marginal cells (Griffin et al., 1998). After shield stage, *spt* is not expressed in the notochord progenitors, whereas lateral and ventral

germ ring and head mesoderm (red arrow) express *spt* (Figure 3.7E).

In *ints5* morpholino injected embryos, expression of *ntl* (Figure 3.7B, D) and *spt* (Figure 3.7F) is normal, and staining is not altered in intensity or extent, similar to that of control morpholino injected embryos (Figure 3.7A, C, E). However, there is a wider gap (open arrow heads in Figure 3.7E, F) in the *spt* expression in the midline. This may indicate defective cell movements towards the dorsal (convergence). The patterning of mesoderm *per se* is not disturbed by knocking-down *ints5*.

For the proper development of ectoderm in *Xenopus* and mouse, a homeodomain transcription activator Distal less 3 (Dlx3) plays important roles (Beanan and Sargent, 2000). In zebrafish, *dlx3* transcription begins during gastrulation, defining a narrow band of cells at the lateral boundary of the presumptive neural plate (Akimenko et al., 1994). In *ints5* morpholino injected embryos, expression pattern of *dlx3* (Figure 3.7H) is generally normal and comparable to control embryos (Figure 3.7G). Although, the specification of ectoderm is not disturbed by knocking-down of *ints5*, the distance between the boundaries of *dlx3* expressing cells become much larger in *ints5* morphant at the end of gastrulation (indicated by black arrows in Figure 3.7G, H). This phenotype once again shows the impaired convergence-extension cell movement induced by knocking-down of *ints5*.

Similarly, the patterning of endoderm was examined based upon the expression of the endoermal marker gene *sox17*. Zebrafish Sox17 protein is highly related to mouse Sox17 and Xenopus Xsox17a and Xsox17b, which are important intrinsic regulators of endoderm formation and contain a high motility group (HMG) DNA binding domain (Alexander and Stainier, 1999; Hudson et al., 1997; Kanai et al., 1996). *sox17* is first

detected in the non-involuting forerunner cells at the onset of gastrulation. Soon thereafter, *sox17* is expressed in the endodermal precursors and this expression continues throughout gastrulation. At 75% epiboly, *sox17* expression in *ints5* morphant is almost the same as in control embryos (Figure 3.7I, J). This suggests that the specification of endoderm is not affected in embryos injected with *ints5* morpholinos.

In summary, the patterning of three germ layers: mesoderm, ectoderm and endoderm is unaffected when *ints5* is knocked-down in zebrafish embryo. Furthermore, the expression of different markers also indicates that the anterior-posterior axis is largely normal.

3.6 CONVERGENT-EXTENSION CELL MOVEMENTS ARE IMPAIRED IN INTS5 MORPHANTS

At 24 hpf, embryos injected with *ints5* splice-junction morpholinos show shortened body axis (Figure 3.5B) and in gastrulating embryos, the distance between the boundaries of *spt* or *dlx3* positive cell are enlarged (Figure 3.7F, H), in comparison to control morpholino injected embryos (Figures 3.5A, 3.7E, G). These phenotypes indicate multiple defects in convergent-extension (CE) cell movements during gastrulation. To characterize the CE movement defects, I performed bi-color WISH to monitor the expression of *hgg1*, *ntl* and *dlx3*. The *hgg1*-expressing cells are the most anterior migrating mesendoerm cells, which will later give rise to the hatching gland. The expression of *ntl* marks the migrating mesendoderm cells in the midline and *dlx3* expression marks the boundary of the neural plate (Akimenko et al., 1994; Schulte-Merker et al., 1992; Thisse et al., 1994).

We observed retarded convergence, marked by the increased distance between *dlx3*

positive cells at the dorsal side, and impaired anterior extension marked by position of *hgg1* positive cells (Figure 3.8B, C) and anterior limit of *ntl* expressing cells in more than 80% embryos (Figure 3.8E, F, H, I). Some embryos (Class II) show more severe convergent-extension defects than others (Class I), referring to the bigger distance between *dlx3* positive cells (marked by dashed lines) and larger gap between animal pole and the anterior limit of *ntl* expression (marked by black arrowheads). These cell movement defects can be rescued by co-injecting *ints5* RNA, where over-expression of *ints5* RNA itself into wild type embryos does not cause CE defects (Figure 3.8 J). Since the expression of different germ layer markers suggests that anterior-posterior patterning is largely normal (Figures 3.6 and 3.7), the shortened axis in *ints5* morphant embryos is likely due to impaired CE cell movements. Therefore, Ints5 is required for proper convergent-extension cell movements during gastrulation.

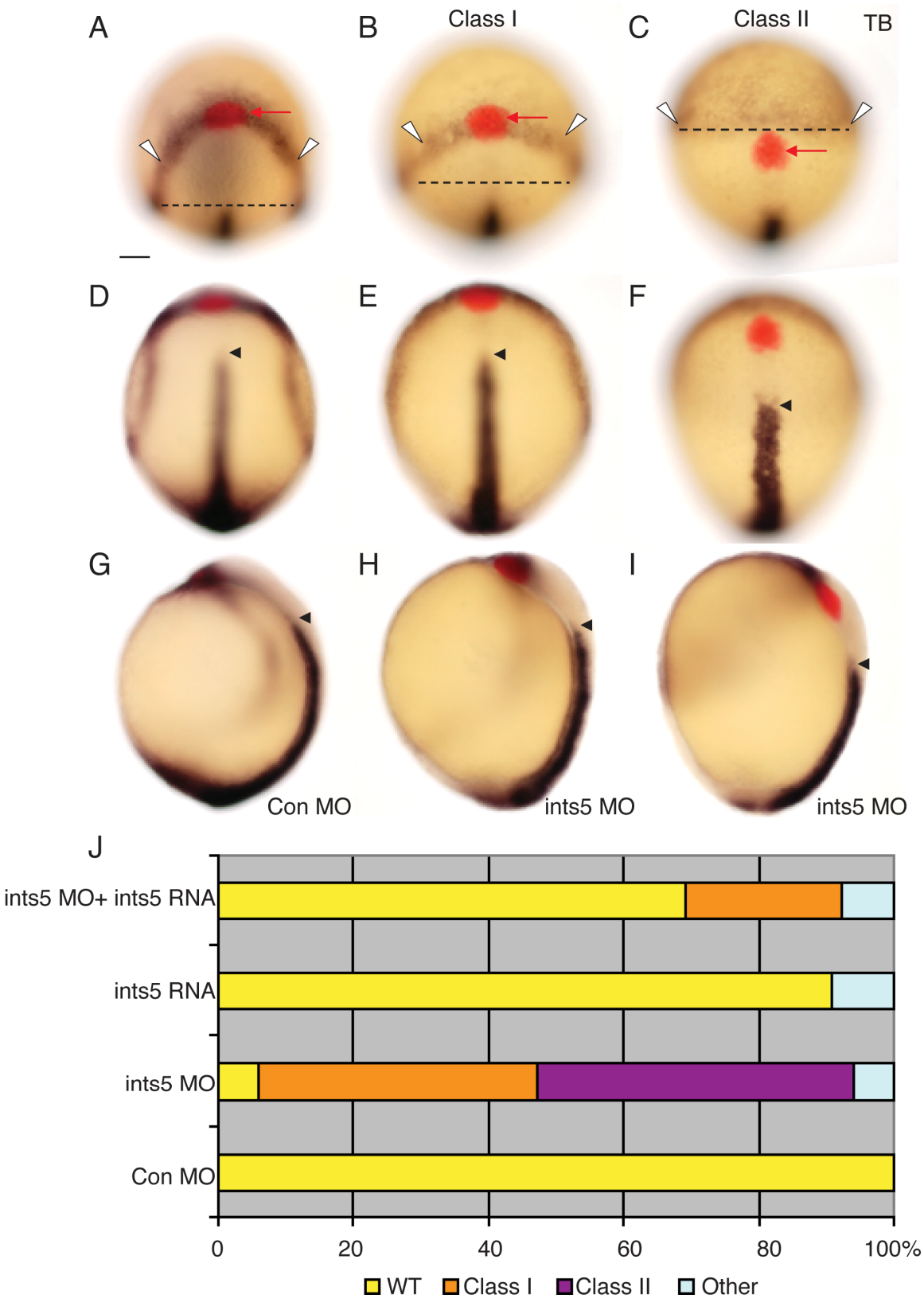
A
B
Class I
C
Class II
TB
D
E
F
G
H
I
Con MO
ints5 MO
ints5 MO
J
ints5 MO+ ints5 RNA
ints5 RNA
ints5 MO
Con MO
0
20
40
60
80
100%
WT
Class I
Class II
Other

Figure 3.8 Knockdown of *ints5* leads to convergent-extension defects during gastrulation.

(A-I) Whole mount in situ hybridization to detect *ntl*, *dlx3* and *hgg1* expression in tailbud (TB, 10 hpf) embryos injected with control morpholinos (A, D, G), *ints5* morpholinos (B, C, E, F, H, I). Black arrowheads indicate the anterior limit of *ntl* expression in the midline, and red arrows indictae *hgg1* staining in the anterior prechordal plate mesendoderm cells. White arrowheads and dotted lines indicate the distance between the lateral limits of *dlx3* expression in the neuroectoderm. (A-C) animal pole views of embryos, (D-F) dorsal views of embryos, (G-I) lateral views of embryos with dorsal to the right.

(M) Histogram showing percentage of injected embryos with wildtype (WT, blue) or impaired (magenta, Class I and yellow, Class II) cell movement marked by *ntl/dlx3/hgg1* expression. Scale bar in (A) and (B), 50 μm.

3.7 KNOCK-DOWN OF INTS5 LEADS TO DEFECTIVE HEMATOPOIESIS.

Since live *ints5* morphant embryos at 24 hpf lack circulating blood, we did two different types of analyses to check whether hematopoiesis is affected by the knock-down of *ints5*.

3.7.1 Ints5 Is Required For Proper Expression Of Hematopoietic Genes.

First, we examined the expression of the hematopoietic genes *stem cell leukemia* (*scl*) and *gata1* by WISH (Detrich et al., 1995; Gering et al., 1998). Expression of *scl* transcripts is severely reduced in *ints5* morphants (Figures 3.9C, D, 3.11B) in comparison to control morphants (Figures 3.9 A, B, 3.11A). In contrast, the adjacent *pax2a* expressing pronephric cells are not affected in *ints5* morphants (Figure 3.11 A, B) (Majumdar et al., 2000).

ints5 morpholino injected embryos have impaired cell movement, and usually grow slower during gastrulation and somitogenesis. To rule out the possibility that their delayed development account for the reduced *scl* expression, we fixed both control and *ints5* morpholino injected embryos at the same stage, 6-somite stage and performed bi-color WISH with *scl* and *myoD* on the stage-matched embryos (Weinberg et al., 1996). The anterior limit of *scl* expression aligns with the anterior somite (marked by *myoD*) in controls (Figure 3.11C), whereas in *ints5* morphants, the anterior limit of major *scl* expression domain aligns with the most posterior somite (Figure 3.11D). Thus, the defects seen in the *ints5* morphants are not due to developmental delay, but rather due to a lack of the anterior *scl* expression domain.

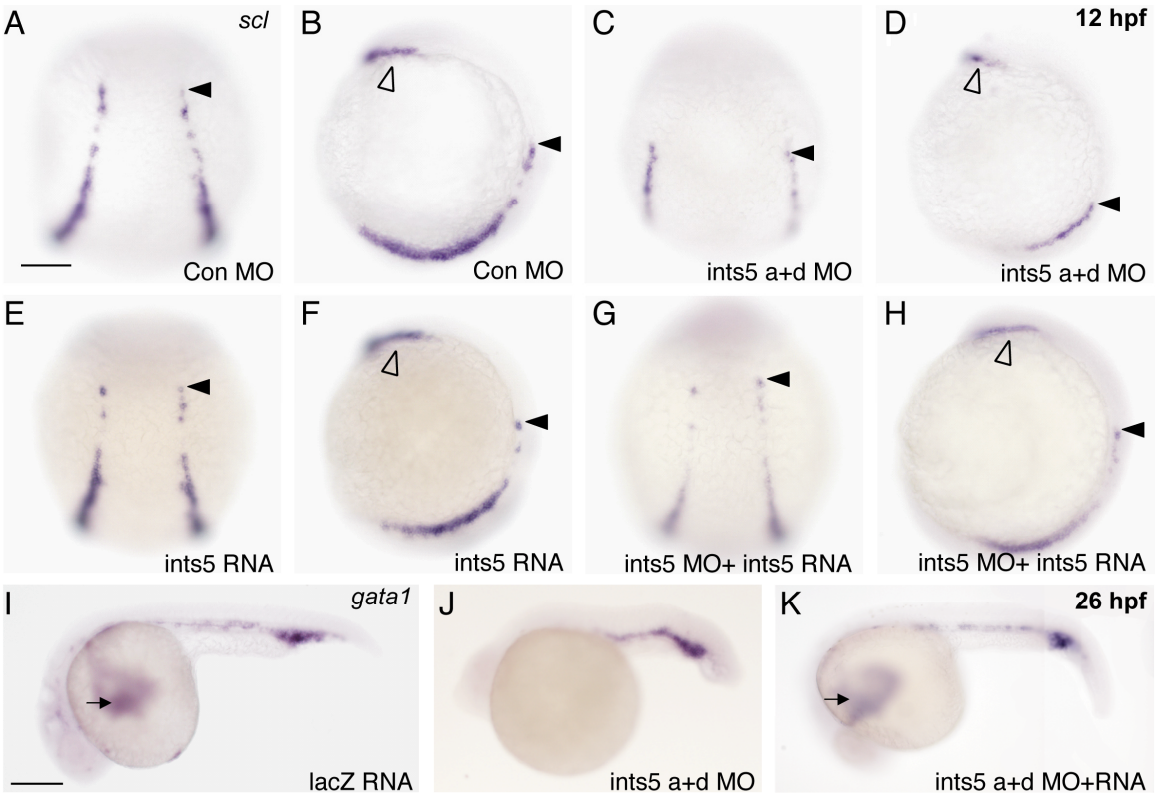
A
scl
Con MO
B
Con MO
C
ints5 a+d MO
D
12 hpf
ints5 a+d MO
E
ints5 RNA
F
ints5 RNA
G
ints5 MO+ ints5 RNA
H
ints5 MO+ ints5 RNA
I
gata1
lacZ RNA
J
ints5 a+d MO
K
26 hpf
ints5 a+d MO+RNA

Figure 3.9 Knockdown of *ints5* leads to reduced expression of hematopoitic genes.

Whole mount *in situ* hybridization to detect expression of *scl* (A-H) at 12 hpf and *gata1* (I-K) at 26 hpf in *ints5* morphants (C, D, J), and control morpholino (A, B) or lacZ RNA (I) injected embryos. Co-injection of *Ints5* RNA can restore *scl* and *gata1* expression in *ints5* morphants (G, H, K), whereas embryos injected with *ints5* RNA alone show normal *scl* expression at 12 hpf (E, F). The black arrowheads indicate the anterior limit of *scl* expression in the intermediate cell mass (ICM), the open arrowheads indicate *scl* expression in rostral blood island (RBI) and black arrows indicate anterior *gata1* expression, which represents the circulating blood cells. (A, C, E, G) show dorsal views of embryos with the anterior to the top. (B, D, F, H) show lateral views of embryos. (I-K) show lateral views of embryo with anterior to the left. Scale bars in (A), 50 μm and in (I), 250μm.

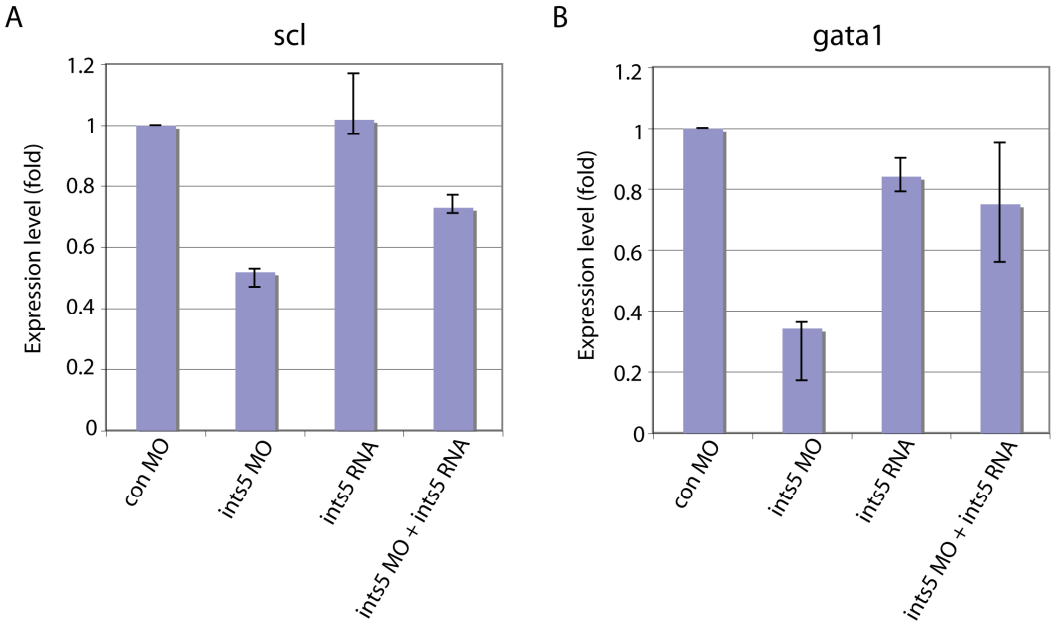
A
scl
Expression level (fold)
1.2
1
0.8
0.6
0.4
0.2
0
con MO
ints5 MO
ints5 RNA
ints5 MO + ints5 RNA
B
gata1
Expression level (fold)
1.2
1
0.8
0.6
0.4
0.2
0
con MO
ints5 MO
ints5 RNA
ints5 MO + ints5 RNA

Figure 3.10 Ints5 regulates hematopoietic gene expression.

Histograms to show expression level of *scl* (A), and *gata1* (B) in injected embryos. Expression levels were measured at 12 hpf by semi-quantitative RT-PCR, normalized with respect to the level of *β-actin* internal control, and shown as fold-change relative to control embryos. Data were obtained from three independent injection experiments.

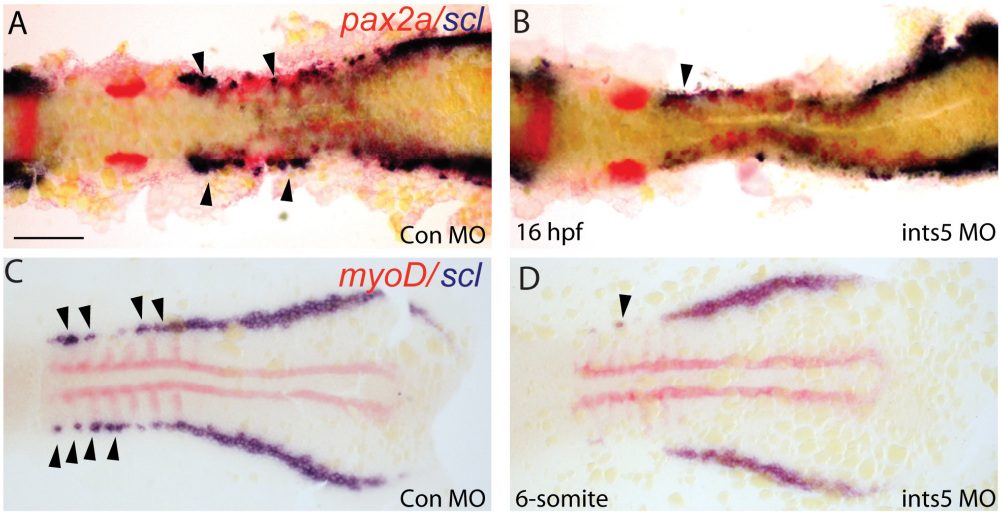
A
pax2a/scl
Con MO
B
16 hpf
ints5 MO
C
myoD/scl
Con MO
D
6-somite
ints5 MO

Figure 3.11 Ints5 knock-down affects hematopoietic progenitors but not pronephric and myotome cells.

Double *in situ* hybridization to detect expression of *scl* (purple) in hematopoietic cells (A-D), *pax2a* (red*)* in the pronephric cells (A, B, 16 hpf) and *myoD* (red*)* in myotome cells (C, D, 12 hpf or 6-somite stage). The black arrowheads indicate the anterior *scl* expression in the ICM, and its reduction in *ints5* morphants. (A-D) show flat-mounted embryos with anterior to the left. Scale bar in (A), 100 μm.

Expression of *gata1*, which is critical for specification of erythrocytes (Orkin and Zon, 1997), is also reduced in *ints5* morphants (Figure 3.9J).The reduction of *scl* and *gata1* can be rescued by co-injecting *ints5* RNA (Figure 3.9G, H, K), whereas over-expression of *ints5* RNA by itself does not affect *scl* expression (Figure 3.9E, F).

To confirm the above results, semi-quantitative real-time PCR was performed to examine the expression levels of *scl* and *gata1* genes (relative to *β-actin*). The expression levels of *scl* and *gata1* are decreased to 50% and 37% of normal levels, respectively, in *ints5* morphants. Co-injection of *ints5* RNA with *ints5* morpholinos can restore the expression of *scl* and *gata1* to normal levels (Figure 3.10).

Together, the above experiments show that Ints5 function is required for proper expression of hematopoietic genes.

As *scl* expression is also critical for the formation of vascular precursors, we examined the expression of endothelial gene, *flk1*, at various stages (de Jong and Zon, 2005; Liao et al., 1997). We find that although early expression of *flk1* is reduced in *ints5* morphants (Figure 3.12A, B), it seems to recover later (at 15 hpf, Figure 3.12C, D), and by 24 hpf, *flk1* experssion is detected in most domains observed in control embryos (Figure 3.12E, F). Expression of *flk1* seems reduced in inter-segmental vessels, but this may reflect cell migration and/or vessel branching defects. These results suggest that the common progenitor of hematopoietic and endothelial cells, the hemangioblast precursors (Vogeli et al., 2006) *per se* are not affected in *ints5* morphants, and that Ints5 function is specifically required for hematopoietic development.

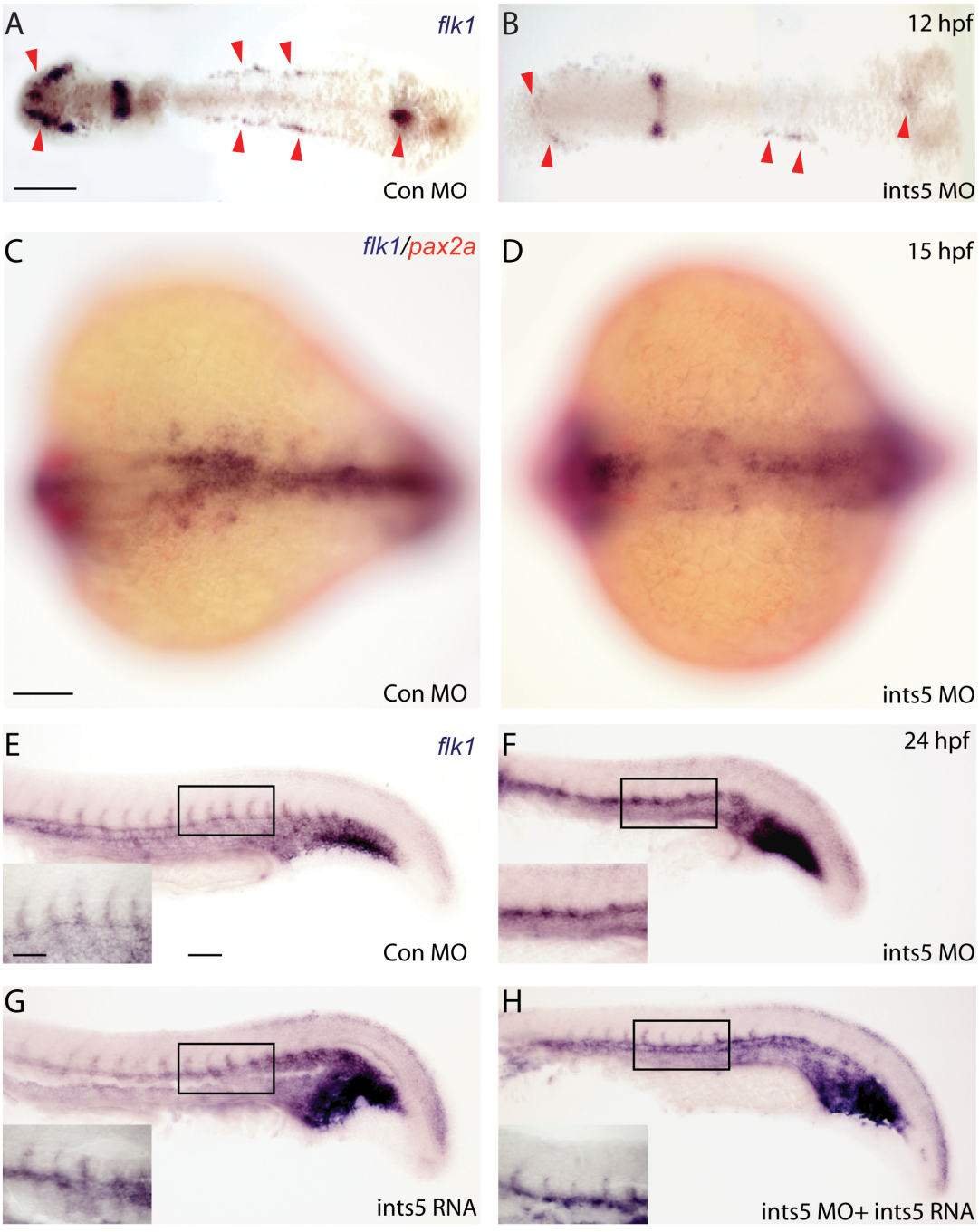
A
flk1
Con MO
B
12 hpf
ints5 MO
C
flk1/pax2a
Con MO
D
15 hpf
ints5 MO
E
flk1
Con MO
F
24 hpf
ints5 MO
G
ints5 RNA
H
ints5 MO+ ints5 RNA

Figure 3.12 Ints5 knockdown does not affect endothelia cells.

(A-H) Whole mount in situ hybridization to detect expression of *flk1* (purple*)* in endothelial cells at 12 hpf (A, B), 15 hpf (C, D) and 24 hpf (E-H). Red arrowheads in (A, B) indicate *flk1* expression. The insets show magnified views of the areas in black box. Inter-segmental *flk1* expression is not detected in *ints5* morphant (F), in comparison to control embryos (E) and *ints5* RNA injected embryos (G). Expression of *flk1* in inter-segmental vessels is rescued by co-injection of *ints5* RNA (H). (A, B) show dorsal views of flat mounted embryos. (C, D) show dorsal views with anterior to the left. (E-H) show lateral views of the trunk with anterior to the left. Scale bars in (A, C), 100μm, in (E, inset) 50μm and in (E, main image) 100μm.

3.7.2 Ints5 Is Required For Erythrocyte Differentiation.

A previous study by Qian *et al*., 2007 showed that *scl* isoforms function in initiation of primitive hematopoiesis and regulate erythroid cell differentiation. Since *ints5* morpholino-injected embryos have reduced *scl* expression, we examined erythroid differentiation in Ints5-manipulated embryos (Qian et al., 2007).

May-Grunwald Giemsa staining of blood smears from wild type embryos shows normal erythrocyte progenitors. These cells differentiate and are typically categorized as: stage I, basophilic erythroblast (30 hpf); stage II, polychromatophilic erythroblast (2 days post fertilization, 2 dpf); stage III, orthochromatophilic erythroblast (4 dpf); stage IV, erythrocyte (5 dpf onwards) (Figure 3.13A-C). The categorization is based on the shape of their nucleus, size and morphology of the cells, and staining of the cytoplasm (Qian et al., 2007).

Blood smear analysis shows that whereas 98% of RBCs (n=589) grow to the polychromatophilic erythroblast stage (stage II) in control embryos by 2 dpf (Figure 3.13D, J), only 58% (n=517) of RBCs in *ints5* morphants develop normally. In *ints5* morphant embryos, 42% (n=517) of cells arrest at the basophilic erythroblast stage (stage I) (Figure 3.13E, J).

To investigate the role of Ints5 in RBC differentiation, we reduced the dosage of the anti-sense morpholinos (*ints5* morpholinos donor+acceptor, 1ng+1ng/embryo) so as to allow embryos to survive till later stages, as embryos injected with normal dose of *ints5* morpholinos usually die by 3 dpf. At 7 dpf, only 30% (n=240) of RBCs in *ints5* morphant embryos injected with the low dose of morpholinos differentiate normally in comparison to control embryos where ~80% (n=265) of the cells are fully-developed,

mature RBCs with flattened elliptical shape (Figure 3.13G, H, K).

Normal differentiation of RBCs in *ints5* morphants was restored by co-injection of *ints5* RNA (Figure 3.13F, I, J, K, 2 dpf n=753, 7 dpf n=209) at both stages. Thus, Ints5 function is required for the normal differentiation of erythrocytes.

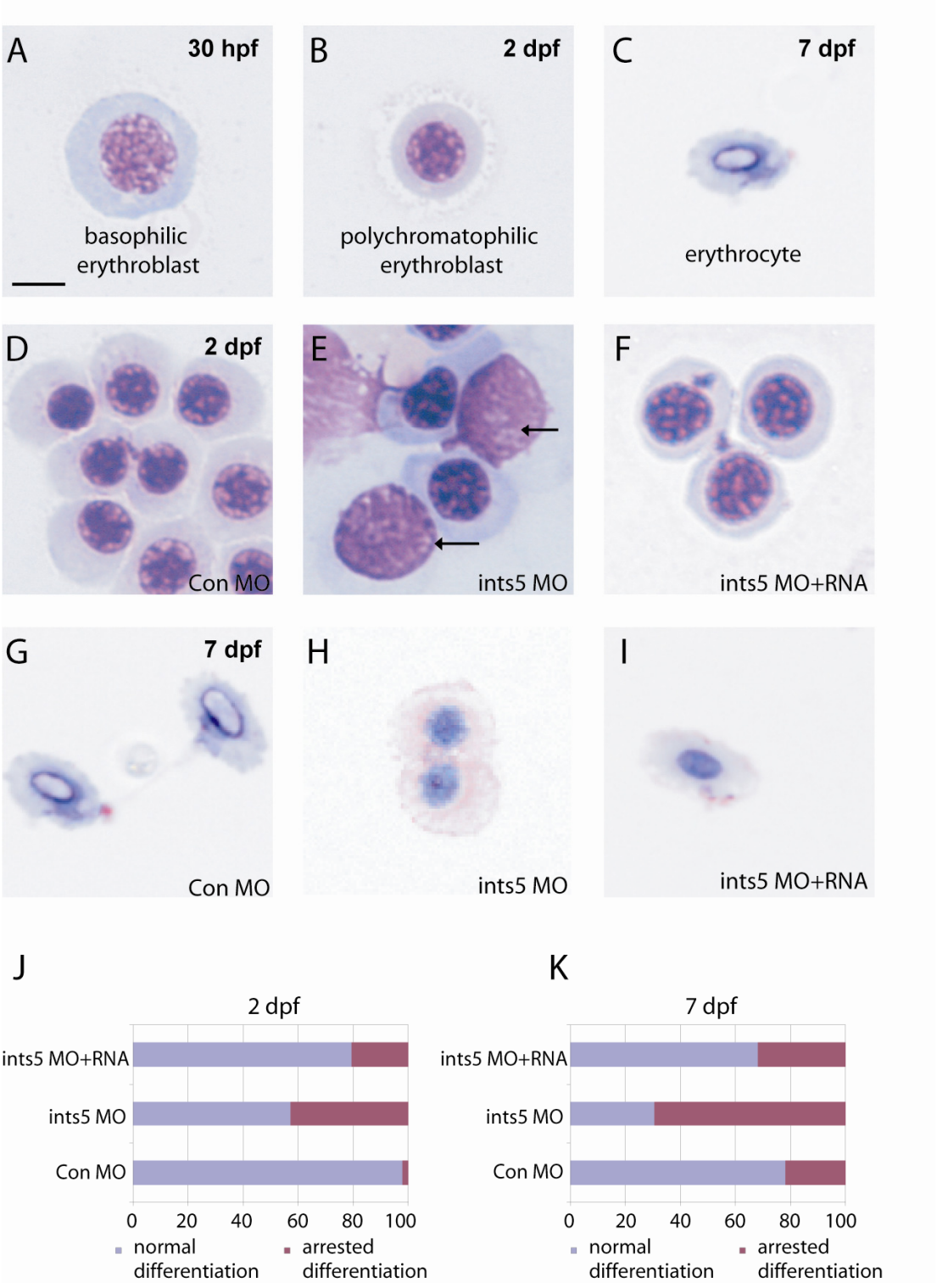
A
30 hpf
basophilic erythroblast
B
2 dpf
polychromatophilic erythroblast
C
7 dpf
erythrocyte
D
2 dpf
Con MO
E
ints5 MO
F
ints5 MO+RNA
G
7 dpf
Con MO
H
ints5 MO
I
ints5 MO+RNA
J
2 dpf
ints5 MO+RNA
ints5 MO
Con MO
0 20 40 60 80 100
normal differentiation
arrested differentiation
K
7 dpf
ints5 MO+RNA
ints5 MO
Con MO
0 20 40 60 80 100
normal differentiation
arrested differentiation

Figure 3.13 Ints5 is required for erythrocyte differentiation.

(A-C) May-Grunwald Giemsa staining shows normal RBCs at various stages. (D-F) RBCs in embryos injected with control morpholinos (D), *ints5* morpholinos (E), or co-injected with *ints5* RNA and morpholinos (F), respectively, at 2 dpf. The arrows indicate the RBCs arrested at basophilic erythroblast stage (E). (G-I) RBCs in embryos injected with control morpholinos (G), *ints5* morpholinos (H), or co-injected with *ints5* RNA and morpholinos (I) respectively at 7 dpf. (J, K) Histograms showing percentage of RBCs with normal (blue) or arrested (magenta) differentiation in injected embryos at 2 dpf (J) and 7 dpf (K), respectively. Scale bar in (A), 10 μm.

CHAPTER IV

THE MECHANISM: INTS5 FUNCTIONS IN HEMATOPOIESIS BY REGULATING SMAD1/SMAD5 SPLICING

4.1 INTS5 IS IMPORTANT FOR PROPER SPLICING OF SMAD1 AND SMAD5 TRANSCRIPTS

The Integrator complex is evolutionarily conserved in metazoans and directly interacts with the C-terminal domain of RNA polymerase II largest subunit. It is recruited to the U1 and U2 snRNA genes and mediates snRNA 3' end processing (Baillat et al., 2005). U1 and U2, together with U4, U5, and U6 small nuclear RNAs, are involved in the major form of pre-mRNA splicing. Each is in a complex of at least seven protein subunits to form an snRNP (small nuclear ribonucleoprotein). These snRNPs form the core of the spliceosome, a large assembly of RNA and protein molecules that performs pre-mRNA splicing in the cell (Alberts et al., 2002). Therefore, knockdown of *ints5* is likely to affect the splicing of target genes.

As Cai Yu's work implied that Ints5 may be required for proper DPP/BMP signaling during *Drosophila* development, and *ints5* morpholino-injected zebrafish embryos have decreased *scl* expression, similar to embryos with mutation in zebrafish *smad5*, (a transcription factor that mediates BMP signaling) (McReynolds et al., 2007), we investigated whether the splicing of *smad5* and its highly related orthologue *smad1* is disrupted in *ints5* morphant embryos. Splicing of *smad2*, *smad3a, smad3b, cyclops*, *squint* and *β-actin* RNAs was also examined as controls. Total RNA was extracted from embryos injected with control or *ints5* splice morpholinos, and RT-PCR was performed with primers for the various genes (Table 2.1-2.6). We found that, the splicing of *smad5* and *smad1* transcripts is impaired, whereas the transcripts for all other examined genes are correctly spliced.

As early as sphere and 30% epiboly stages, aberrantly spliced *smad5* transcripts

accumulate in *ints5* donor morpholino (DM) and acceptor mopholino (AM) injected embryos. In contrast, *β-actin* control transcripts are correctly spliced to yield a 500 bp product from cDNA in comparison to a 700 bp genomic (G) DNA product (Figure 4.1A, B). Figure 4.1C shows the schematic representation of wild type (710 bp) and aberrant *smad5* transcripts that lack exon 4 (466 bp product), or lack both exon 4 and exon 5 (350 bp) (Figure 4.1C).

To test the activity of the aberrant *smad5* splice products, we injected capped synthetic *smad5* RNAs, lacking exon 4 (*smad5Δexon4*), or exons 4 and 5 (*smad5Δexon4, 5*) into one-cell stage zebrafish embryos. Analysis of *scl* expression at 12 hpf shows that embryos injected with *smad5Δexon4* or *smad5Δexon4, 5* RNA have reduced expression in a dose dependent manner at 12 hpf. The phenotype is similar to that of *ints5* morphants (Figures 3.9C, D, 4.2B, C, E-G). So it is possible that *ints5* morpholino induced aberrant *smad5* transcripts can be translated into truncated forms, which may function as dominant-negative Smad5 during development.

To confirm the possibility, I examined the presence of truncated Smad5 by western blot analysis. Using antibodies to detect Smad5 protein in embryo extracts, I detected less full length Smad5 (52KDa), as well as truncated forms of Smad5, corresponding to the aberrant transcripts *smad5Δexon4* (43KDa) and *smad5Δexon4, 5* RNA (39KDa) (Figure 4.3). This result confirms that the *ints5* morpholinos indeed abrogate the production of Smad5 proteins, and lead to the production of truncated Smad5 that have the potential to function as dominant-negative proteins.

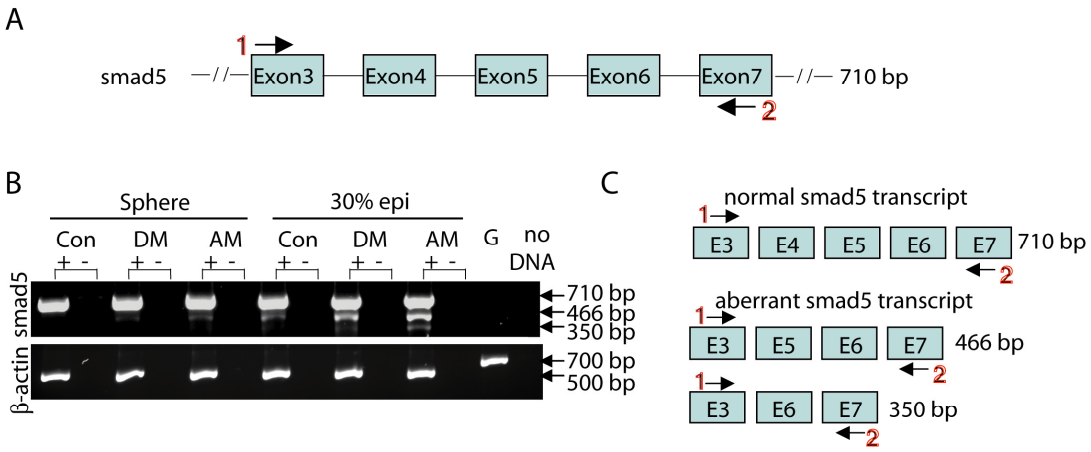
A
smad5
1
Exon3
Exon4
Exon5
Exon6
Exon7
710 bp
2
B
Sphere
30% epi
Con
DM
AM
Con
DM
AM
G
no DNA
+ -
smad5
β-actin
710 bp
466 bp
350 bp
700 bp
500 bp
C
normal smad5 transcript
E3
E4
E5
E6
E7
710 bp
aberrant smad5 transcript
E3
E5
E6
E7
466 bp
E3
E6
E7
350 bp

Figure 4.1 Knock-down of Ints5 perturbs splicing of *smad5* RNA.

(A)Schematic representation of the *smad5* genomic locus. Numbered black arrows indicate the position of primers used in RT-PCRs to detect splicing. The sizes of the predicted products are indicated on the right. (B) At both sphere and 30% epiboly stages, aberrantly spliced *smad5* transcripts accumulate in *ints5* donor morpholino (DM) and acceptor mopholino (AM) injected embryos. Splicing of *β-actin* control is unaffected. (C) Schematic representation of wild type (710 bp) and aberrant (466 bp and 350 bp) *smad5* transcripts.

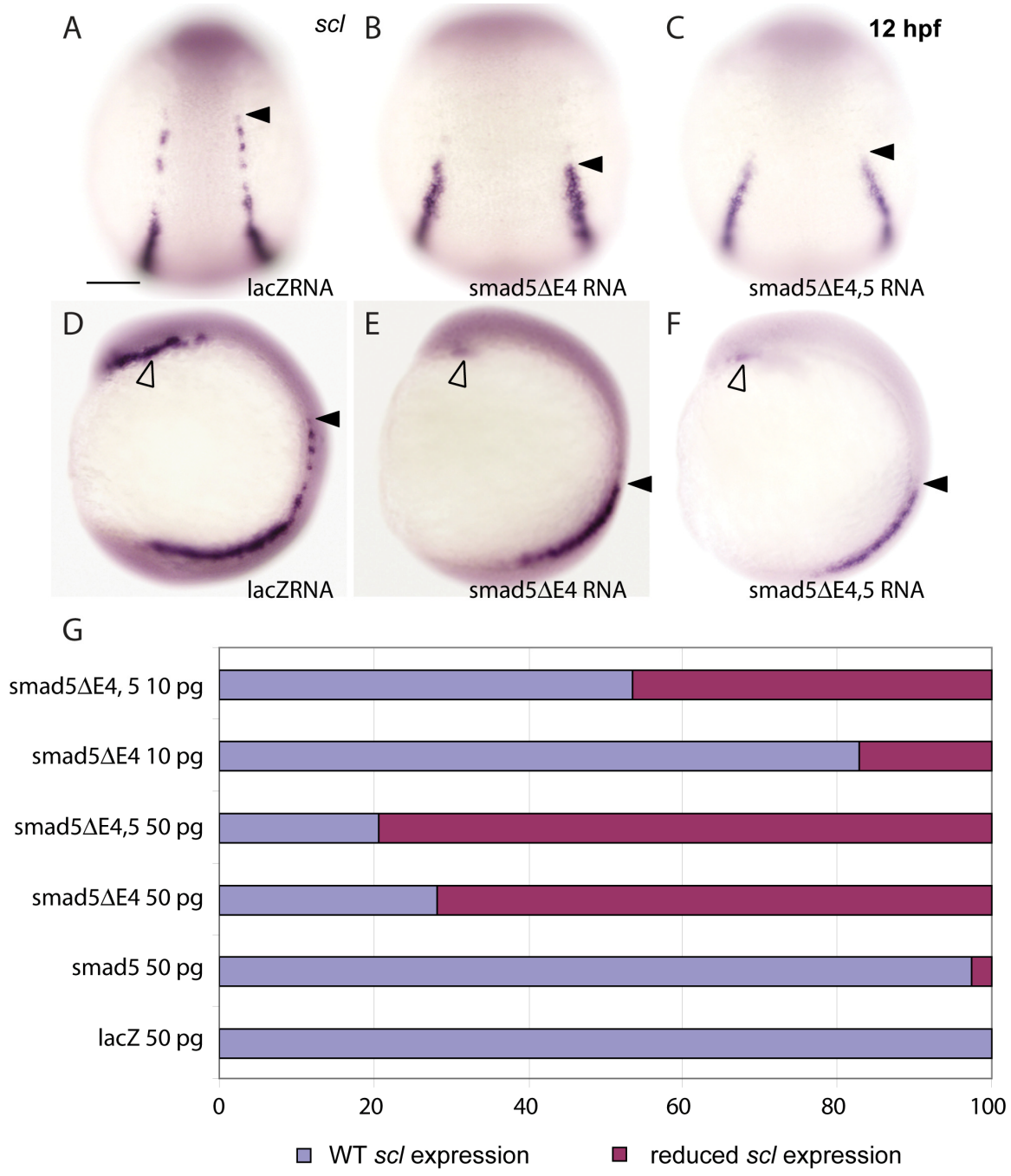
A
scl
B
C
12 hpf
lacZRNA
smad5ΔE4 RNA
smad5ΔE4,5 RNA
D
E
F
lacZRNA
smad5ΔE4 RNA
smad5ΔE4,5 RNA
G
smad5ΔE4, 5 10 pg
smad5ΔE4 10 pg
smad5ΔE4,5 50 pg
smad5ΔE4 50 pg
smad5 50 pg
lacZ 50 pg
0
20
40
60
80
100
WT scl expression
reduced scl expression

Figure 4.2 Over-expression of truncated *smad5* transcripts causes hematopoiesis defects, similar to *ints5* morphants.

(A-F) The whole mount *in situ* hybridization to detect *scl* in control embryos (A, D), embryos injected with *smad5ΔE4* RNA (B, E) or *smad5ΔE4, 5* RNA (C, F) at 12 hpf. The black arrowheads indicate the anterior limit of *scl* expression in the ICM. The open arrowheads mark *scl* expression in RBI. Upper panel shows dorsal views with the anterior to the top; Lower panel shows lateral views with dorsal to the right. (G) Histogram showing percentage of injected embryos with wild type like (blue) or reduced (magenta) *scl* expression. Scale bar in (A), 50 μm.

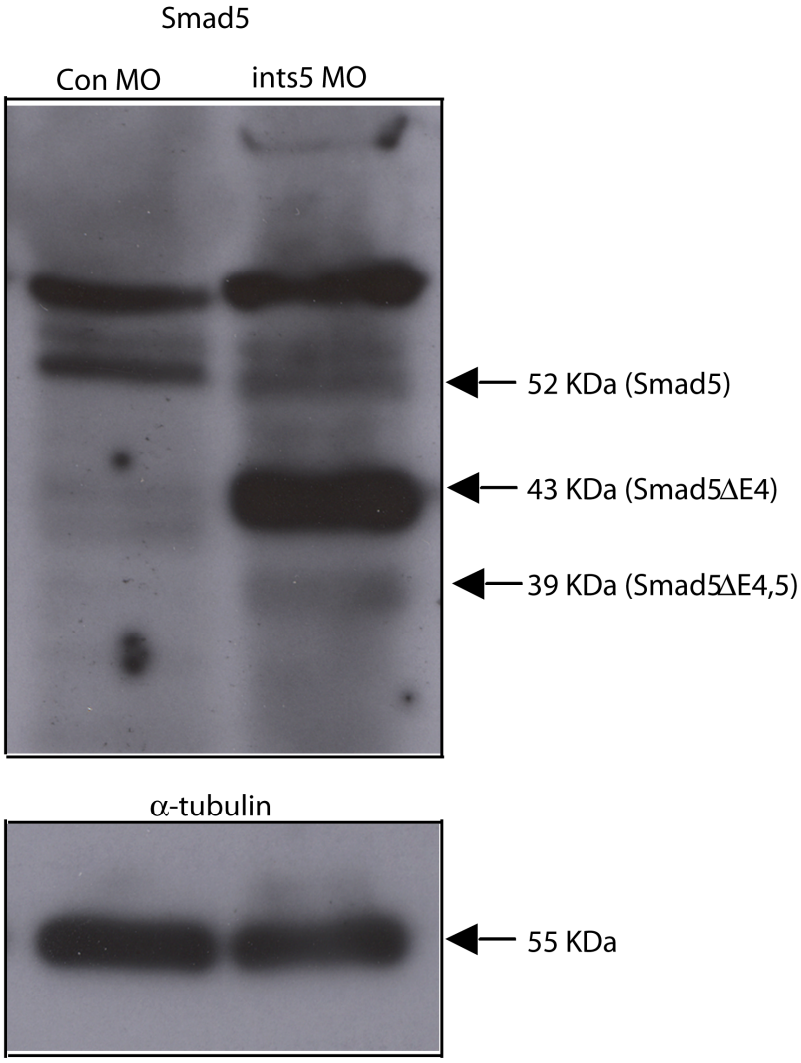
Smad5
Con MO
ints5 MO
52 KDa (Smad5)
43 KDa (Smad5ΔE4)
39 KDa (Smad5ΔE4,5)
α-tubulin
55 KDa

Figure 4.3 Ints5 knockdown leads to production of truncated Smad5 protein in embryos.

Western blots on extracts of embryos injected with control and *ints5* morpholinos. Proteins of each sample were harvested from 20 injected embryos at 8 hpf. Smad5 proteins were detected by using rabbit anti-Smad5 polyclonal antibody (Abcam) (upper panel); the lower panel shows expression of α-tubulin control detected with mouse monoclonal anti-α-tubulin antibodies (Sigma). The black arrows indicate the size of corresponding peptides. In *ints5* morpholino injected embryos, truncated forms of Smad5, Smad5ΔE4 (43kD, lack of 86 amino acids encoded by exon4 of *smad5*) and Smad5EΔ4, 5 (39kD, lack of 123 amino acids encoded by exon4 and exon5 of *smad5*) are accumulated.

Similarly, un-spliced *smad1* transcripts are detected at several exon/intron boundaries in *ints5* morpholino-injected embryos at 30% epiboly stage (Figure 4.4).

However, we did not observe aberrant splicing of any exon/intron boundary of *smad2*, *smad3a* and *smad3b* transcripts or other examined transcripts, such as *cyclops* and *squint* (Figures 4.5, 4.6). Taking *squint* splicing as an example, aberrantly spliced *squint* transcripts were only detected in *squint* morphant but not in control and *ints5* morphant (Figure 4.6)(Gore et al., 2005). These results show that Ints5 is specifically required for the correct splicing of *smad1* and *smad5* RNA.

In fact, the splicing of many genes (including *chordin, vent, vox, ved, gata2, eve1, smurf1, bmp2b, bmp7, ski, sqt, cyc* and others) expressed in early gastrulation was checked in *ints5* morphant and we find that among all the transcripts we examined, only *smad1* and *smad5* RNA splicing are affected. However, this does not exclude the possibility that Ints5 may regulate the splicing of other RNAs directly or indirectly, and *smad1* and *smad5* may not be the only targets for Ints5.

U1 and U2 snRNAs are key components of the spliceosome and function in processing of most pre-mRNAs. It is postulated that knock-down of Ints5 disrupts the production of mature U1 and U2 snRNAs, which in turn affects spliceosome function and leads to aberrant *smad1/5* splicing. To understand the mechanism underlying the *smad1/5* splicing defects, we examined the transcription and processing of U1 and U2 snRNAs with different primer pairs (Figure 4.7A) in *ints5* morphants. RT-PCR analysis shows more accumulation of un-processed primary U1 and U2 snRNAs in *ints5* morpholino injected embryos (Figure 4.7B). Semi-quantitative RT-PCR was performed to determine the change in expression levels of the different U1 and U2 transcripts. The amount of

unprocessed primary U1 and U2 snRNA in *ints5* morphants increased up to 2.4 fold and 2.7 fold respectively (Figure, 4.7C, D). In contrast, levels of mature U1 and U2 snRNAs levels are relatively stable (Figure 4.7E, F). This can be explained by the long half life of U1 and U2 snRNA (Fury and Zieve, 1996).

Therefore, it is likely that Ints5 functions through U1/U2 snRNA processing to regulate the splicing of *smad1/5*.

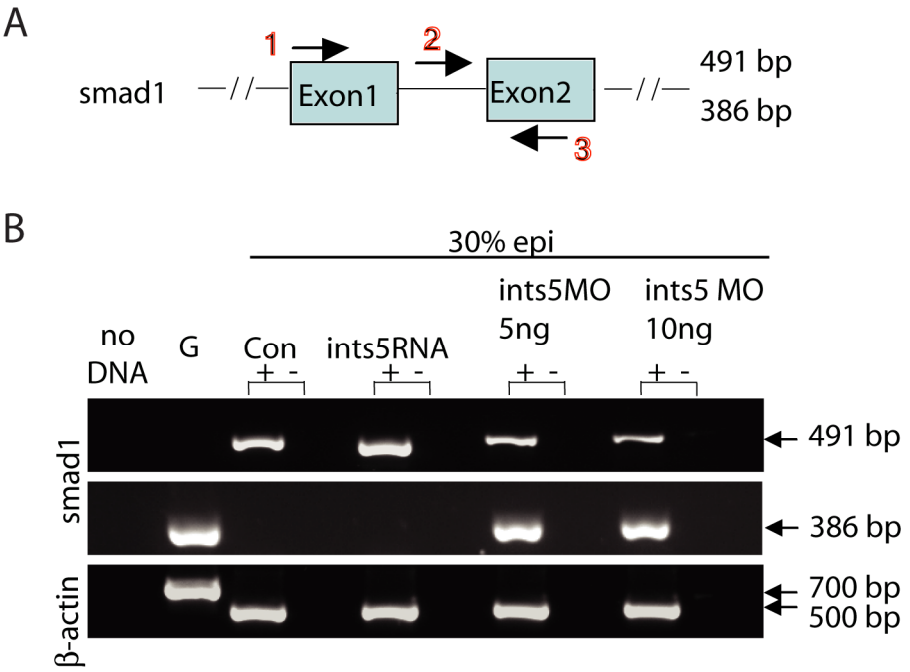
A
smad1
1
2
3
Exon1
Exon2
491 bp
386 bp
B
30% epi
no DNA
G
Con
ints5RNA
ints5MO 5ng
ints5 MO 10ng
+ -
smad1
β-actin
491 bp
386 bp
700 bp
500 bp

Figure 4.4 Knockdown of Ints5 perturbs splicing of *smad1* RNA.

(A) Schematic representation of *smad1* genomic loci. Numbered black arrows indicate the position of primers used in RT-PCRs to detect splicing. The sizes of the predicted products are indicated on the right. (B) Un-spliced *smad1* (386 bp product with primer pair 2+3) and correctly spliced *smad1* (491 bp with primer pair 1+3) transcripts in 30% epiboly *ints5* morpholino injected embryos. Splicing of *β-actin* is shown as control.

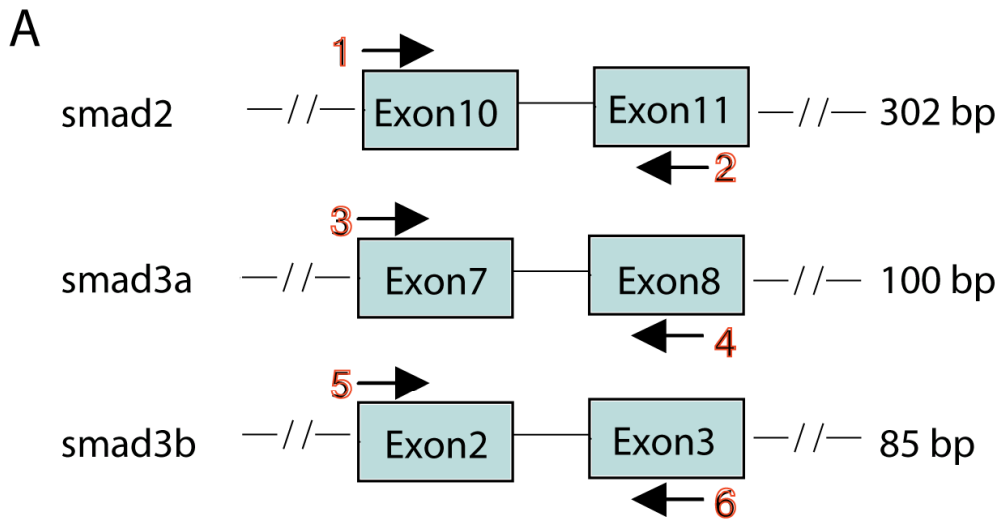
A
smad2
1
Exon10
Exon11
2
302 bp
smad3a
3
Exon7
Exon8
4
100 bp
smad3b
5
Exon2
Exon3
6
85 bp

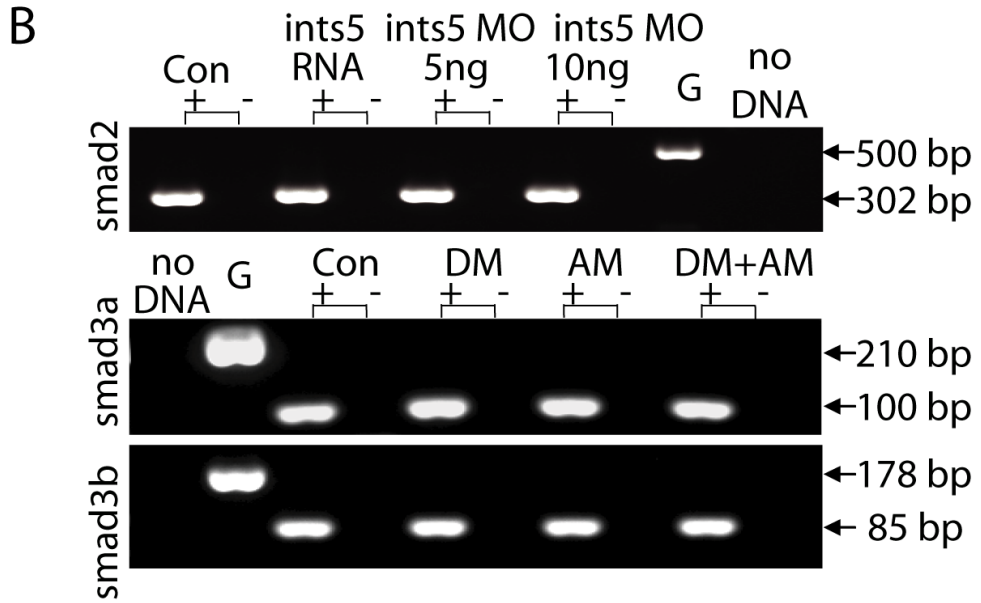
B
Con
ints5 RNA
ints5 MO 5ng
ints5 MO 10ng
G
no DNA
+ -
smad2
500 bp
302 bp
no DNA
G
Con
DM
AM
DM+AM
smad3a
210 bp
100 bp
smad3b
178 bp
85 bp

Figure 4.5 Knockdown of Ints5 does not perturb splicing of *smad2* and *smad3* RNA. (A) Schematic representation of the *smad2, smad3a and smad3b* genomic loci. Numbered black arrows indicate the position of primers used in RT-PCRs to detect splicing. The sizes of the predicted products using various primer pairs (shown in red) are indicated on the right. (B) Amplification of *smad2*, *smad3a* and *smad3b* with indicated primer pairs shows correctly spliced products in *ints5* morphants. Amplification with the primers spanning other regions of these genes did not show aberrant splicing as well (data not.shown).

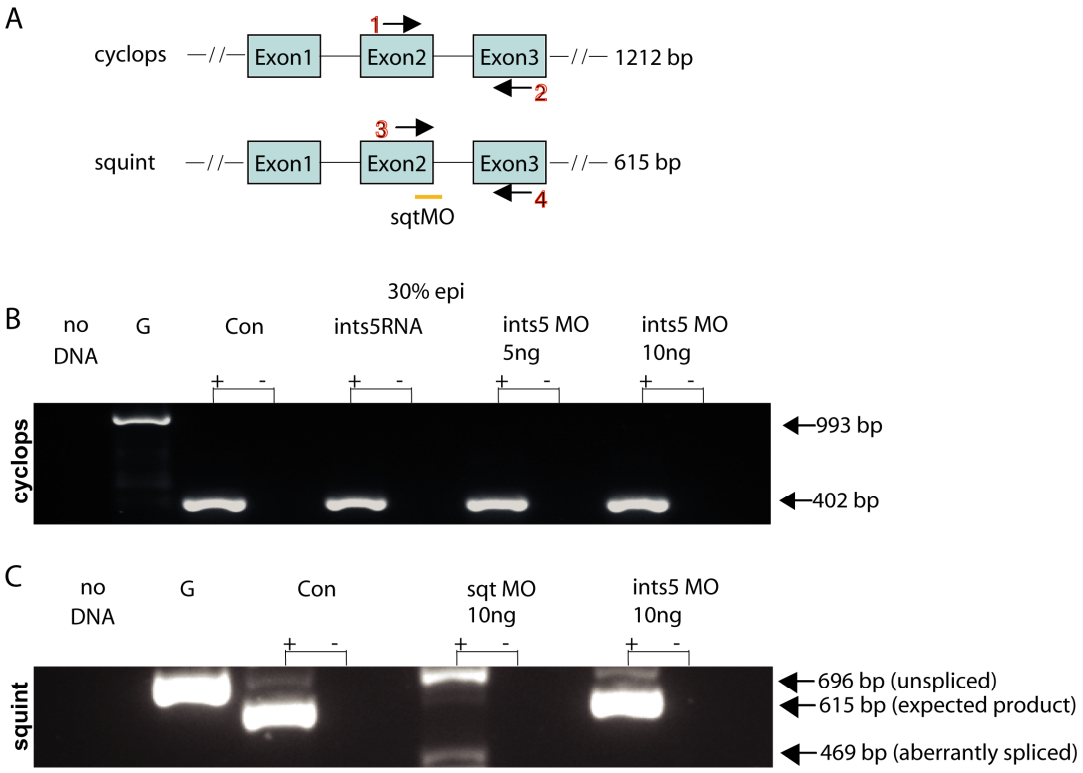
A
cyclops
Exon1
Exon2
Exon3
1212 bp
1
2
squint
615 bp
3
4
sqtMO
B
30% epi
no DNA
G
Con
ints5RNA
ints5 MO 5ng
ints5 MO 10ng
cyclops
993 bp
402 bp
C
no DNA
G
Con
sqt MO 10ng
ints5 MO 10ng
squint
696 bp (unspliced)
615 bp (expected product)
469 bp (aberrantly spliced)

Figure 4.6. Knockdown of Ints5 dose not affect splicing of *cyclops* and *squint* RNA.

(A) Schematic representation of the *cyclops* and *squint* genomic loci. Arrows indicate the position of primer pairs used in RT-PCRs to detect splicing. The orange bar indicates the position of the *squint* splice junction morpholino at the exon2-intron2 boundary (Gore et al., 2005). Expected sizes of the amplified products are shown on the right. (B) At 30% epiboly, a 402 bp cyc product is detected from all cDNA templates, whereas a 993 bp fragment is amplified from genomic DNA. (C) Embryos injected with *ints5* morpholinos or control morpholinos show the expected 615 bp *squint* product. In contrast, embryos injected with *squint* splice-junction morpholinos show either un-spliced (696 bp) or aberrantly spliced *squint* transcripts (469 bp).

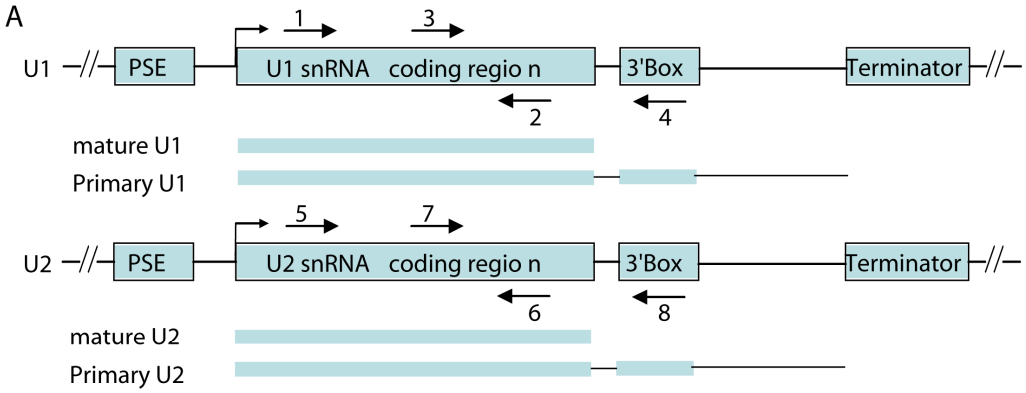
A
U1
PSE
U1 snRNA coding regio n
3'Box
Terminator
1
3
2
4
mature U1
Primary U1
U2
PSE
U2 snRNA coding regio n
3'Box
Terminator
5
7
6
8
mature U2
Primary U2

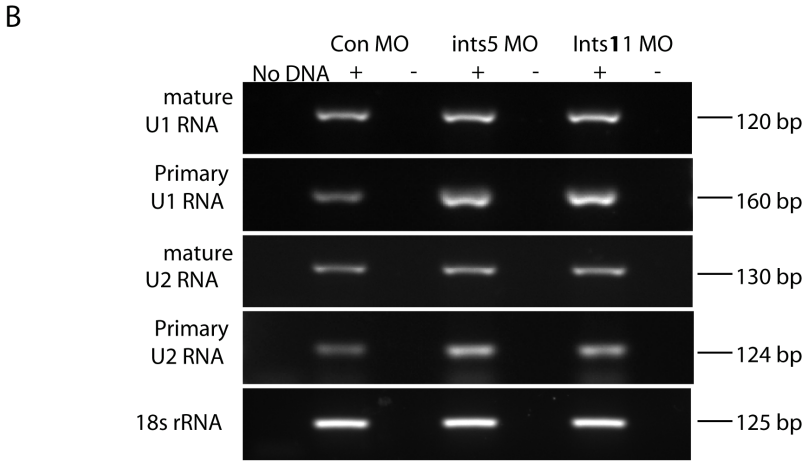
B
Con MO
ints5 MO
Ints11 MO
No DNA + - + - + -
mature U1 RNA
120 bp
Primary U1 RNA
160 bp
mature U2 RNA
130 bp
Primary U2 RNA
124 bp
18s rRNA
125 bp

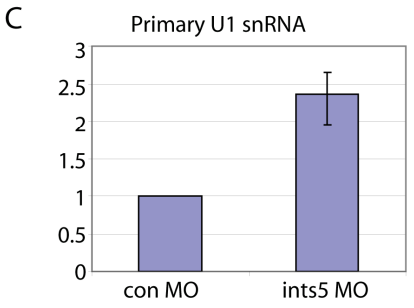
C
Primary U1 snRNA
3
2.5
2
1.5
1
0.5
0
con MO
ints5 MO

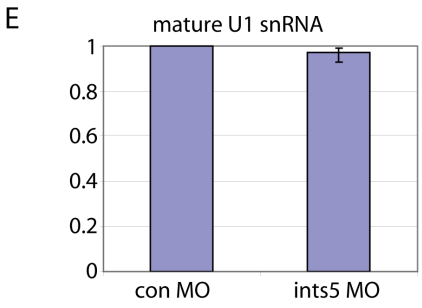
E
mature U1 snRNA
1
0.8
0.6
0.4
0.2
0
con MO
ints5 MO

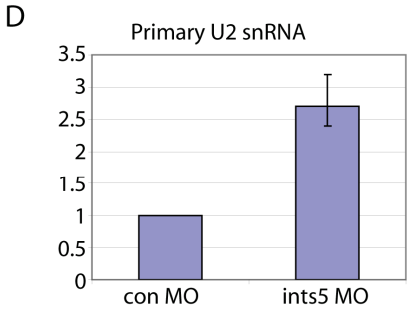
D
Primary U2 snRNA
3.5
3
2.5
2
1.5
1
0.5
0
con MO
ints5 MO

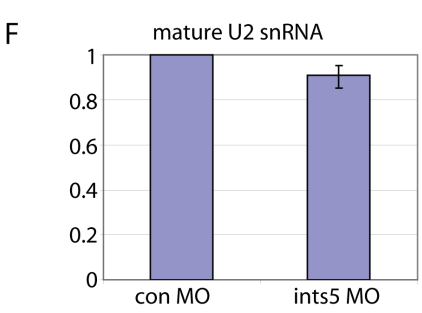
F
mature U2 snRNA
1
0.8
0.6
0.4
0.2
0
con MO
ints5 MO

Figure 4.7 Knockdown of *ints5* leads to accumulation of immature primary U1, U2 snRNAs.

(A) Diagrams of U1 and U2 snRNA genes. Location of the proximal promoter elements (PSE), snRNA coding region, the 3' end formation signals (3' Box) and terminators are indicated with rectangular boxes. The mature and immature primary forms of U snRNA transcripts are represented under each diagram. The numbered arrows indicate the position of primers used to detect the expression of various transcripts of U snRNA genes. (B) The presence of mature and primary U1 and U2 snRNAs was detected by RT-PCRs with labeled primers (mature U1, 1+2; primary U1, 3+4; mature U2, 5+6; primary U2, 7+8) at 8 hpf. The expression of 18s rRNA is shown as control. (C-F) Histograms to show expression level of primary U1(C), Primary U2 (D), mature U1 (E) and mature U2 (F) transcripts in injected embryos. Expression levels were measured at 8 hpf by semi-quantitative RT-PCR, normalized with respect to the level of 18s rRNA internal control, and shown as fold-change relative to control embryos.

4.2 INTS5 MODULATES HEMATOPOIESIS THROUGH SMAD/BMP SIGNALING

If the hematopoiesis defects induced by knock-down of Ints5 are caused by mis-splicing of *smad1* and *smad5*, providing correctly spliced *smad1/5* should rescue the *ints5* morpholino induced defects in these embryos.

To determine the epistatic relationship between Ints5 and Smad1/Smad5, we injected 10 pg of capped synthetic *smad1* or *smad5* RNA together with *ints5* morpholinos into one-cell stage embryos and either fixed them at 6-somite stage (12 hpf) for WISH or raised them for blood extraction at 2 dpf.

We found that co-injected *smad1* or *smad5* RNA can restore *scl* expression in *ints5* morphants, similar to *ints5* RNA co-injections (Figure 4.8C, D, I-M, Table 4.1, $P<<0.01$, z test). Embryos injected with 10 pg of *smad1* or *smad5* RNA alone show normal *scl* expression (Figure 4.8E-H, M), similar to control morpholino-injected embryos (Figure 4.8A, B, M).

To rule out the possibility that the delayed development accounts for the reduced *scl* expression, we did double color WISH with *scl* and *myoD* in stage-matched embryos at 6-somite stage. The anterior *scl* expression domain is missing in *ints5* morphants (Figure 4.9 B). The reduced anterior *scl* expression in *ints5* morphants is rescued by co-injecting *smad1* and *smad5* RNA (Figure 4.9E, F)(Weinberg et al., 1996). The anterior limit of major *scl* expression domain aligns well with the most anterior *myoD* positive cells, similar to control and *smad1/smad5* RNA injected embryos (Figure 4.9A, C, D).

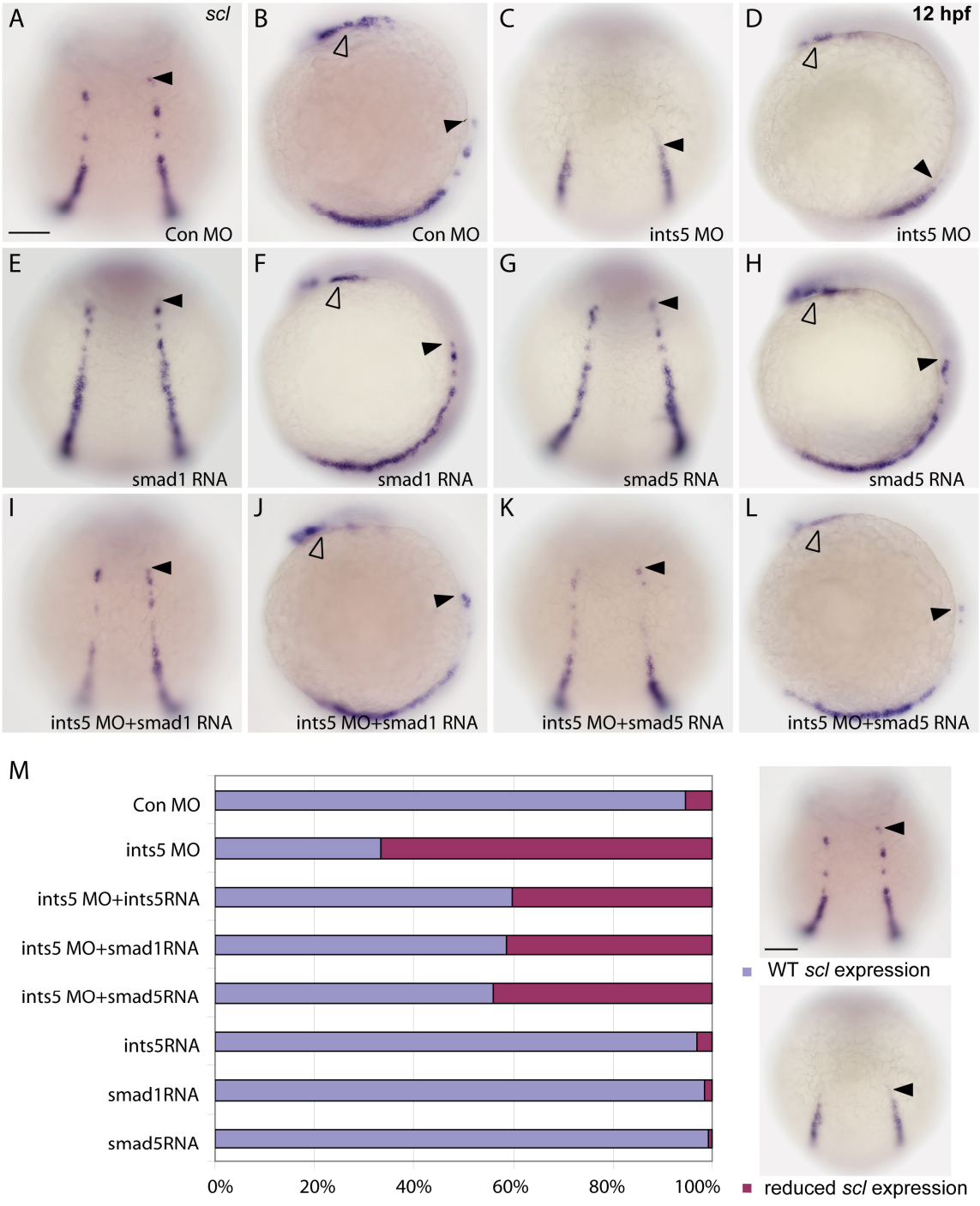
A
scl
Con MO
B
Con MO
C
ints5 MO
D
12 hpf
ints5 MO
E
smad1 RNA
F
smad1 RNA
G
smad5 RNA
H
smad5 RNA
I
ints5 MO+smad1 RNA
J
ints5 MO+smad1 RNA
K
ints5 MO+smad5 RNA
L
ints5 MO+smad5 RNA
M
Con MO
ints5 MO
ints5 MO+ints5RNA
ints5 MO+smad1RNA
ints5 MO+smad5RNA
ints5RNA
smad1RNA
smad5RNA
0%
20%
40%
60%
80%
100%
WT scl expression
reduced scl expression

Figure 4.8 The hematopoiesis defects induced by Ints5 knock-down are rescued by *smad1* and *smad5* RNA.

(A-L) Whole mount *in situ* hybridization to detect *scl* expression in 12 hpf embryos injected with control morpholinos (A, B), *ints5* morpholinos (C, D), *smad1* RNA (E, F), *smad5* RNA (G, H), *ints5* morpholinos and *smad1* RNA (I, J), or *ints5* morpholinos with *smad5* RNA (K, L). The black arrowheads indicate the anterior limit of *scl* expression in ICM. The open arrowheads indicate *scl* expression in RBI. (A, C, E, G, I, K) show dorsal views of embryos with anterior to the top; (B, D, F, H, J, L) show lateral views of embryos with dorsal side to the right. (M) Histogram showing percentage of injected embryos with wild type like (blue) or reduced (magenta) *scl* expression. Scale bar in (A, M), 50 μm.

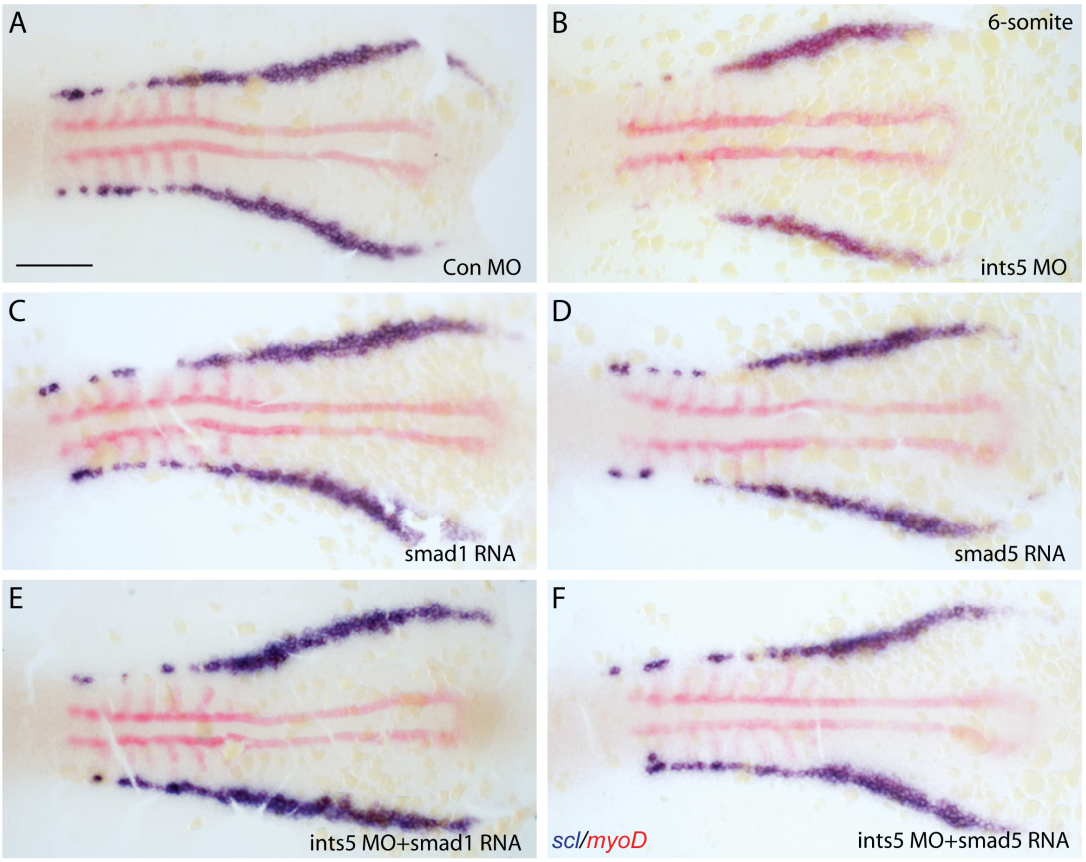
A
Con MO
B
6-somite
ints5 MO
C
smad1 RNA
D
smad5 RNA
E
ints5 MO+smad1 RNA
F
scl/myoD
ints5 MO+smad5 RNA

Figure 4.9 The hematopoiesis defects induced by *ints5* knock-down are rescued by *smad1* and *smad5* RNA.

(A-F) Whole mount in situ hybridization to detect *scl* (purple) and *myoD* (red) expression in 6-somite embryos injected with control morpholinos (A), *ints5* morpholinos (B), *smad1* RNA (C), *smad5 RNA* (D), *ints5* morpholinos with *smad1* RNA (E), or *ints5* morpholinos with *smad5* RNA (F). (A-F) show flat-mounted embryos with anterior to the left. Scale bar in (A), 100 μm.

Table 4.1 Reduced *scl* expression in *ints5* morphant embryos can be rescued by co-injection of *int5*, *smad1* and s*mad5* RNA.

Injected RNA or MO	Dose	Total number of injected embryos	Embryos with normal *scl* expression (%)	embryos with reduced *scl* expression (%)
Con MO	5 ng	360	94.7	5.3
Ints5 RNA	50 pg	253	96.8	3.2
Smad1 RNA	10 pg	220	98.6	1.4
Smad5 RNA	10 pg	221	99.1	0.9
Ints5 acceptor + donor MO	2.5+2.5 ng	295	33.2	66.8
ints5 acceptor + donor MO + int5 RNA	2.5+2.5 ng+50 pg	182	59.9	40.1
ints5 acceptor + donor MO + smad1 RNA	2.5+2.5 ng+10 pg	246	58.5	41.5
ints5 acceptor + donor MO + smad5 RNA	2.5+2.5 ng+10 pg	247	55.9	44.1

To confirm the above results, semi-quantitative real-time PCR was performed to detect the expression level of *scl* and *gata1* genes (relative to *β-actin*). The experiment also shows the reduced expression levels of these genes in *ints5* morphant can be restored to

normal levels by co-injection of *smad1* and *smad5* RNA (Figure 4.10A, B).

Ints5 knock-down inhibits blood formation and erythrocyte differentiation. We have already shown that blood formation can be rescued by wild type *smad1*, *smad5* transcripts. We further investigated red blood cell differentiation defect, and found that ~50% of RBCs arrested in *ints5* morphants (Figure 4.11B, G, n=378). Over-expressing *smad1* or *smad5* at 10 pg dose had no effect on RBC differentiation (Figure 4.11C, D, G, n=255 and n=493). However, normal differentiation of RBCs in *ints5* morphants was restored by co-injection of *smad1* and *smad5* RNA (Figure 4.11 E-G, n=257 and n=380, respectively) at 2 dpf. Thus, co-injecting of *smad1*, *smad5* rescued the RBC differentiation defects seen in the *ints5* morphants.

Taken together, these results show that Ints5 functions in hematopoiesis by regulating *smad1/5* RNA splicing.

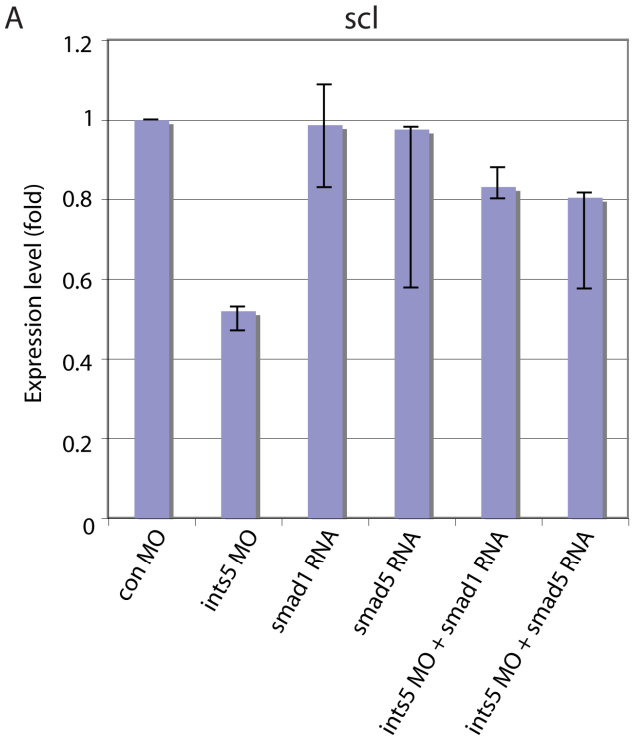
A
scl
Expression level (fold)
1.2
1
0.8
0.6
0.4
0.2
0
con MO
ints5 MO
smad1 RNA
smad5 RNA
ints5 MO + smad1 RNA
ints5 MO + smad5 RNA

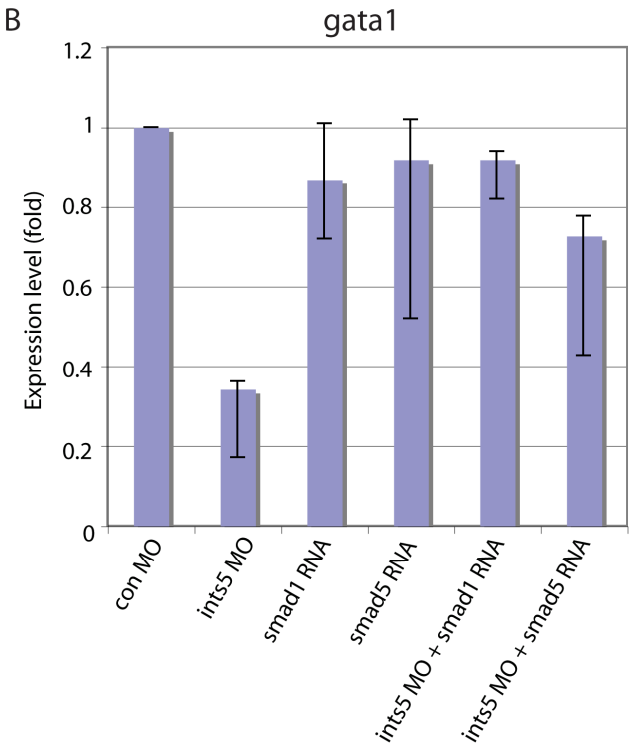
B
gata1
Expression level (fold)
1.2
1
0.8
0.6
0.4
0.2
0
con MO
ints5 MO
smad1 RNA
smad5 RNA
ints5 MO + smad1 RNA
ints5 MO + smad5 RNA

Figure 4.10 The reduced hematopoiesis gene expression induced by *ints5* knock-down are rescued by *smad1* and *smad5* RNA.

Histograms to show expression level of *gata1* (A) and *scl* (B) in injected embryos. Expression levels were measured at 12 hpf by semi-quantitative RT-PCR, normalized with respect to the level of *β-actin* internal control, and shown as fold-change relative to control embryos.

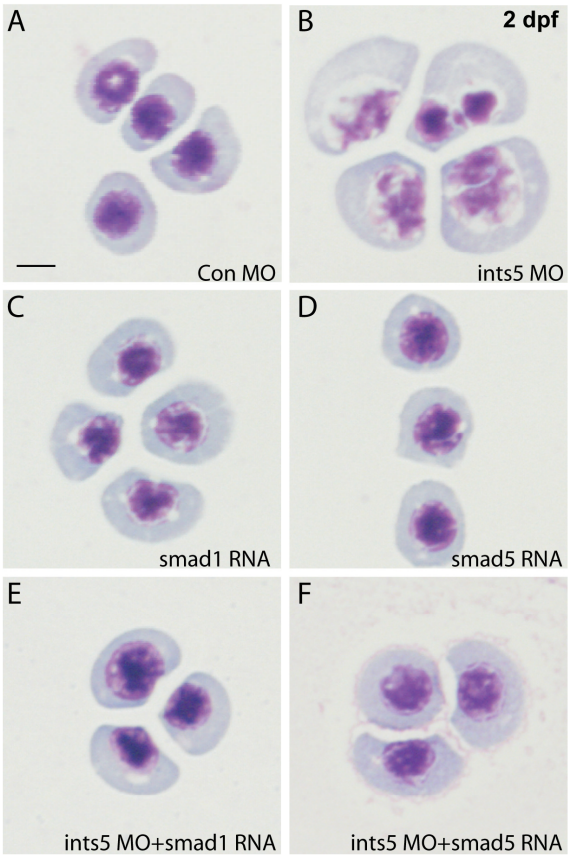
A
Con MO
B
2 dpf
ints5 MO
C
smad1 RNA
D
smad5 RNA
E
ints5 MO+smad1 RNA
F
ints5 MO+smad5 RNA

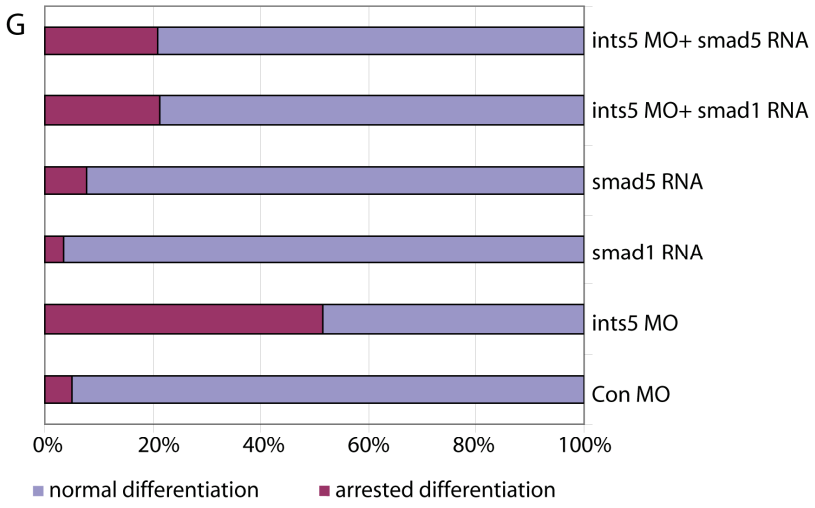
G
ints5 MO+ smad5 RNA
ints5 MO+ smad1 RNA
smad5 RNA
smad1 RNA
ints5 MO
Con MO
0%
20%
40%
60%
80%
100%
normal differentiation
arrested differentiation

Figure 4.11 The red blood cell differentiation defects induced by Ints5 knock-down are rescued by *smad1* and *smad5* RNA.

(A-F) May-Grunwald Giemsa staining to show RBCs differentiation in embryos injected with control morpholinos (A), *ints5* morpholinos (B), *smad1* RNA (C), *smad5* RNA (D), *ints5* morpholinos and *smad1* RNA (E), or *ints5* morpholinos with *smad5* RNA (F) at 2 dpf. (G) Histograms showing percentage of RBCs with normal (blue) or arrested (magenta) differentiation in injected embryos at 2 dpf. Scale bar in (A), 10 μm.

CHAPTER V

THE INTEGRATOR COMPLEX REGULATES PRIMITIVE HEMATOPOIESIS

As Ints5 is a subunit of the Integrator complex (Baillat et al., 2005), to find out whether Ints5 function independently or as a part of the Integrator complex in hematopoiesis, we examined the activity of other Integrator subunits Ints9 and Ints11, which display similarities to the subunits of the cleavage and polyadenylation specificity factor (CPSF) complex (Baillat et al., 2005).

We injected *ints11* ATG morpholinos and splice morpholinos targeting the boundary of intron4-exon5 in the *ints11* gene into one-cell stage embryos and fixed them for WISH at different stages (Figures 5.1, 5.2). Both *ints11* morpholinos cause reduced expression of the hematopoietic markers, *scl* and *gata1* (Figures 5.1C, D, G, 5.2B, D) in more than 50% embryos. In addition, embryos injected with *ints9* splice morpholinos targeting the boundary of intron2-exon3 show similar hematopoiesis defects, albeit to a less extent (Figures 5.1E-G, 5.2C, D). Furthermore, morpholinos targeting the splice junction of *ints11* not only cause aberrant splicing of *ints11* transcripts (Figure 5.3) but also disrupt U1/U2 snRNAs processing (Figure 4.7B) and *smad5* splicing (Figure 5.4) in the same manner as *ints5* splice morpholinos. Therefore, multiple subunits of the Integrator complex, including Ints5, may be required for appropriate hematopoietic gene expression. These results suggest that the Integrator proteins may function as a complex to regulate primitive hematopoiesis in zebrafish by modulating *smad1/5* splicing, via the spliceosome.

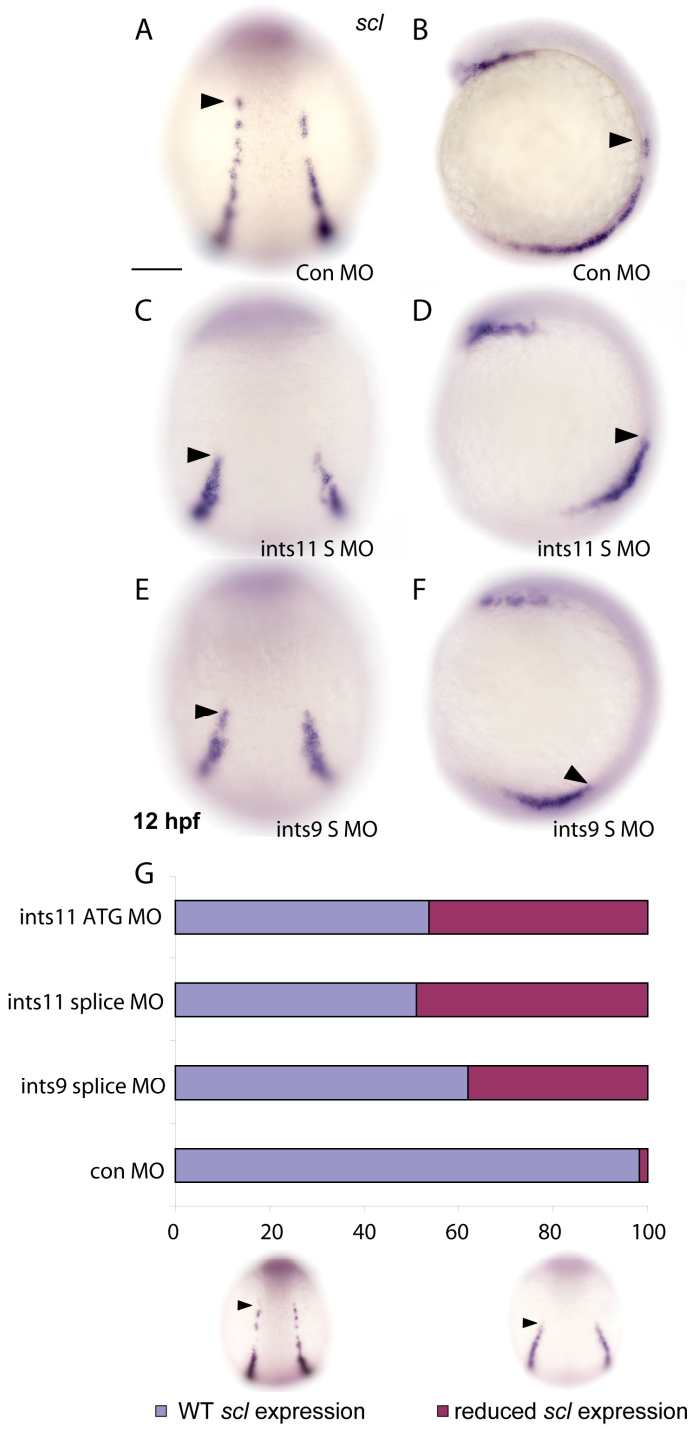
A
scl
Con MO
B
Con MO
C
ints11 S MO
D
ints11 S MO
E
ints9 S MO
12 hpf
F
ints9 S MO
G
ints11 ATG MO
ints11 splice MO
ints9 splice MO
con MO
0
20
40
60
80
100
WT scl expression
reduced scl expression

Figure 5.1 Multiple subunits of the Integrator complex regulate primitive hematopoiesis.

Whole mount *in situ* hybridization to detect *scl* (A-F) in embryos injected with control morpholinos (A, B), *ints11* splice junction morpholinos (C, D) and *ints9* splice junction morpholinos (E, F). The black arrowhead indicates the anterior limit of *scl* expression in the ICM. The *ints9* and *ints11* morphants show substantially reduced *scl* and *gata1* expression in comparison to control morphants. (G) Histograms showing percentage of injected embryos with wild type like (blue) or reduced (magenta) *scl* expression. Scale bars in (A), 50 μm.

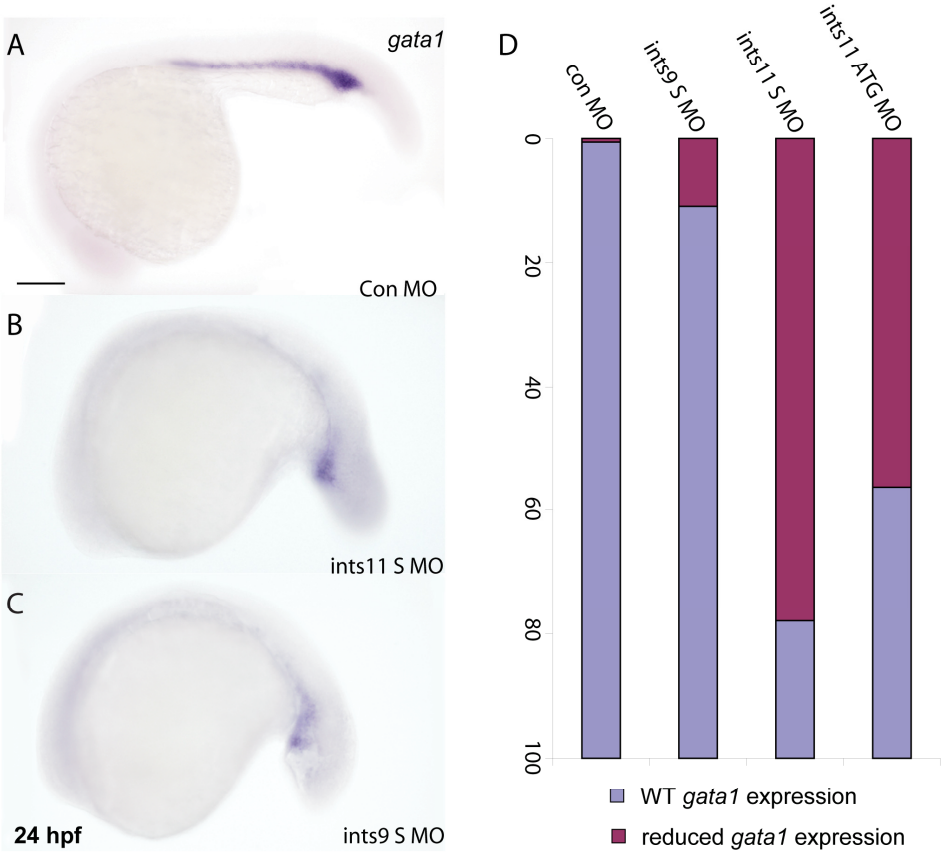
A
gata1
Con MO
B
ints11 S MO
C
24 hpf
ints9 S MO
D
con MO
ints9 S MO
ints11 S MO
ints11 ATG MO
0
20
40
60
80
100
WT gata1 expression
reduced gata1 expression

Figure 5.2 Multiple subunits of the Integrator complex regulate primitive hematopoiesis.

Whole mount *in situ* hybridization to detect *gata1* (A-C) in embryos injected with control morpholinos (A) *ints11* splice junction morpholinos (B) and *ints9* splice junction morpholinos (C). The black arrowhead indicates the anterior limit of *scl* expression in the ICM. The *ints11* morphants show substantially reduced *scl* and *gata1* expression in comparison to control morphants. (D) Histograms showing percentage of injected embryos with wild type like (blue) or reduced (magenta) *gata1*expression. Scale bars in (A), 250 μm.

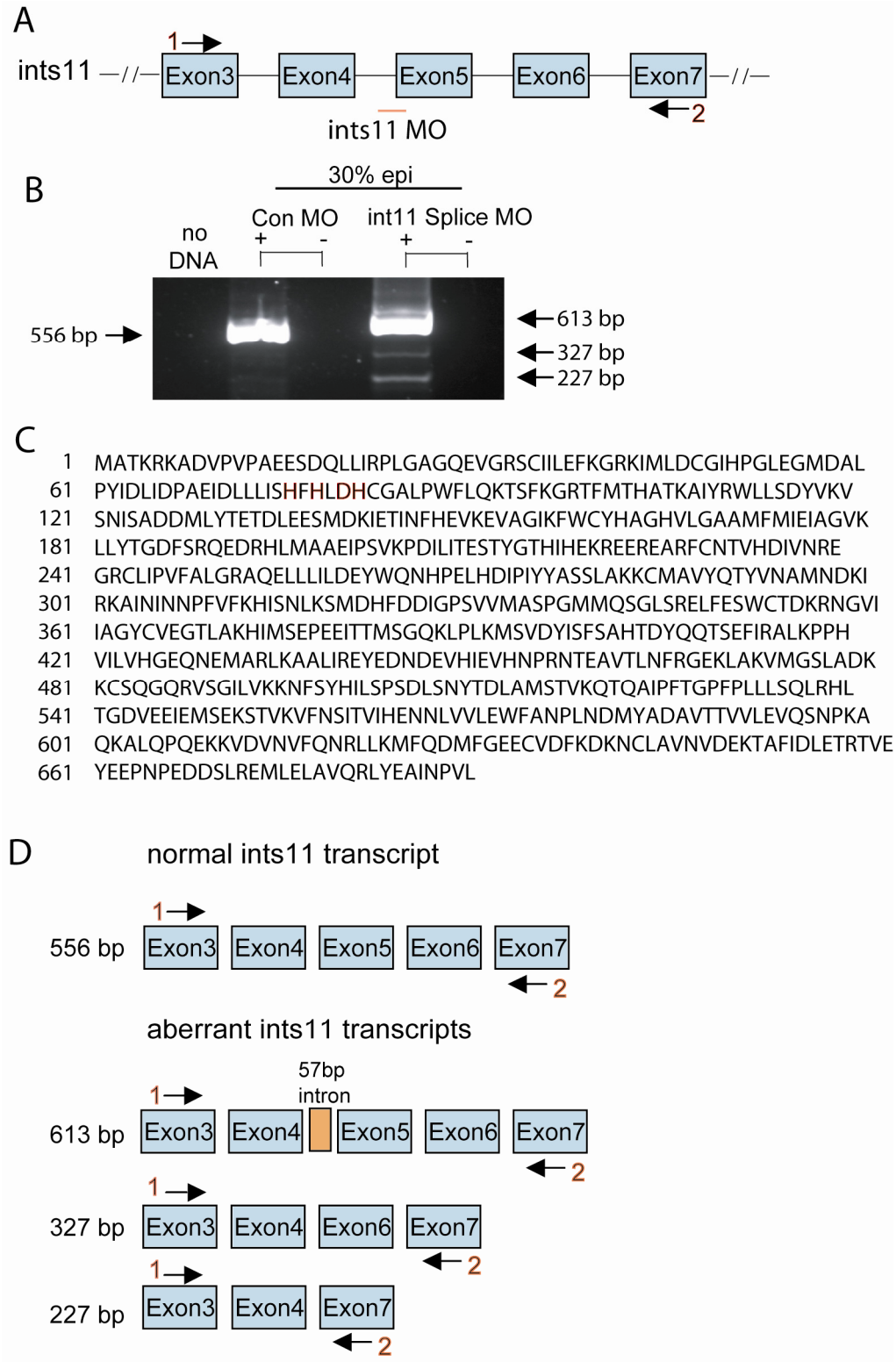
A
ints11
1
Exon3
Exon4
Exon5
Exon6
Exon7
2
ints11 MO
B
30% epi
Con MO
int11 Splice MO
no DNA
+ -
+ -
556 bp
613 bp
327 bp
227 bp
C
1 MATKRKADVPVPAEESDQLLIRPLGAGQEVGRSCIILEFKGRKIMLDCGIHPGLEGMDAL
61 PYIDLIDPAEIDLLLISHFHLDHCGALPWFLQKTSFKGRTFMTHATKAIYRWLLSDYVKV
121 SNISADDMLYTETDLEESMDKIETINFHEVKEVAGIKFWCYHAGHVLGAAMFMIEIAGVK
181 LLYTGDFSRQEDRHLMAAEIPSVKPDILITESTYGTHIHEKREEREARFCNTVHDIVNRE
241 GRCLIPVFALGRAQELLLILDEYWQNHPELHDIPIYYASSLAKKCMAVYQTYVNAMNDKI
301 RKAININNPFVFKHISNLKSMDHFDDIGPSVVMASPGMMQSGLSRELFESWCTDKRNGVI
361 IAGYCVEGTLAKHIMSEPEEITTMSGQKLPLKMSVDYISFSAHTDYQQTSEFIRALKPPH
421 VILVHGEQNEMARLKAALIREYEDNDEVHIEVHNPRNTEAVTLNFRGEKLAKVMGSLADK
481 KCSQGQRVSGILVKKNFSYHILSPSDLSNYTDLAMSTVKQTQAIPFTGPFPLLLSQLRHL
541 TGDVEEIEMSEKSTVKVFNSITVIHENNLVVLEWFANPLNDMYADAVTTVVLEVQSNPKA
601 QKALQPQEKKVDVNVFQNRLLKMFQDMFGEECVDFKDKNCLAVNVDEKTAFIDLETRTVE
661 YEEPNPEDDSLREMLELAVQRLYEAINPVL
D
normal ints11 transcript
556 bp
Exon3
Exon4
Exon5
Exon6
Exon7
aberrant ints11 transcripts
57bp intron
613 bp
327 bp
227 bp

Figure 5.3 The effect of *ints11* splice morpholino.

(A) Schematic representation of the *ints11* genomic locus. Numbered black arrows indicate the position of primers used in RT-PCRs to detect splicing. The orange bar shows the target site of the *ints11* splice-site morpholino. (B) RT-PCR analysis shows that the *ints11* splice junction morpholino disrupts correct splicing of *ints11* RNA. (C) Protein sequence of Ints11. The four amino acids in red form the catalytic center of Ints11, which resides at the beginning of exon5. (D) Schematic representation of normal or aberrant *ints11* transcripts is shown.

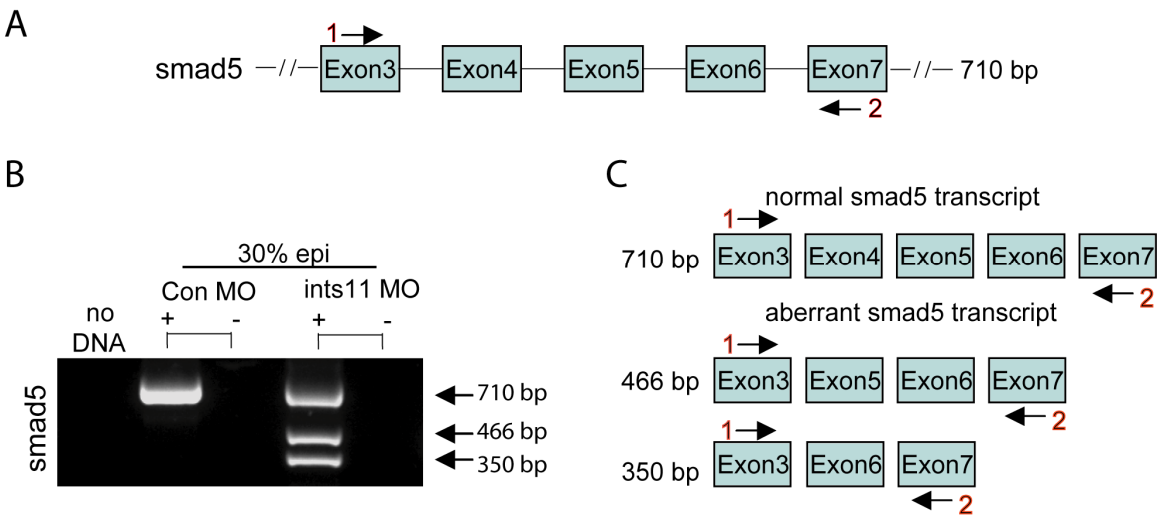
A
smad5
1
Exon3
Exon4
Exon5
Exon6
Exon7
710 bp
2
B
30% epi
Con MO
ints11 MO
no DNA
+
-
+
-
smad5
710 bp
466 bp
350 bp
C
normal smad5 transcript
710 bp
Exon3
Exon4
Exon5
Exon6
Exon7
aberrant smad5 transcript
466 bp
Exon3
Exon5
Exon6
Exon7
350 bp
Exon3
Exon6
Exon7

Figure 5.4 Knock-down of *ints11* perturbs *smad5* splicing.

(A) Schematic representation of the *smad5* genomic locus. Numbered black arrows indicate the position of primers used in RT-PCRs to detect splicing. (B) RT-PCR analysis shows that splicing of *smad5* is impaired in *ints11* morphants at 30% epiboly. (C) Schematic representations of normal and aberrantly spliced *smad5* transcripts.

Chapter VI

DISCUSSION

6.1 INTS5 IS REQUIRED FOR MULTIPLE FUNCTIONS DURING EARLY DEVELOPMENT

A gradient of BMP activity specifics dorsal-ventral fates in early zebrafish embryos (Kishimoto et al., 1997; Schier and Talbot, 2005). It may seem surprising that although Ints5 knockdown affects *smad1/5* splicing, we do not observe early dorso-ventral patterning and germ layer specification defects (Figures 3.6, 3.7), as observed for *smad5* and other BMP pathway mutants (Dick et al., 2000; Hild et al., 1999; Kishimoto et al., 1997; Kodjabachian et al., 1999; Mullins et al., 1996; Schmid et al., 2000; Schulte-Merker et al., 1997). This can be explained by the maternal deposition of Integrator complex factors such as Ints5 (Figure 3.2). The maternal Int proteins may allow normal functioning of the Integrator complex in early embryos, such that the early patterning events that are mediated by BMP signaling are not affected by knockdown of Ints5. The maternal function of Ints5 is difficult to study and remains elusive.

However, hematopoietic marker *scl* is only strongly expressed after gastrulation, when production of Ints5 protein has been disrupted by anti-sense morpholino oligos (Figure 3.4) (Gering et al., 1998). Therefore, the effects of *ints5* morpholino manifested on hematopoiesis.

We also observe convergence-extension (CE) cell movement defects in *ints5* morphants during gastrulation (Figure 3.7E-H). Later during somitogenesis, the bigger distance between the two strips of *scl* expressing cells in the intermediate cell mass (ICM) is also due to the early cell movement defects (Figures 3.9C, 3.11D). We found that, by monitoring the expression of *ntl/dlx3/hgg1*, co-injected *smad1* or *smad5* RNA not only restored blood formation in *ints5* morphants, but also rescued their CE defects (Figure

6.1C, D, I-L, M). Embryos injected with 10 pg of *smad1* or *smad5* RNA alone show normal CE movement (Figure 6.1E-H, M), similar to control morpholino-injected embryos (Figure 6.1A, B, M).

Thus, Ints5 is required for proper CE cell movement at mid-gastrulation stages (Figure 3.7F), and it is possible that the Integrator subunits regulate this process through *smad1/5* splicing as well. However, further investigation is required to confirm this.

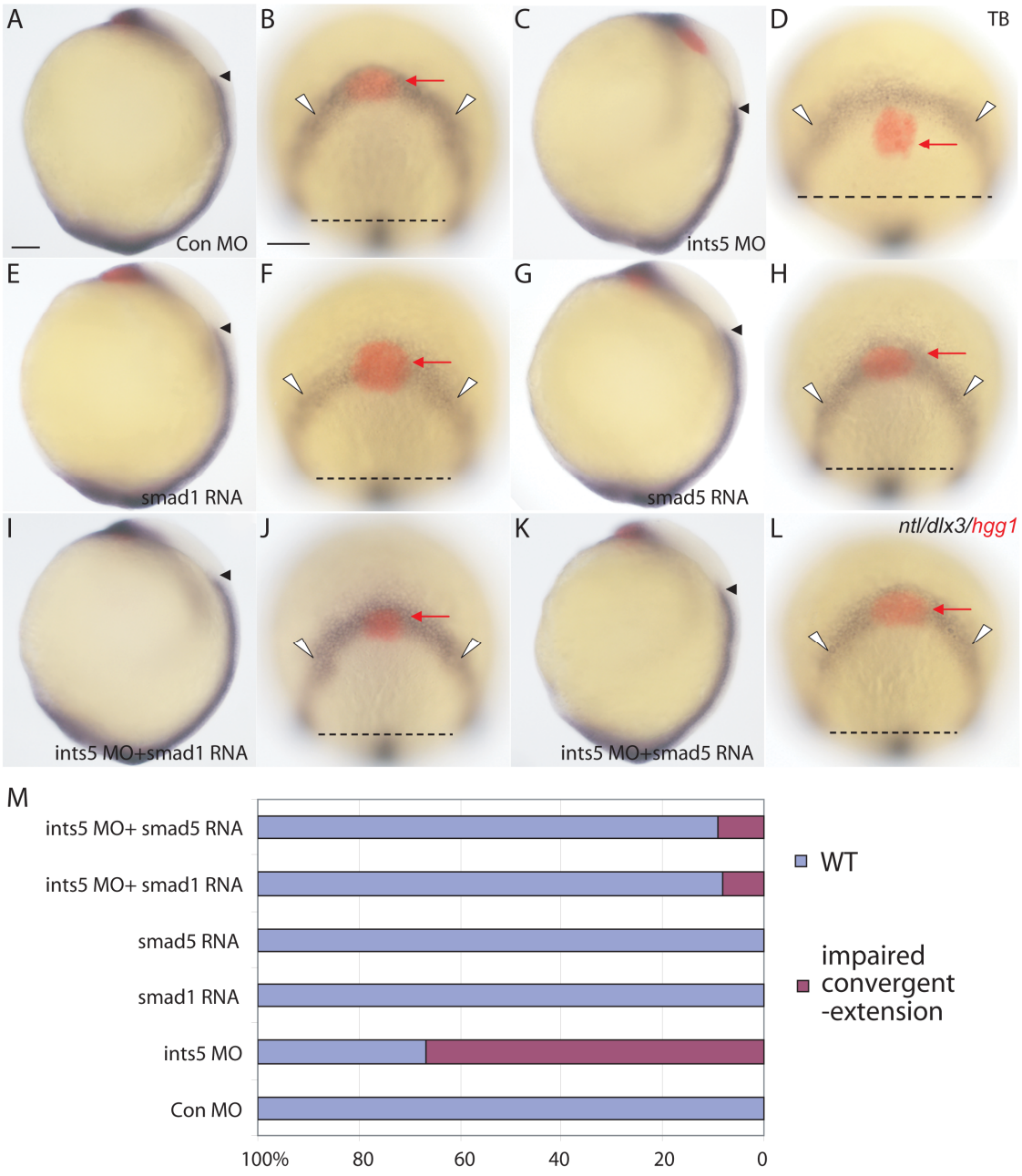
A
Con MO
B
C
ints5 MO
D
TB
E
smad1 RNA
F
G
smad5 RNA
H
I
ints5 MO+smad1 RNA
J
K
ints5 MO+smad5 RNA
L
ntl/dlx3/hgg1
M
ints5 MO+ smad5 RNA
ints5 MO+ smad1 RNA
smad5 RNA
smad1 RNA
ints5 MO
Con MO
100%
80
60
40
20
0
WT
impaired convergent -extension

Figure 6.1 Convergent-extension defects in *ints5* morphants are rescued by *smad1* and *smad5* RNA.

(A-L) Whole mount in situ hybridization to detect *ntl*, *dlx3* and *hgg1* expression in tailbud (TB, 10 hpf) embryos injected with control morpholinos (A, B), *ints5* morpholinos (C, D), *smad1* RNA (E, F), *smad5* RNA (G, H), *ints5* morpholinos and *smad1* RNA (I, J), or *ints5* morpholinos with *smad5* RNA (K, L). Black arrowheads indicate the anterior limit of *ntl* expression in the midline, and red arrows indictae *hgg1* staining in the anterior prechordal plate mesendoderm cells. White arrowheads and dotted lines indicate the distance between the lateral limits of *dlx3* expression in the neuroectoderm. (A, C, E, G, I, K) show lateral views of embryos with dorsal to the right; (B, D, F, H, J, L) show animal pole views of embryos. (M) Histogram showing percentage of injected embryos with wild type (WT, blue) or impaired (magenta) cell movement marked by *ntl/dlx3/hgg1* expression. Scale bar in (A) and (B), 50 μm.

6.2 THE INTEGRATOR SPECIFICALLY REGULATES BMP/SMAD SIGNALING.

The Integrator complex is thought to function in RNA processing, which is important for every cell. However, my findings show that only *smad1* and *smad5* splicing are affected in *ints5* morphants whereas expression of other *smads* (for e.g., *smad 2*, *smad3a*, *smad3b*) is not disrupted, suggesting that the Int complex does not generally affect all *smad* splicing. Furthermore, our analysis of several other genes (eg, *sqt, cyc* and others) shows that disruption of Integrator complex function does not generally affect genes expressed during gastrulation. In addition, depletion of Ints5 in *Drosophila* germarium specifically affects Dpp signaling activities, which in turn leads to no differentiated mature oocytes (Cai et al., unpublished data). This raises the possibility that the Integrator complex has a specific effect on BMP/SMAD signaling or functions specifically in the cells that respond to BMP signaling, so as to regulate hematopoiesis.

One interesting question is to understand how Integrator subunits specifically regulate BMP/SMAD signaling, although they are proteins with presumed house keeping functions. In fact, it is gradually known that mutations in some transcription or translation machinery components can lead to very specific defects in distinct cell-types (Pellizzoni, 2007; van der Knaap et al., 2006). For example, the vanishing white matter disease (VWM) is characterized by early childhood onset of chronic neurological deterioration. The basic defect of this striking disease resides in any of the five genes encoding the subunits of eukaryotic translation initiation factor eIF2B, which is essential in all cells for protein synthesis. Although the defect is in housekeeping genes, oligodendrocytes and astrocytes are predominantly affected, whereas other cell types are surprisingly spared.

The selective vulnerability of glia for defects in eIF2B mutant is poorly understood (van der Knaap et al., 2006).

In addition, the survival motor neuron (SMN) protein is part of a macromolecular complex that functions in the biogenesis of small nuclear ribonucleoproteins (snRNPs), which are essential for pre-mRNA splicing. Reduced level of SMN expression causes the inherited motor neuron disease spinal muscular atrophy (SMA) (Pellizzoni, 2007). Work in recent years show that the SMN complex acts as a macromolecular chaperone of snRNPs to increase the efficiency and fidelity of RNA–protein interactions *in vivo*, and to provide an opportunity for these interactions to be regulated (Pellizzoni, 2007). It is indicated that the RNA metabolism deficiencies underlying SMA affect the homeostasis of specific mRNAs encoding proteins essential for motor neuron development and function.

Similarly, Diamond-Blackfan anemia (DBA) has long been a puzzle for hematologists. This syndrome is characterized by defective erythropoiesis, low stature and malformations (Shimamura, 2008). It is caused by mutations in human ribosomal proteins, mainly ribosomal protein S19 (RPS19). Human cells with RPS mutation are not able to process ribosomal RNA (rRNA) (Dianzani and Loreni, 2008). Recently, Uechi et al. developed an RPS19-deficient zebrafish by knocking down *rps19* using an anti-sense morpholino oligo. The RPS19-deficient animals showed a dramatic decrease in blood cells as well at early developmental stages. These phenotypes can be rescued by injection of zebrafish *rps19* mRNA, but not by injection of *rps19* mRNAs with mutations that have been identified in DBA patients (Uechi et al., 2008). These results indicate that *rps19* is essential for hematopoietic differentiation during early embryogenesis. It is also reported

that increased abnormally spliced forms of FLVCR1 are observed in DBA immature erythroid cells, although *FLVCR1* itself is not mutated (Rey et al., 2008). The FLVCR protein is a heme exporter and the receptor for the subgroup C leukemia retrovirus. A phenotype similar to DBA is shown by *Flvcr1* null mice as well (Keel et al., 2008). These discoveries suggest a possible functional link between rRNA processing and erythropoiesis through *FLVCR1* transcript splicing. However, the definite role of FLVCR1 in regulating erythropoiesis is not clear. Neither it is known how exactly a defect in RPS19 or other RPS genes can influence *FLVCR1* splicing specifically.

Recent work by Watanabe et al. has shown that SF3b4, a subunit of SF3b which is a common RNA splicing complex, specifically binds to BMPR-1A and inhibits BMP signaling during osteochondral cell differentiation (Watanabe et al., 2007). There may be a potential connection between TGFβ/BMP signaling and the small RNA or RNA processing machinery. So it is possible that Ints5, which is involved in U1/U2 snRNA maturation, which in turn is important for the pre-mRNA splicing, may cooperate with other RNA splicing factors in specific cellular contexts (such as hematopoietic progenitors), to specifically modulate BMP signaling via *smad1/smad5* RNA splicing. Alternatively, the post-transcriptional process of certain BMP signaling components (such as Smad1/5) is simply more sensitive than that of other genes during early zebrafish development.

6.3 SMAD5 SPLICING IS IMPORTANT FOR HEMATOPOIESIS

Although hematopoiesis has been extensively studied, the molecular program of hematopoietic stem cell induction and self-renewal remains unclear. Smads are

evolutionarily conserved transducers of the differentiation and growth arrest signals from the transforming growth factor β/BMP (TGF-β/BMP) family of ligands. Upon BMP receptor activation, the receptor regulated Smad1, 5, 8 are phosphorylated in the C-terminal MH2 domain and recruit the common subunit Smad4 to the nucleus to mediate target gene expression (Heldin et al., 1997; Kretzschmar and Massague, 1998; Massague, 1998). The TGF-β/BMP superfamily of multifunctional cytokines regulates proliferation, differentiation, and apoptosis in hematopoietic cells and a variety of other tissues and cell types (Eaves et al., 1991). Homozygous *SMAD5* null mice undergo embryonic lethality with abnormal vasculature and blood cells (Chang et al., 1999; Yang et al., 1999). Recent studies demonstrate that SMAD1 and SMAD5, as well as the type I receptors ALK3 and ALK6, are expressed in $CD34^{+}CD38^{-}lin^{-}$ human hematopoietic stem cells, which are capable of giving rise to all the lineages in nonobese diabetic/severe combined immune deficient (NOD/SCID) mice (Bhatia et al., 1999). Despite the growing body of evidence, very little is known about the mechanisms underlying the differential regulation of hematopoiesis by TGF-β/BMP.

Recent work has revealed that the post-transcriptional processing of BMP Smads is involved in maintenance of hematopoietic stem cell identity. Jiang *et al*. identified a ubiquitously expressed novel isoform, SMAD5β, which encodes a 351 amino acid protein with a truncated MH2 domain and a unique C-terminal tail of 18 amino acids (Jiang et al., 2000). Yeast 2-hybrid interaction assays reveal that the SMAD5β isoform does not homodimerize or heterodimerize with SMAD5 or SMAD4, so it may be the functional equivalent of inactivating mutations. Smad5β is expressed in both normal hematopoiesis and leukemogenesis (Jiang et al., 2000). Interestingly, the expression level

of the *smad5β* isoform is higher in CD34+ hematopoietic stem cells than in terminally differentiated peripheral blood leukocytes, thereby implicating a function for the β form in stem cell homeostasis (Jiang et al., 2000). It is also indicated that the alternative splicing of *smad5* is differentially regulated during maturation of hematopoietic cells. Our work shows that the splicing of *smad1/5* is impaired by knockdown of Ints5. Aberrant splicing of *smad5* leads to production of dominant negative forms of Smad5, the over-expression of which phenocopies the hematopoiesis phenotypes we observe in *ints5* morphants. These include reduced expression of *scl*, and eventually, failure in erythrocyte differentiation. Thus, accurate splicing of *smad5* is crucial for the normal progression of hematopoiesis and erythropoietic differentiation, and the failure to generate appropriate Smad5 products can lead to a reduction of hematopoietic progenitors.

6.4 SPECULATION: DYSFUNCTION OF INTEGRATOR SUBUNITS IS INVOLVED IN DISEASE

Eukaryotic pre-mRNA splicing allows for a large, diverse proteome to be coded by a relatively small genome. Usually alternative splicing events are well regulated, but when mutations disrupt the splicing machinery, disease can occur, as mutations can cause disease through aberrant transcript production. As the Integrator complex plays a vital role in transcription and processing of snRNA, which in turn regulate pre-mRNA processing, dysfunction of the Integrator subunits may lead to various defects.

In our study, knockdown of Integrator subunits leads to defects in zebrafish erythropoiesis differentiation. It is possible that mutations of *ints* can cause syndromes

similar to DBA disease in human. Therefore, it is worth sequencing each Integrator subunit in the human patients with anemia or unidentified anemia cell lines. If *ints* are anemia related genes, the ints-deficient zebrafish will provide a valuable model for investigating the molecular mechanisms of anemia development in humans.

Besides, deficiencies in mRNA splicing have also been shown to cause many other genetic disorders (Pellizzoni, 2007; Solis et al., 2008). In fact, recent work has shown that disruption of the murine Integrator subunit 1 (Ints1) causes growth arrest and eventual apoptosis at early blastocyst stages (Hata and Nakayama, 2007). *Ints1*$^{-/-}$ embryos have increased levels of unprocessed primary U2 snRNA transcripts but decreased levels of mature U2 snRNA transcripts compared to heterozygotes. Thus, Ints1 is suggested to play a non-redundant role, for instance, as a scaffold for the assembly of the Integrator complex, in the mouse embryo (Hata and Nakayama, 2007). In addition, Integrator subunit 3 is a probable target for the 1q21 amplification found in most hepatocellular carcinoma (HCC) tumors, and may be involved in the development and/or progression of this cancer (Inagaki et al., 2008).

However, it is still unclear how these genes function, and how their malfunction leads to profound defects in specific biological processes. The study presented here reveals a potential link between snRNA processing and BMP signaling in hematopoiesis. Understanding the precise mechanisms by which the individual subunits function may provide insights into the roles played by the Integrator complex during development and tumorigenesis.

Reference

Abe, E. (2006). Function of BMPs and BMP antagonists in adult bone. *Ann N Y Acad Sci* **1068**, 41-53.

Akimenko, M. A., Ekker, M., Wegner, J., Lin, W. and Westerfield, M. (1994). Combinatorial expression of three zebrafish genes related to distal-less: part of a homeobox gene code for the head. *J Neurosci* **14**, 3475-86.

Alberts, B., Johnson, A., Lewis, J., Raff, M., Roberts, K. and Walter, P. (2002). molecular biology of the cell. 319-320.

Alexander, J. and Stainier, D. Y. (1999). A molecular pathway leading to endoderm formation in zebrafish. *Curr Biol* **9**, 1147-57.

Aono, A., Hazama, M., Notoya, K., Taketomi, S., Yamasaki, H., Tsukuda, R., Sasaki, S. and Fujisawa, Y. (1995). Potent ectopic bone-inducing activity of bone morphogenetic protein-4/7 heterodimer. *Biochem Biophys Res Commun* **210**, 670-7.

Attisano, L. and Wrana, J. L. (2002). Signal transduction by the TGF-beta superfamily. *Science* **296**, 1646-7.

Aubin, J., Davy, A. and Soriano, P. (2004). In vivo convergence of BMP and MAPK signaling pathways: impact of differential Smad1 phosphorylation on development and homeostasis. *Genes Dev* **18**, 1482-94.

Baillat, D., Hakimi, M. A., Naar, A. M., Shilatifard, A., Cooch, N. and Shiekhattar, R. (2005). Integrator, a multiprotein mediator of small nuclear RNA processing, associates with the C-terminal repeat of RNA polymerase II. *Cell* **123**, 265-76.

Bauer, H., Lele, Z., Rauch, G. J., Geisler, R. and Hammerschmidt, M. (2001). The type I serine/threonine kinase receptor Alk8/Lost-a-fin is required for Bmp2b/7 signal transduction during dorsoventral patterning of the zebrafish embryo. *Development* **128**, 849-58.

Beanan, M. J. and Sargent, T. D. (2000). Regulation and function of Dlx3 in vertebrate development. *Dev Dyn* **218**, 545-53.

Bennett, C. M., Kanki, J. P., Rhodes, J., Liu, T. X., Paw, B. H., Kieran, M. W., Langenau, D. M., Delahaye-Brown, A., Zon, L. I., Fleming, M. D. et al. (2001). Myelopoiesis in the zebrafish, Danio rerio. *Blood* **98**, 643-51.

Berman, J. N., Kanki, J. P. and Look, A. T. (2005). Zebrafish as a model for myelopoiesis during embryogenesis. *Exp Hematol* **33**, 997-1006.

Bhardwaj, G., Murdoch, B., Wu, D., Baker, D. P., Williams, K. P., Chadwick, K., Ling, L. E., Karanu, F. N. and Bhatia, M. (2001). Sonic hedgehog induces the proliferation of primitive human hematopoietic cells via BMP regulation. *Nat Immunol* **2**, 172-80.

Bhatia, M., Bonnet, D., Wu, D., Murdoch, B., Wrana, J., Gallacher, L. and Dick, J. E. (1999). Bone morphogenetic proteins regulate the developmental program of human hematopoietic stem cells. *J Exp Med* **189**, 1139-48.

Blader, P., Rastegar, S., Fischer, N. and Strahle, U. (1997). Cleavage of the BMP-4 antagonist chordin by zebrafish tolloid. *Science* **278**, 1937-40.

Breslin, M. B., Lindberg, I., Benjannet, S., Mathis, J. P., Lazure, C. and Seidah, N. G. (1993). Differential processing of proenkephalin by prohormone convertases 1(3) and 2 and furin. *J Biol Chem* **268**, 27084-93.

Bresnahan, P. A., Leduc, R., Thomas, L., Thorner, J., Gibson, H. L., Brake, A. J., Barr, P. J. and Thomas, G. (1990). Human fur gene encodes a yeast KEX2-like endoprotease that cleaves pro-beta-NGF in vivo. *J Cell Biol* **111**, 2851-9.

Brownlie, A., Donovan, A., Pratt, S. J., Paw, B. H., Oates, A. C., Brugnara, C., Witkowska, H. E., Sassa, S. and Zon, L. I. (1998). Positional cloning of the zebrafish sauternes gene: a model for congenital sideroblastic anaemia. *Nat Genet* **20**, 244-50.

Brownlie, A., Hersey, C., Oates, A. C., Paw, B. H., Falick, A. M., Witkowska, H. E., Flint, J., Higgs, D., Jessen, J., Bahary, N. et al. (2003). Characterization of embryonic globin genes of the zebrafish. *Dev Biol* **255**, 48-61.

Burns, C. E., DeBlasio, T., Zhou, Y., Zhang, J., Zon, L. and Nimer, S. D. (2002). Isolation and characterization of runxa and runxb, zebrafish members of the runt family of transcriptional regulators. *Exp Hematol* **30**, 1381-9.

Byrd, N., Becker, S., Maye, P., Narasimhaiah, R., St-Jacques, B., Zhang, X., McMahon, J., McMahon, A. and Grabel, L. (2002). Hedgehog is required for murine yolk sac angiogenesis. *Development* **129**, 361-72.

Callebaut, I., Moshous, D., Mornon, J. P. and de Villartay, J. P. (2002). Metallo-beta-lactamase fold within nucleic acids processing enzymes: the beta-CASP family. *Nucleic Acids Res* **30**, 3592-601.

Carradice, D. and Lieschke, G. J. (2008). Zebrafish in hematology: sushi or science? *Blood* **111**, 3331-42.

Catlett, I. M. and Hedrick, S. M. (2005). Suppressor of cytokine signaling 1 is required for the differentiation of CD4+ T cells. *Nat Immunol* **6**, 715-21.

Cebe-Suarez, S., Zehnder-Fjallman, A. and Ballmer-Hofer, K. (2006). The role of VEGF receptors in angiogenesis; complex partnerships. *Cell Mol Life Sci* **63**, 601-15.

Chadwick, K., Wang, L., Li, L., Menendez, P., Murdoch, B., Rouleau, A. and Bhatia, M. (2003). Cytokines and BMP-4 promote hematopoietic differentiation of human embryonic stem cells. *Blood* **102**, 906-15.

Chang, H., Huylebroeck, D., Verschueren, K., Guo, Q., Matzuk, M. M. and Zwijsen, A. (1999). Smad5 knockout mice die at mid-gestation due to multiple embryonic and extraembryonic defects. *Development* **126**, 1631-42.

Chen, Y. and Struhl, G. (1998). In vivo evidence that Patched and Smoothened constitute distinct binding and transducing components of a Hedgehog receptor complex. *Development* **125**, 4943-8.

Chen, Y. G. and Massague, J. (1999). Smad1 recognition and activation by the ALK1 group of transforming growth factor-beta family receptors. *J Biol Chem* **274**, 3672-7.

Childs, S., Weinstein, B. M., Mohideen, M. A., Donohue, S., Bonkovsky, H. and Fishman, M. C. (2000). Zebrafish dracula encodes ferrochelatase and its mutation provides a model for erythropoietic protoporphyria. *Curr Biol* **10**, 1001-4.

Christian, J. L. and Nakayama, T. (1999). Can't get no SMADisfaction: Smad proteins as positive and negative regulators of TGF-beta family signals. *Bioessays* **21**, 382-90.

Clarke, T. R., Hoshiya, Y., Yi, S. E., Liu, X., Lyons, K. M. and Donahoe, P. K. (2001). Mullerian inhibiting substance signaling uses a bone morphogenetic protein (BMP)-like pathway mediated by ALK2 and induces SMAD6 expression. *Mol Endocrinol* **15**, 946-59.

Connors, S. A., Trout, J., Ekker, M. and Mullins, M. C. (1999). The role of tolloid/mini fin in dorsoventral pattern formation of the zebrafish embryo. *Development* **126**, 3119-30.

Creemers, J. W., Groot Kormelink, P. J., Roebroek, A. J., Nakayama, K. and Van de Ven, W. J. (1993). Proprotein processing activity and cleavage site selectivity of the Kex2-like endoprotease PACE4. *FEBS Lett* **336**, 65-9.

Croker, B. A., Kiu, H. and Nicholson, S. E. (2008). SOCS regulation of the JAK/STAT signalling pathway. *Semin Cell Dev Biol* **19**, 414-22.

Cui, Y., Hackenmiller, R., Berg, L., Jean, F., Nakayama, T., Thomas, G. and Christian, J. L. (2001). The activity and signaling range of mature BMP-4 is regulated by sequential cleavage at two sites within the prodomain of the precursor. *Genes Dev* **15**, 2797-802.

Cui, Y., Jean, F., Thomas, G. and Christian, J. L. (1998). BMP-4 is proteolytically activated by furin and/or PC6 during vertebrate embryonic development. *Embo J* **17**, 4735-43.

Dale, L. and Jones, C. M. (1999). BMP signalling in early Xenopus development. *Bioessays* **21**, 751-60.

Dale, L. and Wardle, F. C. (1999). A gradient of BMP activity specifies dorsal-ventral fates in early Xenopus embryos. *Semin Cell Dev Biol* **10**, 319-26.

Davidson, A. J., Ernst, P., Wang, Y., Dekens, M. P., Kingsley, P. D., Palis, J., Korsmeyer, S. J., Daley, G. Q. and Zon, L. I. (2003). cdx4 mutants fail to specify blood progenitors and can be rescued by multiple hox genes. *Nature* **425**, 300-6.

Davidson, A. J. and Zon, L. I. (2004). The 'definitive' (and 'primitive') guide to zebrafish hematopoiesis. *Oncogene* **23**, 7233-46.

de Caestecker, M. P., Piek, E. and Roberts, A. B. (2000). Role of transforming growth factor-beta signaling in cancer. *J Natl Cancer Inst* **92**, 1388-402.

de Jong, J. L. and Zon, L. I. (2005). Use of the zebrafish system to study primitive and definitive hematopoiesis. *Annu Rev Genet* **39**, 481-501.

De Robertis, E. M., Larrain, J., Oelgeschlager, M. and Wessely, O. (2000). The establishment of Spemann's organizer and patterning of the vertebrate embryo. *Nat Rev Genet* **1**, 171-81.

De Robertis, E. M., Wessely, O., Oelgeschlager, M., Brizuela, B., Pera, E., Larrain, J., Abreu, J. and Bachiller, D. (2001). Molecular mechanisms of cell-cell signaling by the Spemann-Mangold organizer. *Int J Dev Biol* **45**, 189-97.

Denef, N., Neubuser, D., Perez, L. and Cohen, S. M. (2000). Hedgehog induces opposite changes in turnover and subcellular localization of patched and smoothened. *Cell* **102**, 521-31.

Deng, Z., Morse, J. H., Slager, S. L., Cuervo, N., Moore, K. J., Venetos, G., Kalachikov, S., Cayanis, E., Fischer, S. G., Barst, R. J. et al. (2000). Familial primary pulmonary hypertension (gene PPH1) is caused by mutations in the bone morphogenetic protein receptor-II gene. *Am J Hum Genet* **67**, 737-44.

Derynck, R. and Zhang, Y. E. (2003). Smad-dependent and Smad-independent pathways in TGF-beta family signalling. *Nature* **425**, 577-84.

Detrich, H. W., 3rd, Kieran, M. W., Chan, F. Y., Barone, L. M., Yee, K., Rundstadler, J. A., Pratt, S., Ransom, D. and Zon, L. I. (1995). Intraembryonic

hematopoietic cell migration during vertebrate development. *Proc Natl Acad Sci U S A* **92**, 10713-7.

Dianzani, I. and Loreni, F. (2008). Diamond-Blackfan anemia: a ribosomal puzzle. *Haematologica* **93**, 1601-4.

Dick, A., Hild, M., Bauer, H., Imai, Y., Maifeld, H., Schier, A. F., Talbot, W. S., Bouwmeester, T. and Hammerschmidt, M. (2000). Essential role of Bmp7 (snailhouse) and its prodomain in dorsoventral patterning of the zebrafish embryo. *Development* **127**, 343-54.

Dick, A., Meier, A. and Hammerschmidt, M. (1999). Smad1 and Smad5 have distinct roles during dorsoventral patterning of the zebrafish embryo. *Dev Dyn* **216**, 285-98.

Dominski, Z., Yang, X. C., Purdy, M., Wagner, E. J. and Marzluff, W. F. (2005). A CPSF-73 homologue is required for cell cycle progression but not cell growth and interacts with a protein having features of CPSF-100. *Mol Cell Biol* **25**, 1489-500.

Donovan, A., Brownlie, A., Dorschner, M. O., Zhou, Y., Pratt, S. J., Paw, B. H., Phillips, R. B., Thisse, C., Thisse, B. and Zon, L. I. (2002). The zebrafish mutant gene chardonnay (cdy) encodes divalent metal transporter 1 (DMT1). *Blood* **100**, 4655-9.

Donovan, A., Brownlie, A., Zhou, Y., Shepard, J., Pratt, S. J., Moynihan, J., Paw, B. H., Drejer, A., Barut, B., Zapata, A. et al. (2000). Positional cloning of zebrafish ferroportin1 identifies a conserved vertebrate iron exporter. *Nature* **403**, 776-81.

Dooley, K. A., Davidson, A. J. and Zon, L. I. (2005). Zebrafish scl functions independently in hematopoietic and endothelial development. *Dev Biol* **277**, 522-36.

Driever, W., Solnica-Krezel, L., Schier, A. F., Neuhauss, S. C., Malicki, J., Stemple, D. L., Stainier, D. Y., Zwartkruis, F., Abdelilah, S., Rangini, Z. et al. (1996). A

genetic screen for mutations affecting embryogenesis in zebrafish. *Development* **123**, 37-46.

Dubois, C. M., Laprise, M. H., Blanchette, F., Gentry, L. E. and Leduc, R. (1995). Processing of transforming growth factor beta 1 precursor by human furin convertase. *J Biol Chem* **270**, 10618-24.

Eaves, C. J., Cashman, J. D., Kay, R. J., Dougherty, G. J., Otsuka, T., Gaboury, L. A., Hogge, D. E., Lansdorp, P. M., Eaves, A. C. and Humphries, R. K. (1991). Mechanisms that regulate the cell cycle status of very primitive hematopoietic cells in long-term human marrow cultures. II. Analysis of positive and negative regulators produced by stromal cells within the adherent layer. *Blood* **78**, 110-7.

Ebisawa, T., Fukuchi, M., Murakami, G., Chiba, T., Tanaka, K., Imamura, T. and Miyazono, K. (2001). Smurf1 interacts with transforming growth factor-beta type I receptor through Smad7 and induces receptor degradation. *J Biol Chem* **276**, 12477-80.

Echelard, Y., Epstein, D. J., St-Jacques, B., Shen, L., Mohler, J., McMahon, J. A. and McMahon, A. P. (1993). Sonic hedgehog, a member of a family of putative signaling molecules, is implicated in the regulation of CNS polarity. *Cell* **75**, 1417-30.

Egloff, S. and Murphy, S. (2008). Role of the C-terminal domain of RNA polymerase II in expression of small nuclear RNA genes. *Biochem Soc Trans* **36**, 537-9.

Egloff, S., O'Reilly, D., Chapman, R. D., Taylor, A., Tanzhaus, K., Pitts, L., Eick, D. and Murphy, S. (2007). Serine-7 of the RNA polymerase II CTD is specifically required for snRNA gene expression. *Science* **318**, 1777-9.

Egloff, S., O'Reilly, D. and Murphy, S. (2008). Expression of human snRNA genes from beginning to end. *Biochem Soc Trans* **36**, 590-4.

Fainsod, A., Steinbeisser, H. and De Robertis, E. M. (1994). On the function of BMP-4 in patterning the marginal zone of the Xenopus embryo. *Embo J* **13**, 5015-25.

Fehling, H. J., Lacaud, G., Kubo, A., Kennedy, M., Robertson, S., Keller, G. and Kouskoff, V. (2003). Tracking mesoderm induction and its specification to the hemangioblast during embryonic stem cell differentiation. *Development* **130**, 4217-27.

Foley, R. N. (2008). Erythropoietin: physiology and molecular mechanisms. *Heart Fail Rev* **13**, 405-14.

Fried, W. (2009). Erythropoietin and Erythropoiesis. *Exp Hematol*.

Fury, M. G. and Zieve, G. W. (1996). U6 snRNA maturation and stability. *Exp Cell Res* **228**, 160-3.

Galloway, J. L., Wingert, R. A., Thisse, C., Thisse, B. and Zon, L. I. (2005). Loss of gata1 but not gata2 converts erythropoiesis to myelopoiesis in zebrafish embryos. *Dev Cell* **8**, 109-16.

Galloway, J. L. and Zon, L. I. (2003). Ontogeny of hematopoiesis: examining the emergence of hematopoietic cells in the vertebrate embryo. *Curr Top Dev Biol* **53**, 139-58.

Gering, M. and Patient, R. (2005). Hedgehog signaling is required for adult blood stem cell formation in zebrafish embryos. *Dev Cell* **8**, 389-400.

Gering, M., Rodaway, A. R., Gottgens, B., Patient, R. K. and Green, A. R. (1998). The SCL gene specifies haemangioblast development from early mesoderm. *Embo J* **17**, 4029-45.

Gering, M., Yamada, Y., Rabbitts, T. H. and Patient, R. K. (2003). Lmo2 and Scl/Tal1 convert non-axial mesoderm into haemangioblasts which differentiate into endothelial cells in the absence of Gata1. *Development* **130**, 6187-99.

Gluecksohn-Schoenheimer, S. (1944). The Development of Normal and Homozygous Brachy (T/T) Mouse Embryos in the Extraembryonic Coelom of the Chick. *Proc Natl Acad Sci U S A* **30**, 134-40.

Gore, A. V., Maegawa, S., Cheong, A., Gilligan, P. C., Weinberg, E. S. and Sampath, K. (2005). The zebrafish dorsal axis is apparent at the four-cell stage. *Nature* **438**, 1030-5.

Graff, J. M. (1997). Embryonic patterning: to BMP or not to BMP, that is the question. *Cell* **89**, 171-4.

Griffin, K. J., Amacher, S. L., Kimmel, C. B. and Kimelman, D. (1998). Molecular identification of spadetail: regulation of zebrafish trunk and tail mesoderm formation by T-box genes. *Development* **125**, 3379-88.

Guo, X. and Wang, X. F. (2009). Signaling cross-talk between TGF-beta/BMP and other pathways. *Cell Res* **19**, 71-88.

Haerry, T. E., Khalsa, O., O'Connor, M. B. and Wharton, K. A. (1998). Synergistic signaling by two BMP ligands through the SAX and TKV receptors controls wing growth and patterning in Drosophila. *Development* **125**, 3977-87.

Haffter, P., Granato, M., Brand, M., Mullins, M. C., Hammerschmidt, M., Kane, D. A., Odenthal, J., van Eeden, F. J., Jiang, Y. J., Heisenberg, C. P. et al. (1996). The identification of genes with unique and essential functions in the development of the zebrafish, Danio rerio. *Development* **123**, 1-36.

Hammerschmidt, M., Brook, A. and McMahon, A. P. (1997). The world according to hedgehog. *Trends Genet* **13**, 14-21.

Hammerschmidt, M., Pelegri, F., Mullins, M. C., Kane, D. A., van Eeden, F. J., Granato, M., Brand, M., Furutani-Seiki, M., Haffter, P., Heisenberg, C. P. et al. (1996). dino and mercedes, two genes regulating dorsal development in the zebrafish embryo. *Development* **123**, 95-102.

Hara, T. and Miyajima, A. (1996). Function and signal transduction mediated by the interleukin 3 receptor system in hematopoiesis. *Stem Cells* **14**, 605-18.

Harland, R. and Gerhart, J. (1997). Formation and function of Spemann's organizer. *Annu Rev Cell Dev Biol* **13**, 611-67.

Hassel, S., Eichner, A., Yakymovych, M., Hellman, U., Knaus, P. and Souchelnytskyi, S. (2004). Proteins associated with type II bone morphogenetic protein receptor (BMPR-II) and identified by two-dimensional gel electrophoresis and mass spectrometry. *Proteomics* **4**, 1346-58.

Hata, A., Lagna, G., Massague, J. and Hemmati-Brivanlou, A. (1998). Smad6 inhibits BMP/Smad1 signaling by specifically competing with the Smad4 tumor suppressor. *Genes Dev* **12**, 186-97.

Hata, T. and Nakayama, M. (2007). Targeted disruption of the murine large nuclear KIAA1440/Ints1 protein causes growth arrest in early blastocyst stage embryos and eventual apoptotic cell death. *Biochim Biophys Acta* **1773**, 1039-51.

He, C. and Chen, X. (2005). Transcription regulation of the vegf gene by the BMP/Smad pathway in the angioblast of zebrafish embryos. *Biochem Biophys Res Commun* **329**, 324-30.

Heldin, C. H., Miyazono, K. and ten Dijke, P. (1997). TGF-beta signalling from cell membrane to nucleus through SMAD proteins. *Nature* **390**, 465-71.

Herbomel, P., Thisse, B. and Thisse, C. (1999). Ontogeny and behaviour of early macrophages in the zebrafish embryo. *Development* **126**, 3735-45.

Hild, M., Dick, A., Rauch, G. J., Meier, A., Bouwmeester, T., Haffter, P. and Hammerschmidt, M. (1999). The smad5 mutation somitabun blocks Bmp2b signaling during early dorsoventral patterning of the zebrafish embryo. *Development* **126**, 2149-59.

Holley, S. A. and Ferguson, E. L. (1997). Fish are like flies are like frogs: conservation of dorsal-ventral patterning mechanisms. *Bioessays* **19**, 281-4.

Holley, S. A., Jackson, P. D., Sasai, Y., Lu, B., De Robertis, E. M., Hoffmann, F. M. and Ferguson, E. L. (1995). A conserved system for dorsal-ventral patterning in insects and vertebrates involving sog and chordin. *Nature* **376**, 249-53.

Howe, J. R., Bair, J. L., Sayed, M. G., Anderson, M. E., Mitros, F. A., Petersen, G. M., Velculescu, V. E., Traverso, G. and Vogelstein, B. (2001). Germline mutations of the gene encoding bone morphogenetic protein receptor 1A in juvenile polyposis. *Nat Genet* **28**, 184-7.

Hsia, N. and Zon, L. I. (2005). Transcriptional regulation of hematopoietic stem cell development in zebrafish. *Exp Hematol* **33**, 1007-14.

Huber, T. L. and Zon, L. I. (1998). Transcriptional regulation of blood formation during Xenopus development. *Semin Immunol* **10**, 103-9.

Hudson, C., Clements, D., Friday, R. V., Stott, D. and Woodland, H. R. (1997). Xsox17alpha and -beta mediate endoderm formation in Xenopus. *Cell* **91**, 397-405.

Iemura, S., Yamamoto, T. S., Takagi, C., Uchiyama, H., Natsume, T., Shimasaki, S., Sugino, H. and Ueno, N. (1998). Direct binding of follistatin to a complex of bone-morphogenetic protein and its receptor inhibits ventral and epidermal cell fates in early Xenopus embryo. *Proc Natl Acad Sci U S A* **95**, 9337-42.

Inagaki, Y., Yasui, K., Endo, M., Nakajima, T., Zen, K., Tsuji, K., Minami, M., Tanaka, S., Taniwaki, M., Itoh, Y. et al. (2008). CREB3L4, INTS3, and SNAPAP are targets for the 1q21 amplicon frequently detected in hepatocellular carcinoma. *Cancer Genet Cytogenet* **180**, 30-6.

Itoh, S. and ten Dijke, P. (2007). Negative regulation of TGF-beta receptor/Smad signal transduction. *Curr Opin Cell Biol* **19**, 176-84.

Jagadeeswaran, P., Sheehan, J. P., Craig, F. E. and Troyer, D. (1999). Identification and characterization of zebrafish thrombocytes. *Br J Haematol* **107**, 731-8.

Jay, K. E., Gallacher, L. and Bhatia, M. (2002). Emergence of muscle and neural hematopoiesis in humans. *Blood* **100**, 3193-202.

Jegalian, A. G. and Wu, H. (2002). Differential roles of SOCS family members in EpoR signal transduction. *J Interferon Cytokine Res* **22**, 853-60.

Jiang, Y., Liang, H., Guo, W., Kottickal, L. V. and Nagarajan, L. (2000). Differential expression of a novel C-terminally truncated splice form of SMAD5 in hematopoietic stem cells and leukemia. *Blood* **95**, 3945-50.

Johansson, B. M. and Wiles, M. V. (1995). Evidence for involvement of activin A and bone morphogenetic protein 4 in mammalian mesoderm and hematopoietic development. *Mol Cell Biol* **15**, 141-51.

Johnson, S. L., Midson, C. N., Ballinger, E. W. and Postlethwait, J. H. (1994). Identification of RAPD primers that reveal extensive polymorphisms between laboratory strains of zebrafish. *Genomics* **19**, 152-6.

Joly, J. S., Joly, C., Schulte-Merker, S., Boulekbache, H. and Condamine, H. (1993). The ventral and posterior expression of the zebrafish homeobox gene eve1 is perturbed in dorsalized and mutant embryos. *Development* **119**, 1261-75.

Jurica, M. S. and Moore, M. J. (2003). Pre-mRNA splicing: awash in a sea of proteins. *Mol Cell* **12**, 5-14.

Kalev-Zylinska, M. L., Horsfield, J. A., Flores, M. V., Postlethwait, J. H., Vitas, M. R., Baas, A. M., Crosier, P. S. and Crosier, K. E. (2002). Runx1 is required for zebrafish blood and vessel development and expression of a human RUNX1-CBF2T1 transgene advances a model for studies of leukemogenesis. *Development* **129**, 2015-30.

Kanai, Y., Kanai-Azuma, M., Noce, T., Saido, T. C., Shiroishi, T., Hayashi, Y. and Yazaki, K. (1996). Identification of two Sox17 messenger RNA isoforms, with and without the high mobility group box region, and their differential expression in mouse spermatogenesis. *J Cell Biol* **133**, 667-81.

Karanu, F. N., Murdoch, B., Gallacher, L., Wu, D. M., Koremoto, M., Sakano, S. and Bhatia, M. (2000). The notch ligand jagged-1 represents a novel growth factor of human hematopoietic stem cells. *J Exp Med* **192**, 1365-72.

Kavsak, P., Rasmussen, R. K., Causing, C. G., Bonni, S., Zhu, H., Thomsen, G. H. and Wrana, J. L. (2000). Smad7 binds to Smurf2 to form an E3 ubiquitin ligase that targets the TGF beta receptor for degradation. *Mol Cell* **6**, 1365-75.

Kawabata, M., Inoue, H., Hanyu, A., Imamura, T. and Miyazono, K. (1998). Smad proteins exist as monomers in vivo and undergo homo- and hetero-oligomerization upon activation by serine/threonine kinase receptors. *Embo J* **17**, 4056-65.

Kawahara, A. and Dawid, I. B. (2000). Expression of the Kruppel-like zinc finger gene biklf during zebrafish development. *Mech Dev* **97**, 173-6.

Keel, S. B., Doty, R. T., Yang, Z., Quigley, J. G., Chen, J., Knoblaugh, S., Kingsley, P. D., De Domenico, I., Vaughn, M. B., Kaplan, J. et al. (2008). A heme export protein is required for red blood cell differentiation and iron homeostasis. *Science* **319**, 825-8.

Khalsa, O., Yoon, J. W., Torres-Schumann, S. and Wharton, K. A. (1998). TGF-beta/BMP superfamily members, Gbb-60A and Dpp, cooperate to provide pattern information and establish cell identity in the Drosophila wing. *Development* **125**, 2723-34.

Kile, B. T. and Alexander, W. S. (2001). The suppressors of cytokine signalling (SOCS). *Cell Mol Life Sci* **58**, 1627-35.

Kimmel, C. B., Ballard, W. W., Kimmel, S. R., Ullmann, B. and Schilling, T. F. (1995). Stages of embryonic development of the zebrafish. *Dev Dyn* **203**, 253-310.

Kishimoto, Y., Lee, K. H., Zon, L., Hammerschmidt, M. and Schulte-Merker, S. (1997). The molecular nature of zebrafish swirl: BMP2 function is essential during early dorsoventral patterning. *Development* **124**, 4457-66.

Kitisin, K., Saha, T., Blake, T., Golestaneh, N., Deng, M., Kim, C., Tang, Y., Shetty, K., Mishra, B. and Mishra, L. (2007). Tgf-Beta signaling in development. *Sci STKE* **2007**, cm1.

Klug, C. A., Morrison, S. J., Masek, M., Hahm, K., Smale, S. T. and Weissman, I. L. (1998). Hematopoietic stem cells and lymphoid progenitors express different Ikaros isoforms, and Ikaros is localized to heterochromatin in immature lymphocytes. *Proc Natl Acad Sci U S A* **95**, 657-62.

Kodjabachian, L., Dawid, I. B. and Toyama, R. (1999). Gastrulation in zebrafish: what mutants teach us. *Dev Biol* **213**, 231-45.

Koipally, J., Kim, J., Jones, B., Jackson, A., Avitahl, N., Winandy, S., Trevisan, M., Nichogiannopoulou, A., Kelley, C. and Georgopoulos, K. (1999). Ikaros chromatin remodeling complexes in the control of differentiation of the hemo-lymphoid system. *Cold Spring Harb Symp Quant Biol* **64**, 79-86.

Kopan, R. and Ilagan, M. X. (2009). The canonical Notch signaling pathway: unfolding the activation mechanism. *Cell* **137**, 216-33.

Kretzschmar, M., Doody, J. and Massague, J. (1997). Opposing BMP and EGF signalling pathways converge on the TGF-beta family mediator Smad1. *Nature* **389**, 618-22.

Kretzschmar, M. and Massague, J. (1998). SMADs: mediators and regulators of TGF-beta signaling. *Curr Opin Genet Dev* **8**, 103-11.

Lane, K. B., Machado, R. D., Pauciulo, M. W., Thomson, J. R., Phillips, J. A., 3rd, Loyd, J. E., Nichols, W. C. and Trembath, R. C. (2000). Heterozygous germline mutations in BMPR2, encoding a TGF-beta receptor, cause familial primary pulmonary hypertension. The International PPH Consortium. *Nat Genet* **26**, 81-4.

Larsson, J. and Karlsson, S. (2005). The role of Smad signaling in hematopoiesis. *Oncogene* **24**, 5676-92.

Leung, A. Y., Mendenhall, E. M., Kwan, T. T., Liang, R., Eckfeldt, C., Chen, E., Hammerschmidt, M., Grindley, S., Ekker, S. C. and Verfaillie, C. M. (2005). Characterization of expanded intermediate cell mass in zebrafish chordin morphant embryos. *Dev Biol* **277**, 235-54.

Levanon, D., Negreanu, V., Bernstein, Y., Bar-Am, I., Avivi, L. and Groner, Y. (1994). AML1, AML2, and AML3, the human members of the runt domain gene-family: cDNA structure, expression, and chromosomal localization. *Genomics* **23**, 425-32.

Li, X., Claesson-Welsh, L. and Shibuya, M. (2008). VEGF receptor signal transduction. *Methods Enzymol* **443**, 261-84.

Liao, E. C., Paw, B. H., Peters, L. L., Zapata, A., Pratt, S. J., Do, C. P., Lieschke, G. and Zon, L. I. (2000). Hereditary spherocytosis in zebrafish riesling illustrates evolution of erythroid beta-spectrin structure, and function in red cell morphogenesis and membrane stability. *Development* **127**, 5123-32.

Liao, W., Bisgrove, B. W., Sawyer, H., Hug, B., Bell, B., Peters, K., Grunwald, D. J. and Stainier, D. Y. (1997). The zebrafish gene cloche acts upstream of a flk-1 homologue to regulate endothelial cell differentiation. *Development* **124**, 381-9.

Lieschke, G. J., Oates, A. C., Crowhurst, M. O., Ward, A. C. and Layton, J. E. (2001). Morphologic and functional characterization of granulocytes and macrophages in embryonic and adult zebrafish. *Blood* **98**, 3087-96.

Lieschke, G. J., Oates, A. C., Paw, B. H., Thompson, M. A., Hall, N. E., Ward, A. C., Ho, R. K., Zon, L. I. and Layton, J. E. (2002). Zebrafish SPI-1 (PU.1) marks a site of myeloid development independent of primitive erythropoiesis: implications for axial patterning. *Dev Biol* **246**, 274-95.

Lin, H. K., Bergmann, S. and Pandolfi, P. P. (2005). Deregulated TGF-beta signaling in leukemogenesis. *Oncogene* **24**, 5693-700.

Long, Q., Meng, A., Wang, H., Jessen, J. R., Farrell, M. J. and Lin, S. (1997). GATA-1 expression pattern can be recapitulated in living transgenic zebrafish using GFP reporter gene. *Development* **124**, 4105-11.

Lyons, S. E., Lawson, N. D., Lei, L., Bennett, P. E., Weinstein, B. M. and Liu, P. P. (2002). A nonsense mutation in zebrafish gata1 causes the bloodless phenotype in vlad tepes. *Proc Natl Acad Sci U S A* **99**, 5454-9.

Majumdar, A., Lun, K., Brand, M. and Drummond, I. A. (2000). Zebrafish no isthmus reveals a role for pax2.1 in tubule differentiation and patterning events in the pronephric primordia. *Development* **127**, 2089-98.

Marine, J. C., McKay, C., Wang, D., Topham, D. J., Parganas, E., Nakajima, H., Pendeville, H., Yasukawa, H., Sasaki, A., Yoshimura, A. et al. (1999). SOCS3 is essential in the regulation of fetal liver erythropoiesis. *Cell* **98**, 617-27.

Marston, N. J., Richards, W. J., Hughes, D., Bertwistle, D., Marshall, C. J. and Ashworth, A. (1999). Interaction between the product of the breast cancer susceptibility gene BRCA2 and DSS1, a protein functionally conserved from yeast to mammals. *Mol Cell Biol* **19**, 4633-42.

Massague, J. (1998). TGF-beta signal transduction. *Annu Rev Biochem* **67**, 753-91.

Massague, J., Blain, S. W. and Lo, R. S. (2000). TGFbeta signaling in growth control, cancer, and heritable disorders. *Cell* **103**, 295-309.

Massague, J., Seoane, J. and Wotton, D. (2005). Smad transcription factors. *Genes Dev* **19**, 2783-810.

Matsumura, K., Hirashima, M., Ogawa, M., Kubo, H., Hisatsune, H., Kondo, N., Nishikawa, S., Chiba, T. and Nishikawa, S. (2003). Modulation of VEGFR-2-mediated endothelial-cell activity by VEGF-C/VEGFR-3. *Blood* **101**, 1367-74.

Maxson, R. and Ishii, M. (2008). The Bmp pathway in skull vault development. *Front Oral Biol* **12**, 197-208.

McMahon, A. P. (2000). More surprises in the Hedgehog signaling pathway. *Cell* **100**, 185-8.

McReynolds, L. J., Gupta, S., Figueroa, M. E., Mullins, M. C. and Evans, T. (2007). Smad1 and Smad5 differentially regulate embryonic hematopoiesis. *Blood* **110**, 3881-90.

Miller-Bertoglio, V. E., Fisher, S., Sanchez, A., Mullins, M. C. and Halpern, M. E. (1997). Differential regulation of chordin expression domains in mutant zebrafish. *Dev Biol* **192**, 537-50.

Mintzer, K. A., Lee, M. A., Runke, G., Trout, J., Whitman, M. and Mullins, M. C. (2001). Lost-a-fin encodes a type I BMP receptor, Alk8, acting maternally and zygotically in dorsoventral pattern formation. *Development* **128**, 859-69.

Miyazono, K., Maeda, S. and Imamura, T. (2005). BMP receptor signaling: transcriptional targets, regulation of signals, and signaling cross-talk. *Cytokine Growth Factor Rev* **16**, 251-63.

Molloy, S. S., Bresnahan, P. A., Leppla, S. H., Klimpel, K. R. and Thomas, G. (1992). Human furin is a calcium-dependent serine endoprotease that recognizes the sequence Arg-X-X-Arg and efficiently cleaves anthrax toxin protective antigen. *J Biol Chem* **267**, 16396-402.

Moustakas, A., Souchelnytskyi, S. and Heldin, C. H. (2001). Smad regulation in TGF-beta signal transduction. *J Cell Sci* **114**, 4359-69.

Mucenski, M. L., McLain, K., Kier, A. B., Swerdlow, S. H., Schreiner, C. M., Miller, T. A., Pietryga, D. W., Scott, W. J., Jr. and Potter, S. S. (1991). A functional c-myb gene is required for normal murine fetal hepatic hematopoiesis. *Cell* **65**, 677-89.

Mukouyama, Y., Chiba, N., Mucenski, M. L., Satake, M., Miyajima, A., Hara, T. and Watanabe, T. (1999). Hematopoietic cells in cultures of the murine embryonic aorta-gonad-mesonephros region are induced by c-Myb. *Curr Biol* **9**, 833-6.

Mullins, M. C., Hammerschmidt, M., Kane, D. A., Odenthal, J., Brand, M., van Eeden, F. J., Furutani-Seiki, M., Granato, M., Haffter, P., Heisenberg, C. P. et al. (1996). Genes establishing dorsoventral pattern formation in the zebrafish embryo: the ventral specifying genes. *Development* **123**, 81-93.

Munoz-Sanjuan, I. and A, H. B. (2001). Early posterior/ventral fate specification in the vertebrate embryo. *Dev Biol* **237**, 1-17.

Murakami, G., Watabe, T., Takaoka, K., Miyazono, K. and Imamura, T. (2003). Cooperative inhibition of bone morphogenetic protein signaling by Smurf1 and inhibitory Smads. *Mol Biol Cell* **14**, 2809-17.

Murone, M., Rosenthal, A. and de Sauvage, F. J. (1999a). Hedgehog signal transduction: from flies to vertebrates. *Exp Cell Res* **253**, 25-33.

Murone, M., Rosenthal, A. and de Sauvage, F. J. (1999b). Sonic hedgehog signaling by the patched-smoothened receptor complex. *Curr Biol* **9**, 76-84.

Nakayama, K. (1997). Furin: a mammalian subtilisin/Kex2p-like endoprotease involved in processing of a wide variety of precursor proteins. *Biochem J* **327 (Pt 3)**, 625-35.

Nakayama, T., Cui, Y. and Christian, J. L. (2000). Regulation of BMP/Dpp signaling during embryonic development. *Cell Mol Life Sci* **57**, 943-56.

Nerlov, C., Querfurth, E., Kulessa, H. and Graf, T. (2000). GATA-1 interacts with the myeloid PU.1 transcription factor and represses PU.1-dependent transcription. *Blood* **95**, 2543-51.

Neul, J. L. and Ferguson, E. L. (1998). Spatially restricted activation of the SAX receptor by SCW modulates DPP/TKV signaling in Drosophila dorsal-ventral patterning. *Cell* **95**, 483-94.

Nguyen, M., Park, S., Marques, G. and Arora, K. (1998). Interpretation of a BMP activity gradient in Drosophila embryos depends on synergistic signaling by two type I receptors, SAX and TKV. *Cell* **95**, 495-506.

Nishimatsu, S. and Thomsen, G. H. (1998). Ventral mesoderm induction and patterning by bone morphogenetic protein heterodimers in Xenopus embryos. *Mech Dev* **74**, 75-88.

Nishinakamura, R., Miyajima, A., Mee, P. J., Tybulewicz, V. L. and Murray, R. (1996). Hematopoiesis in mice lacking the entire granulocyte-macrophage colony-stimulating factor/interleukin-3/interleukin-5 functions. *Blood* **88**, 2458-64.

Orkin, S. H. (1992). GATA-binding transcription factors in hematopoietic cells. *Blood* **80**, 575-81.

Orkin, S. H. and Zon, L. I. (1997). Genetics of erythropoiesis: induced mutations in mice and zebrafish. *Annu Rev Genet* **31**, 33-60.

Park, C., Afrikanova, I., Chung, Y. S., Zhang, W. J., Arentson, E., Fong Gh, G., Rosendahl, A. and Choi, K. (2004). A hierarchical order of factors in the generation of

FLK1- and SCL-expressing hematopoietic and endothelial progenitors from embryonic stem cells. *Development* **131**, 2749-62.

Paw, B. H., Davidson, A. J., Zhou, Y., Li, R., Pratt, S. J., Lee, C., Trede, N. S., Brownlie, A., Donovan, A., Liao, E. C. et al. (2003). Cell-specific mitotic defect and dyserythropoiesis associated with erythroid band 3 deficiency. *Nat Genet* **34**, 59-64.

Pellizzoni, L. (2007). Chaperoning ribonucleoprotein biogenesis in health and disease. *EMBO Rep* **8**, 340-5.

Pera, E. M., Ikeda, A., Eivers, E. and De Robertis, E. M. (2003). Integration of IGF, FGF, and anti-BMP signals via Smad1 phosphorylation in neural induction. *Genes Dev* **17**, 3023-8.

Piccolo, S., Agius, E., Leyns, L., Bhattacharyya, S., Grunz, H., Bouwmeester, T. and De Robertis, E. M. (1999). The head inducer Cerberus is a multifunctional antagonist of Nodal, BMP and Wnt signals. *Nature* **397**, 707-10.

Piccolo, S., Agius, E., Lu, B., Goodman, S., Dale, L. and De Robertis, E. M. (1997). Cleavage of Chordin by Xolloid metalloprotease suggests a role for proteolytic processing in the regulation of Spemann organizer activity. *Cell* **91**, 407-16.

Piccolo, S., Sasai, Y., Lu, B. and De Robertis, E. M. (1996). Dorsoventral patterning in Xenopus: inhibition of ventral signals by direct binding of chordin to BMP-4. *Cell* **86**, 589-98.

Pierre, M., Yoshimoto, M., Huang, L. and Yoder, M. C. (2009). VEGF and IHH Rescue Definitive Hematopoiesis in Gata-4 and Gata-6 Deficient Murine Embryoid Bodies. *Exp Hematol*.

Porter, A. C. and Vaillancourt, R. R. (1998). Tyrosine kinase receptor-activated signal transduction pathways which lead to oncogenesis. *Oncogene* **17**, 1343-52.

Pratt, S. J., Drejer, A., Foott, H., Barut, B., Brownlie, A., Postlethwait, J., Kato, Y., Yamamoto, M. and Zon, L. I. (2002). Isolation and characterization of zebrafish NFE2. *Physiol Genomics* **11**, 91-8.

Qian, F., Zhen, F., Xu, J., Huang, M., Li, W. and Wen, Z. (2007). Distinct functions for different scl isoforms in zebrafish primitive and definitive hematopoiesis. *PLoS Biol* **5**, e132.

Raftery, L. A. and Sutherland, D. J. (2003). Gradients and thresholds: BMP response gradients unveiled in Drosophila embryos. *Trends Genet* **19**, 701-8.

Ransom, D. G., Bahary, N., Niss, K., Traver, D., Burns, C., Trede, N. S., Paffett-Lugassy, N., Saganic, W. J., Lim, C. A., Hersey, C. et al. (2004). The zebrafish moonshine gene encodes transcriptional intermediary factor 1gamma, an essential regulator of hematopoiesis. *PLoS Biol* **2**, E237.

Reilly, J. T. (2003a). FLT3 and its role in the pathogenesis of acute myeloid leukaemia. *Leuk Lymphoma* **44**, 1-7.

Reilly, J. T. (2003b). Receptor tyrosine kinases in normal and malignant haematopoiesis. *Blood Rev* **17**, 241-8.

Rekhtman, N., Radparvar, F., Evans, T. and Skoultchi, A. I. (1999). Direct interaction of hematopoietic transcription factors PU.1 and GATA-1: functional antagonism in erythroid cells. *Genes Dev* **13**, 1398-411.

Rey, M. A., Duffy, S. P., Brown, J. K., Kennedy, J. A., Dick, J. E., Dror, Y. and Tailor, C. S. (2008). Enhanced alternative splicing of the FLVCR1 gene in Diamond

Blackfan anemia disrupts FLVCR1 expression and function that are critical for erythropoiesis. *Haematologica* **93**, 1617-26.

Robb, L., Lyons, I., Li, R., Hartley, L., Kontgen, F., Harvey, R. P., Metcalf, D. and Begley, C. G. (1995). Absence of yolk sac hematopoiesis from mice with a targeted disruption of the scl gene. *Proc Natl Acad Sci U S A* **92**, 7075-9.

Roberts, A. B. and Derynck, R. (2001). Meeting report: signaling schemes for TGF-beta. *Sci STKE* **2001**, PE43.

Rosnet, O. and Birnbaum, D. (1993). Hematopoietic receptors of class III receptor-type tyrosine kinases. *Crit Rev Oncog* **4**, 595-613.

Rosnet, O., Schiff, C., Pebusque, M. J., Marchetto, S., Tonnelle, C., Toiron, Y., Birg, F. and Birnbaum, D. (1993). Human FLT3/FLK2 gene: cDNA cloning and expression in hematopoietic cells. *Blood* **82**, 1110-9.

Sabbattini, P., Lundgren, M., Georgiou, A., Chow, C., Warnes, G. and Dillon, N. (2001). Binding of Ikaros to the lambda5 promoter silences transcription through a mechanism that does not require heterochromatin formation. *Embo J* **20**, 2812-22.

Sandberg, M. L., Sutton, S. E., Pletcher, M. T., Wiltshire, T., Tarantino, L. M., Hogenesch, J. B. and Cooke, M. P. (2005). c-Myb and p300 regulate hematopoietic stem cell proliferation and differentiation. *Dev Cell* **8**, 153-66.

Schier, A. F. and Talbot, W. S. (2005). Molecular genetics of axis formation in zebrafish. *Annu Rev Genet* **39**, 561-613.

Schmid, B., Furthauer, M., Connors, S. A., Trout, J., Thisse, B., Thisse, C. and Mullins, M. C. (2000). Equivalent genetic roles for bmp7/snailhouse and bmp2b/swirl in dorsoventral pattern formation. *Development* **127**, 957-67.

Schulte-Merker, S., Ho, R. K., Herrmann, B. G. and Nusslein-Volhard, C. (1992). The protein product of the zebrafish homologue of the mouse T gene is expressed in nuclei of the germ ring and the notochord of the early embryo. *Development* **116**, 1021-32.

Schulte-Merker, S., Lee, K. J., McMahon, A. P. and Hammerschmidt, M. (1997). The zebrafish organizer requires chordino. *Nature* **387**, 862-3.

Schulte-Merker, S., van Eeden, F. J., Halpern, M. E., Kimmel, C. B. and Nusslein-Volhard, C. (1994). no tail (ntl) is the zebrafish homologue of the mouse T (Brachyury) gene. *Development* **120**, 1009-15.

Schulze, H. and Shivdasani, R. A. (2004). Molecular mechanisms of megakaryocyte differentiation. *Semin Thromb Hemost* **30**, 389-98.

Serra, R. (2002). Transforming Grwoth Factor beta (TGFb). *Encyclooedia of Life Science*, 1-7.

Shafizadeh, E. and Paw, B. H. (2004). Zebrafish as a model of human hematologic disorders. *Curr Opin Hematol* **11**, 255-61.

Shafizadeh, E., Paw, B. H., Foott, H., Liao, E. C., Barut, B. A., Cope, J. J., Zon, L. I. and Lin, S. (2002). Characterization of zebrafish merlot/chablis as non-mammalian vertebrate models for severe congenital anemia due to protein 4.1 deficiency. *Development* **129**, 4359-70.

Shi, Y., Hata, A., Lo, R. S., Massague, J. and Pavletich, N. P. (1997). A structural basis for mutational inactivation of the tumour suppressor Smad4. *Nature* **388**, 87-93.

Shi, Y. and Massague, J. (2003). Mechanisms of TGF-beta signaling from cell membrane to the nucleus. *Cell* **113**, 685-700.

Shimamura, A. (2008). Diamond-Blackfan anemia: a new facet. *Blood* **112**, 1552-3.

Shimmi, O. and O'Connor, M. B. (2003). Physical properties of Tld, Sog, Tsg and Dpp protein interactions are predicted to help create a sharp boundary in Bmp signals during dorsoventral patterning of the Drosophila embryo. *Development* **130**, 4673-82.

Shin, M., Nagai, H. and Sheng, G. (2009). Notch mediates Wnt and BMP signals in the early separation of smooth muscle progenitors and blood/endothelial common progenitors. *Development* **136**, 595-603.

Shivdasani, R. A., Mayer, E. L. and Orkin, S. H. (1995). Absence of blood formation in mice lacking the T-cell leukaemia oncoprotein tal-1/SCL. *Nature* **373**, 432-4.

Snyder, A., Fraser, S. T. and Baron, M. H. (2004). Bone morphogenetic proteins in vertebrate hematopoietic development. *J Cell Biochem* **93**, 224-32.

Solis, A. S., Shariat, N. and Patton, J. G. (2008). Splicing fidelity, enhancers, and disease. *Front Biosci* **13**, 1926-42.

Solnica-Krezel, L., Stemple, D. L., Mountcastle-Shah, E., Rangini, Z., Neuhauss, S. C., Malicki, J., Schier, A. F., Stainier, D. Y., Zwartkruis, F., Abdelilah, S. et al. (1996). Mutations affecting cell fates and cellular rearrangements during gastrulation in zebrafish. *Development* **123**, 67-80.

Spiekermann, K., Bagrintseva, K., Schwab, R., Schmieja, K. and Hiddemann, W. (2003). Overexpression and constitutive activation of FLT3 induces STAT5 activation in primary acute myeloid leukemia blast cells. *Clin Cancer Res* **9**, 2140-50.

Spivak, J. L. (1986). The mechanism of action of erythropoietin. *Int J Cell Cloning* **4**, 139-66.

Stachel, S. E., Grunwald, D. J. and Myers, P. Z. (1993). Lithium perturbation and goosecoid expression identify a dorsal specification pathway in the pregastrula zebrafish. *Development* **117**, 1261-74.

Steiner, D. F. (1998). The proprotein convertases. *Curr Opin Chem Biol* **2**, 31-9.

Sumoy, L., Keasey, J. B., Dittman, T. D. and Kimelman, D. (1997). A role for notochord in axial vascular development revealed by analysis of phenotype and the expression of VEGR-2 in zebrafish flh and ntl mutant embryos. *Mech Dev* **63**, 15-27.

Tanaka, K., Ichiyama, K., Hashimoto, M., Yoshida, H., Takimoto, T., Takaesu, G., Torisu, T., Hanada, T., Yasukawa, H., Fukuyama, S. et al. (2008). Loss of suppressor of cytokine signaling 1 in helper T cells leads to defective Th17 differentiation by enhancing antagonistic effects of IFN-gamma on STAT3 and Smads. *J Immunol* **180**, 3746-56.

Thisse, C., Thisse, B., Halpern, M. E. and Postlethwait, J. H. (1994). Goosecoid expression in neurectoderm and mesendoderm is disrupted in zebrafish cyclops gastrulas. *Dev Biol* **164**, 420-9.

Thompson, M. A., Ransom, D. G., Pratt, S. J., MacLennan, H., Kieran, M. W., Detrich, H. W., 3rd, Vail, B., Huber, T. L., Paw, B., Brownlie, A. J. et al. (1998). The cloche and spadetail genes differentially affect hematopoiesis and vasculogenesis. *Dev Biol* **197**, 248-69.

Tian, J., Yam, C., Balasundaram, G., Wang, H., Gore, A. and Sampath, K. (2003). A temperature-sensitive mutation in the nodal-related gene cyclops reveals that the floor plate is induced during gastrulation in zebrafish. *Development* **130**, 3331-42.

Toyama, R., O'Connell, M. L., Wright, C. V., Kuehn, M. R. and Dawid, I. B. (1995). Nodal induces ectopic goosecoid and lim1 expression and axis duplication in zebrafish. *Development* **121**, 383-91.

Traver, D. (2004). Cellular dissection of zebrafish hematopoiesis. *Methods Cell Biol* **76**, 127-49.

Trinh, L. A., Ferrini, R., Cobb, B. S., Weinmann, A. S., Hahm, K., Ernst, P., Garraway, I. P., Merkenschlager, M. and Smale, S. T. (2001). Down-regulation of TDT transcription in CD4(+)CD8(+) thymocytes by Ikaros proteins in direct competition with an Ets activator. *Genes Dev* **15**, 1817-32.

Tsai, F. Y., Keller, G., Kuo, F. C., Weiss, M., Chen, J., Rosenblatt, M., Alt, F. W. and Orkin, S. H. (1994). An early haematopoietic defect in mice lacking the transcription factor GATA-2. *Nature* **371**, 221-6.

Tsuneizumi, K., Nakayama, T., Kamoshida, Y., Kornberg, T. B., Christian, J. L. and Tabata, T. (1997). Daughters against dpp modulates dpp organizing activity in Drosophila wing development. *Nature* **389**, 627-31.

Uechi, T., Nakajima, Y., Chakraborty, A., Torihara, H., Higa, S. and Kenmochi, N. (2008). Deficiency of ribosomal protein S19 during early embryogenesis leads to reduction of erythrocytes in a zebrafish model of Diamond-Blackfan anemia. *Hum Mol Genet* **17**, 3204-11.

Uguen, P. and Murphy, S. (2003). The 3' ends of human pre-snRNAs are produced by RNA polymerase II CTD-dependent RNA processing. *Embo J* **22**, 4544-54.

Uhmann, A., Dittmann, K., Nitzki, F., Dressel, R., Koleva, M., Frommhold, A., Zibat, A., Binder, C., Adham, I., Nitsche, M. et al. (2007). The Hedgehog receptor Patched controls lymphoid lineage commitment. *Blood* **110**, 1814-23.

van der Knaap, M. S., Pronk, J. C. and Scheper, G. C. (2006). Vanishing white matter disease. *Lancet Neurol* **5**, 413-23.

Vandenbunder, B., Pardanaud, L., Jaffredo, T., Mirabel, M. A. and Stehelin, D. (1989). Complementary patterns of expression of c-ets 1, c-myb and c-myc in the blood-forming system of the chick embryo. *Development* **107**, 265-74.

Varnum-Finney, B., Xu, L., Brashem-Stein, C., Nourigat, C., Flowers, D., Bakkour, S., Pear, W. S. and Bernstein, I. D. (2000). Pluripotent, cytokine-dependent, hematopoietic stem cells are immortalized by constitutive Notch1 signaling. *Nat Med* **6**, 1278-81.

Visser, J. A., Olaso, R., Verhoef-Post, M., Kramer, P., Themmen, A. P. and Ingraham, H. A. (2001). The serine/threonine transmembrane receptor ALK2 mediates Mullerian inhibiting substance signaling. *Mol Endocrinol* **15**, 936-45.

Vogeli, K. M., Jin, S. W., Martin, G. R. and Stainier, D. Y. (2006). A common progenitor for haematopoietic and endothelial lineages in the zebrafish gastrula. *Nature* **443**, 337-9.

von Bubnoff, A. and Cho, K. W. (2001). Intracellular BMP signaling regulation in vertebrates: pathway or network? *Dev Biol* **239**, 1-14.

Wagner, D. S. and Mullins, M. C. (2002). Modulation of BMP activity in dorsal-ventral pattern formation by the chordin and ogon antagonists. *Dev Biol* **245**, 109-23.

Wang, H., Long, Q., Marty, S. D., Sassa, S. and Lin, S. (1998). A zebrafish model for hepatoerythropoietic porphyria. *Nat Genet* **20**, 239-43.

Warren, D. J. and Moore, M. A. (1988). Synergism among interleukin 1, interleukin 3, and interleukin 5 in the production of eosinophils from primitive hemopoietic stem cells. *J Immunol* **140**, 94-9.

Watanabe, H., Shionyu, M., Kimura, T. and Kimata, K. (2007). Splicing factor 3b subunit 4 binds BMPR-IA and inhibits osteochondral cell differentiation. *J Biol Chem* **282**, 20728-38.

Weinberg, E. S., Allende, M. L., Kelly, C. S., Abdelhamid, A., Murakami, T., Andermann, P., Doerre, O. G., Grunwald, D. J. and Riggleman, B. (1996). Developmental regulation of zebrafish MyoD in wild-type, no tail and spadetail embryos. *Development* **122**, 271-80.

Weinstein, B. M., Schier, A. F., Abdelilah, S., Malicki, J., Solnica-Krezel, L., Stemple, D. L., Stainier, D. Y., Zwartkruis, F., Driever, W. and Fishman, M. C. (1996). Hematopoietic mutations in the zebrafish. *Development* **123**, 303-9.

Westerfield, M. (2000). The zebrafish book.A guide for the laboratory use of zebrafish (Danio rerio).

Wieben, E. D., Nenninger, J. M. and Pederson, T. (1985). Ribonucleoprotein organization of eukaryotic RNA. XXXII. U2 small nuclear RNA precursors and their accurate 3' processing in vitro as ribonucleoprotein particles. *J Mol Biol* **183**, 69-78.

Willett, C. E., Cherry, J. J. and Steiner, L. A. (1997). Characterization and expression of the recombination activating genes (rag1 and rag2) of zebrafish. *Immunogenetics* **45**, 394-404.

Willett, C. E., Cortes, A., Zuasti, A. and Zapata, A. G. (1999). Early hematopoiesis and developing lymphoid organs in the zebrafish. *Dev Dyn* **214**, 323-36.

Willett, C. E., Kawasaki, H., Amemiya, C. T., Lin, S. and Steiner, L. A. (2001). Ikaros expression as a marker for lymphoid progenitors during zebrafish development. *Dev Dyn* **222**, 694-8.

Wingert, R. A., Brownlie, A., Galloway, J. L., Dooley, K., Fraenkel, P., Axe, J. L., Davidson, A. J., Barut, B., Noriega, L., Sheng, X. et al. (2004). The chianti zebrafish mutant provides a model for erythroid-specific disruption of transferrin receptor 1. *Development* **131**, 6225-35.

Winnier, G., Blessing, M., Labosky, P. A. and Hogan, B. L. (1995). Bone morphogenetic protein-4 is required for mesoderm formation and patterning in the mouse. *Genes Dev* **9**, 2105-16.

Wozney, J. M., Rosen, V., Celeste, A. J., Mitsock, L. M., Whitters, M. J., Kriz, R. W., Hewick, R. M. and Wang, E. A. (1988). Novel regulators of bone formation: molecular clones and activities. *Science* **242**, 1528-34.

Wrana, J. L. (2000). Regulation of Smad activity. *Cell* **100**, 189-92.

Yanagisawa, K. O., Fujimoto, H. and Urushihara, H. (1981). Effects of the brachyury (T) mutation on morphogenetic movement in the mouse embryo. *Dev Biol* **87**, 242-8.

Yang, X., Castilla, L. H., Xu, X., Li, C., Gotay, J., Weinstein, M., Liu, P. P. and Deng, C. X. (1999). Angiogenesis defects and mesenchymal apoptosis in mice lacking SMAD5. *Development* **126**, 1571-80.

Zhang, J., Niu, C., Ye, L., Huang, H., He, X., Tong, W. G., Ross, J., Haug, J., Johnson, T., Feng, J. Q. et al. (2003). Identification of the haematopoietic stem cell niche and control of the niche size. *Nature* **425**, 836-41.

Zhang, P., Behre, G., Pan, J., Iwama, A., Wara-Aswapati, N., Radomska, H. S., Auron, P. E., Tenen, D. G. and Sun, Z. (1999). Negative cross-talk between hematopoietic regulators: GATA proteins repress PU.1. *Proc Natl Acad Sci U S A* **96**, 8705-10.

Zhang, P., Zhang, X., Iwama, A., Yu, C., Smith, K. A., Mueller, B. U., Narravula, S., Torbett, B. E., Orkin, S. H. and Tenen, D. G. (2000). PU.1 inhibits GATA-1 function and erythroid differentiation by blocking GATA-1 DNA binding. *Blood* **96**, 2641-8.

Zhang, Y. E. (2009). Non-Smad pathways in TGF-beta signaling. *Cell Res* **19**, 128-39.

Zimmerman, L. B., De Jesus-Escobar, J. M. and Harland, R. M. (1996). The Spemann organizer signal noggin binds and inactivates bone morphogenetic protein 4. *Cell* **86**, 599-606.

Zon, L. I. (1995). Developmental biology of hematopoiesis. *Blood* **86**, 2876-91.

Development ePress online publication date 15 July 2009

Development 136, 2757-2765 (2009) doi:10.1242/dev.034959

The Integrator subunits function in hematopoiesis by modulating Smad/BMP signaling

Shijie Tao[1,2], Yu Cai[1,2] and Karuna Sampath[1,2,3,*]

Hematopoiesis, the dynamic process of blood cell development, is regulated by the activity of the bone morphogenetic protein (BMP) signaling pathway and by many transcription factors. However, the molecules and mechanisms that regulate BMP/Smad signaling in hematopoiesis are largely unknown. Here, we show that the Integrator complex, an evolutionarily conserved group of proteins, functions in zebrafish hematopoiesis by modulating Smad/BMP signaling. The Integrator complex proteins are known to directly interact with RNA polymerase II to mediate 3′ end processing of U1 and U2 snRNAs. We have identified several subunits of the Integrator complex in zebrafish. Antisense morpholino-mediated knockdown of the Integrator subunit 5 (Ints5) in zebrafish embryos affects U1 and U2 snRNA processing, leading to aberrant splicing of *smad1* and *smad5* RNA, and reduced expression of the hematopoietic genes *stem cell leukemia* (*scl*, also known as *tal1*) and *gata1*. Blood smears from *ints5* morphant embryos show arrested red blood cell differentiation, similar to *scl*-deficient embryos. Interestingly, targeting other Integrator subunits also leads to defects in *smad5* RNA splicing and arrested hematopoiesis, suggesting that the Ints proteins function as a complex to regulate the BMP pathway during hematopoiesis. Our work establishes a link between the RNA processing machinery and the downstream effectors of BMP signaling, and reveals a new group of proteins that regulates the switch from primitive hematopoietic stem cell identity and blood cell differentiation by modulating Smad function.

KEY WORDS: Hematopoiesis, Integrator proteins, RNA splicing, Smad/BMP signaling, Zebrafish

INTRODUCTION

Hematopoiesis is the process that gives rise to all types of blood cells. It is generally believed that hematopoietic development branches at an early stage into myeloid and lymphoid cell fates. The lymphoid branch differentiates to T, B and natural killer cells, and the myeloid branch develops into all the other cell types, including monocytes/macrophages, granulocytes, megakaryoctyes and erythrocytes (red blood cells, RBCs) (Hsu et al., 2001; Larsson and Karlsson, 2005). In the mouse, the hemangioblast progenitors (common progenitors for both hematopoietic and endothelial lineages) arise from a mesodermal population of cells positive for brachyury (T) expression (Fehling et al., 2003). Similarly, in zebrafish, hemangioblasts originate from the ventral margin of the embryo (Vogeli et al., 2006). Primitive hematopoiesis occurs at two anatomical sites: the rostral blood island (RBI) arising from the cephalic mesoderm and the intermediate cell mass (ICM) located in the trunk, ventral to the notochord. Cells within the ICM predominantly differentiate into vascular cells and primitive erythrocytes, which enter the blood circulation around 24 hours post fertilization (hpf) (Al-Adhami and Kunz, 1977; Davidson and Zon, 2004).

Recent work has shown that the process of blood cell formation is regulated by a variety of intrinsic transcription factors. These include the Stem cell leukemia (Scl, Tal1 – ZFIN) basic helix-loop-helix transcription factor, and a zinc-finger transcription factor, Gata1. *scl* is expressed in the RBI and the ICM, where its expression marks the formation of primitive hematopoietic stem cells (HSCs) and vascular precursors. *gata1* is expressed in the lateral plate mesoderm that will migrate medially to form the ICM and is crucial for myeloid differentiation (de Jong and Zon, 2005). Many extracellular signaling molecules present in the environment are also involved in hematopoietic regulation. These include the bone morphogenetic proteins (BMPs). BMPs belong to the Transforming growth factor β (TGF-β) family of secreted proteins, and signal via the downstream transcription factors, Smad1, 5 and 8 (Smad9 – ZFIN) (von Bubnoff and Cho, 2001). BMP signaling is important not only for the patterning of ventral mesoderm from where the primitive HSCs arise, but also for regulating the specification and proliferation of blood progenitors (Larsson and Karlsson, 2005; Winnier et al., 1995). Loss of either Smad1 or Smad5 leads to a failure in the generation of definitive hematopoietic progenitors in zebrafish (McReynolds et al., 2007).

Integrator is a multiprotein complex that associates with the C-terminal repeats of RNA polymerase II and mediates U1 and U2 snRNA 3′ end processing (Baillat et al., 2005). Here, we report that the snRNA metabolism-related factor Ints5, a subunit of the Integrator complex, functions in zebrafish hematopoiesis by modulating the splicing of *smad1* and *smad5* RNA, thereby establishing a potential link between the RNA processing machinery and downstream effectors of BMP signaling in the regulation of hematopoiesis.

MATERIALS AND METHODS

Fish maintenance

Zebrafish were maintained under standard conditions at 28.5°C and embryos were obtained by standard breeding methods. All experimental procedures were carried out according to the guidelines of the Institutional Animal Care Use Committee at Temasek Life Sciences Laboratory.

5′ and 3′ RACE

Total RNA was extracted from wild-type embryos and subjected to 5′ and 3′ RACE using the FirstChoice RLM-RACE Kit (Ambion) according to the manufacturer's instructions. The following primers were used: Ints5 5′

[1]Temasek Life Sciences Laboratory, 1 Research Link, National University of Singapore, Singapore 117604. [2]Department of Biological Sciences, 14 Science Drive, National University of Singapore, Singapore 117543. [3]School of Biological Sciences, Nanyang Technological University, 30 Nanyang Drive, Singapore 637551.

*Author for correspondence (e-mail: karuna@tll.org.sg)

Accepted 11 June 2009

RACE, 5′-TCACCCTATGCAGGCCTTGTAGA-3′ and 5′-GGGAGTAGCACTCCATTAGTGA-3′; Ints5 3′ RACE, 5′-GCTACTTCCTCCAGTCTTGAGT-3′ and 5′-CGCTGTGCTATTGCTCTGTCAT-3′. The RACE products were cloned into the plasmid pCS2+ and sequenced.

In situ hybridization analyses

Whole-mount in situ hybridization was performed as described (Tian et al., 2003). The following plasmids were linearized and antisense probes were synthesized by in vitro transcription: pBS*ints5* (*Bam*HI, T3 RNA Polymerase), pGEMT-Easy*scl* (*Nco*I, SP6 RNA Polymerase), pBS*gata1* (*Xba*I, T7 RNA Polymerase), pBS*flk1* (*Sma*I, T7), pKS*pax2a* (*Bam*HI, T7) (Detrich et al., 1995; Gering et al., 1998; Liao et al., 1997; Majumdar et al., 2000), pBS*hgg1* (*Xba*I, T7) (Thisse et al., 1994), pBS*gsc* (*Eco*RI, T7) (Thisse et al., 1994), pBS*ntl* (*Xho*I, T7) (Schulte-Merker et al., 1994), pBS*spt* (*Eco*RI, T7) (Griffin et al., 1998), pBS*sox17* (*Eco*RI, T7) (Alexander and Stainier, 1999), pBS*myoD* (*Bam*HI, T7) (Weinberg et al., 1996) and pBS*dlx3* (*Sal*I, T7) (Akimenko et al., 1994). For digoxigenin- and fluorescein-labeled probes, BM Purple (Roche) and Fast Red (Sigma) substrates were used.

Injection of morpholinos and RNA

All morpholinos were obtained from GeneTools. The *ints5* donor and acceptor morpholinos were designed to target the splice site. Co-injection of the two *ints5* morpholinos (donor and acceptor MO) at an optimal dose of 2.5 ng each was found to have better efficiency, and all injections, unless otherwise specified, were performed using this combination. The *ints11* ATG morpholino was injected at a dose of 25 ng/embryo. The *ints9* SMO targeting the intron2-exon3 boundary of *ints9* was used at a dose of 12.5 ng/embryo. The *ints11* SMO targeting the intron4-exon5 boundary was injected at a dose of 2.5 ng/embryo. The morpholino sequences are: Ints5 donor MO, 5′-CTTGTATTGCTCACCTGTAA-3′; Ints5 acceptor MO, 5′-AGCTCTTGAGGACTGATGGA-3′; Ints9 SMO, 5′-GATAATCGTGGACTGTAAATCCAAC-3′; Ints11 ATG MO, 5′-AAGGCGTAACTTTGATATCAGGCAT-3′; Ints11 SMO, 5′-AGATGGAAATGACTGAGAGGAAGAG-3′. cDNAs encoding Ints5, Ints9, Ints11, Smad1 and Smad5 were cloned in pCS2+. For injection, constructs were digested with *Not*I and the capped mRNA was synthesized with the mMESSAGE mMACHINE SP6 Kit (Ambion) according to the manufacturer's instructions. For rescue experiments, 50 pg of *ints5* RNA or 10 pg of *smad1* and *smad5* RNA was co-injected with *ints5* morpholinos.

RT-PCR

Total RNA from injected embryos (1 μg) was used to generate cDNA with Superscript II Reverse Transcriptase (Invitrogen) and $p(dT)_{15}$ or random $p(dN)_6$ primers (Roche). The cDNA was then used in a PCR reaction. Primer details are available upon request.

May-Grunwald Giemsa staining

Fish embryos were anesthetized in PBS (pH 7.4, calcium- and magnesium-free) with 0.02% tricane (Sigma) and 1% BSA. After tail clipping, red blood cells were collected and cytospun onto slides by centrifugation at 400 rpm for 3 minutes using a Cytospin 4 Cytocentrifuge (Thermo Scientific). The slides were air-dried and subjected to May-Grunwald Giemsa staining (Qian et al., 2007).

Smad cDNA constructs

Smad5Δexon4 and Smad5Δexon4,5 were generated by PCR amplification from cDNA templates (Dick et al., 1999) using the following primers: Smad5Δexon4 F, 5′-CACTACAAACGAGTTGAAAGTCCAGCTGATACTCCTCCTCCTGCCTACAT-3′; Smad5Δexon4 R, 5′-ATGTAGGCAGGAGGAGGAGTATCAGCTGGACTTTCAACTCGTTTGTAGTG-3′; Smad5Δexon4,5 F, 5′-CACTACAAACGAGTTGAAAGTCCAGATGTGCAGCCAGTGGAGTATCAGGA-3′; Smad5Δexon4,5 R, 5′-TCCTGATACTCCACTGGCTGCACATCTGGACTTTCAACTCGTTTGTAGTG-3′. Constructs were linearized with *Not*I and capped mRNA was synthesized with the mMESSAGE mMACHINE SP6 Kit (Ambion).

Quantitative real-time PCR

First-strand cDNA was synthesized using Superscript II Reverse Transcriptase (Invitrogen). Semi-quantitative real-time PCR was performed with the Power SYBR Green PCR Mix (Applied Biosystems) on the

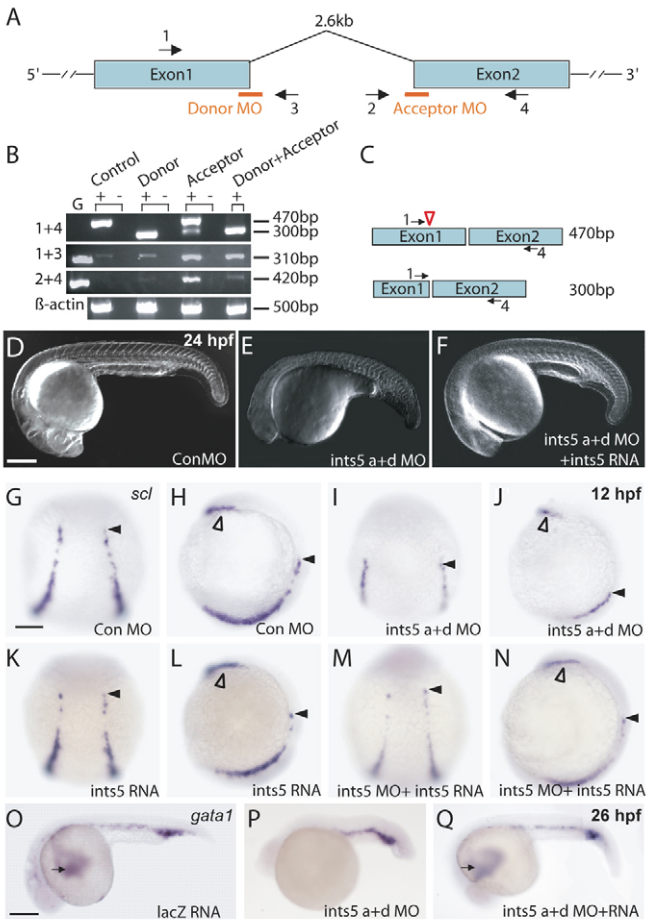

Fig. 1. Ints5 functions during hematopoiesis. (**A**) Schematic representation of the *ints5* genomic locus; orange bars indicate target sites of the donor and acceptor morpholinos (MOs); numbered black arrows show the position of the primers used in RT-PCRs to examine splicing of *ints5* RNA. (**B**) RT-PCR to detect splicing of *ints5* and control β-actin (encoded by *bactin1*). RNA from sphere stage (4 hours post fertilization, hpf) embryos injected with control or *ints5* donor and acceptor morpholinos at the 1-cell stage. Primers used (left) and transcript sizes (right) are indicated. G, genomic DNA. (**C**) Schematic representation of correctly spliced (upper) and aberrantly spliced (lower) *ints5* transcripts. The size of bands amplified by primer pair 1 and 4 is indicated on the right. Red open arrowhead indicates the position of a cryptic splice site in exon 1. (**D-F**) DIC images of live embryos at 24 hpf injected with control morpholinos (D), *ints5* acceptor and donor (a+d) morpholinos (E) or co-injected with *ints5* morpholinos and *ints5* RNA (F). (**G-Q**) Whole-mount in situ hybridization to detect expression of *scl* (G-N) at 12 hpf and *gata1* (O-Q) at 26 hpf shows reduced expression of both genes in *ints5* morphants (I,J,P), in comparison to control morpholino- or *lacZ* RNA-injected embryos (G,H,O). Black arrowheads indicate the anterior limit of *scl* expression in the intermediate cell mass (ICM); open arrowheads indicate *scl* expression in the rostral blood island (RBI); black arrows indicate anterior *gata1* expression, which represents the circulating blood cells. Co-injection of *ints5* RNA can restore *scl* and *gata1* expression in *ints5* morphants (M,N,Q), whereas embryos injected with *ints5* RNA alone show normal *scl* expression at 12 hpf (K,L). D-F,O-Q show lateral views of embryos with anterior to the left; G,I,K,M show dorsal views of embryos with anterior at the top; H,J,L,N show lateral views of embryos with dorsal to the right. Scale bars: 250 μm in D,O; 50 μm in G.

7900HT Fast Real-Time PCR System (Applied Biosystems). Each PCR reaction was performed in triplicate, and each experiment was repeated three times. The PCR cycle conditions were 95°C, 10 minutes and then 94°C, 15 seconds; 60°C, 1 minute, for 45 cycles. The CT values were analyzed using the 2-ΔΔT method. Primer details are available upon request.

Western blots

Western blots were performed on extracts of embryos after removing the yolk. Proteins of each sample were harvested from 20 injected embryos at 8 hpf, separated using SDS-PAGE and transferred to a nitrocellulose membrane (Amersham Biosciences, RPN203E). Ints5 proteins were detected using rabbit anti-Ints5 antibody (1:1000, Bethyl Laboratories). Smad5 proteins were detected using rabbit anti-Smad5 polyclonal antibody (1:500, Abcam). The expression of the α-Tubulin control was detected using anti-α-Tubulin antibody (1:1000, Sigma). Anti-mouse immunoglobulins (1:5000, DAKO) or anti-rabbit immunoglobulins (1:5000, DAKO) were used as secondary antibodies and were detected with SuperSignal West Femto Maximum Sensitivity Substrate (Pierce) or with SuperSignal West Pico Chemiluminescent Substrate (Pierce).

RESULTS

Ints5 functions during primitive hematopoiesis.

To investigate the function of Ints5 during early zebrafish development, two antisense morpholinos were designed to target the intronic donor and acceptor sites of the *ints5* gene (Fig. 1A). Reverse transcription-PCR (RT-PCR) analysis shows the accumulation of nonspliced *ints5* transcripts in embryos injected with *ints5* splice-junction morpholinos (Fig. 1B). Sequence analysis of RT-PCR products from the transcripts shows that the correct exon-intron boundary is not chosen and, instead, a cryptic site in exon 1 of *ints5* is used in the morphant embryos. This leads to the production of

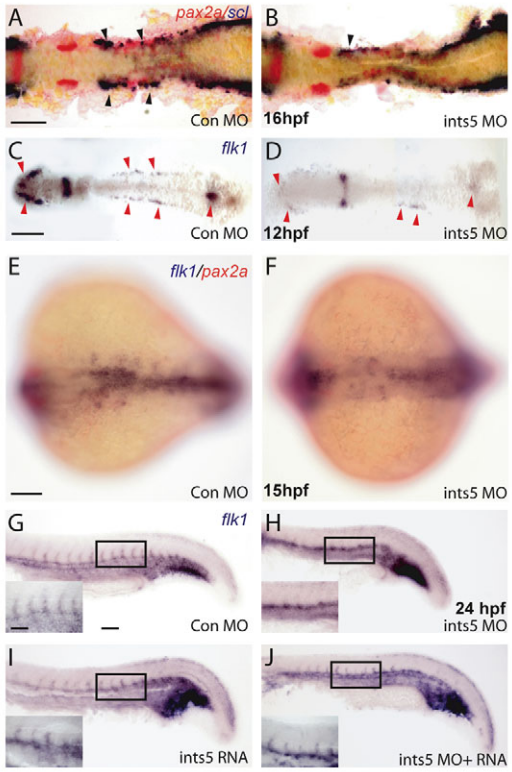

Fig. 2. Ints5 knockdown affects hematopoietic progenitors but not pronephric cells. (**A-F**) In situ hybridization to detect expression of *scl* (purple) in hematopoietic cells, *pax2a* (red) in the pronephric cells and *flk1* (purple) in endothelial cells. (A,B) *scl* and *pax2a* expression in control (A) and *ints5* morphants (B) at 16 hpf. Black arrowheads indicate the anterior *scl* expression in the ICM, and its reduction in *ints5* morphants; *pax2a* expression is unaffected. (C-F) Expression of *flk1* in control (C,E) and *ints5* morphants (D,F) at 12 hpf (C,D) and 15 hpf (E,F). Red arrowheads indicate *flk1* expression, which is much reduced in *ints5* morphants at an early stage (C,D) but recovers later in development (E,F). (**G-J**) Expression of *flk1* in injected embryos at 24 hpf. Insets show enlarged views of the boxed areas. Inter-segmental *flk1* expression is not detected in *ints5* morphants (H), in comparison to control embryos (G) and *ints5* RNA-injected embryos (I). Expression of *flk1* in inter-segmental vessels is rescued by co-injection of *ints5* RNA (J). A-D show dorsal views of flat-mounted embryos; E,F show dorsal views with anterior to the left; G-J show lateral views of the trunk with anterior to the left. Scale bars: 100 μm in A,C,E,G; 50 μm in inset in G.

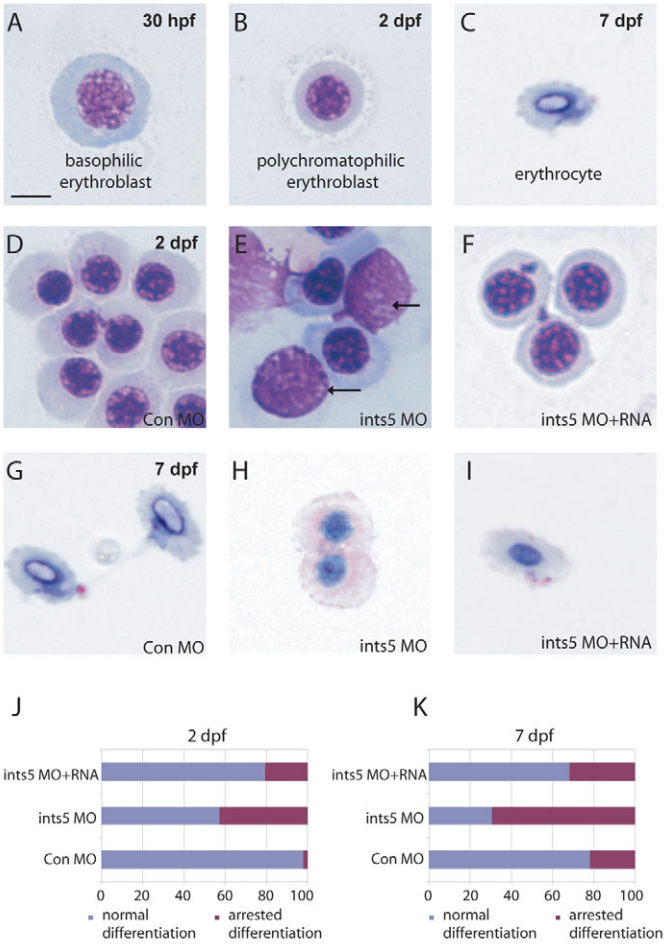

Fig. 3. Ints5 is required for erythrocyte differentiation. (**A-C**) May-Grunwald Giemsa staining shows normal red blood cells (RBCs) at various stages of differentiation at the indicated embryonic stages. (**D-F**) RBCs in embryos injected with control morpholinos (D), *ints5* morpholinos (E), or co-injected with *ints5* RNA and morpholinos (F) at 2 dpf. Arrows indicate the RBCs arrested at the basophilic erythroblast stage (E). (**G-I**) RBCs in embryos injected with control morpholinos (G), *ints5* morpholinos (H), or co-injected with *ints5* RNA and morpholinos (I) at 7 dpf. (**J**,**K**) Histograms showing the percentage of RBCs with normal (blue) or arrested (magenta) differentiation in injected embryos at 2 dpf (J) and 7 dpf (K). Scale bar: 10 μm.

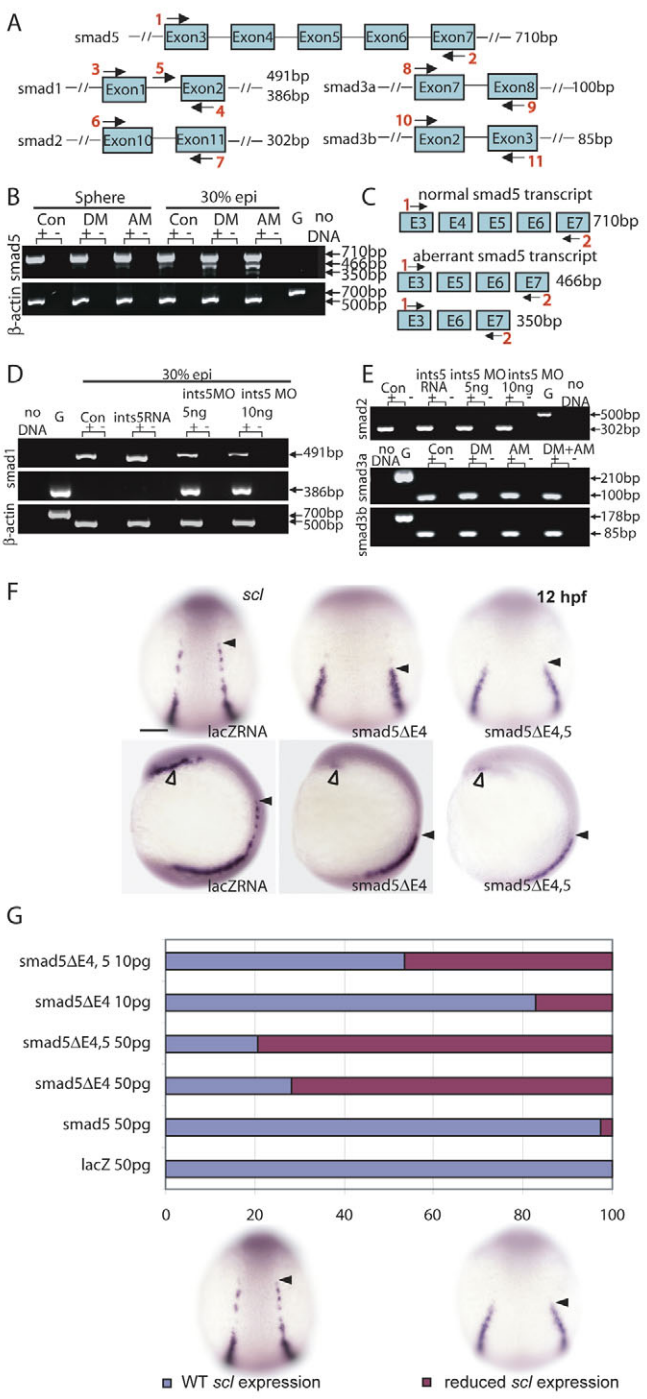

Fig. 4. Knockdown of Ints5 perturbs splicing of *smad1* and *smad5* RNA. (**A**) Schematic representation of the *smad5*, *smad1*, *smad2*, *smad3a* and *smad3b* genomic loci. Numbered black arrows indicate the position of primers used in RT-PCRs to detect splicing. The sizes of the predicted products using various primer pairs are indicated on the right. (**B**) At both sphere and 30% epiboly stages, aberrantly spliced *smad5* transcripts accumulate in *ints5* donor morpholino (DM)- and acceptor mopholino (AM)-injected embryos. β-actin control transcripts are correctly spliced to yield a 500 bp product from cDNA in comparison to a 700 bp genomic DNA product, G. (**C**) Schematic representation to show the wild-type 710 bp *smad5* transcript, and aberrant *smad5* transcripts that lack exon 4 (466 bp product), or lack both exon 4 and exon 5 (350 bp product). (**D**) Unspliced *smad1* (386 bp product with primer pair 4 and 5) and correctly spliced *smad1* (491 bp with primer pair 3 and 4) transcripts in 30% epiboly *ints5* morpholino-injected embryos. (**E**) Amplification of *smad2*, *smad3a* and *smad3b* with the primer pairs indicated in A shows correctly spliced products in *ints5* morphants. Amplification with primers spanning other regions of these genes also did not show aberrant splicing (data not shown). (**F**,**G**) Overexpression of truncated *smad5* transcripts causes hematopoiesis defects, similar to *ints5* morphants. (F) Whole-mount in situ hybridization to detect *scl* in control embryos (left), and in embryos injected with *smad5ΔE4* RNA (middle) or *smad5ΔE4,5* RNA (right) at 12 hpf. Black arrowheads indicate the anterior limit of *scl* expression in the ICM; open arrowheads mark *scl* expression in the RBI. Upper panel shows dorsal views with anterior to the top; lower panel shows lateral views with dorsal to the right. (G) Histogram showing the percentage of injected embryos with wild-type (blue) or reduced (magenta) *scl* expression levels. Scale bar: 50 μm.

incorrectly spliced *ints5* transcripts lacking 170 bp of the coding sequence (Fig. 1C). Western blot analysis using antibodies to detect Ints5 protein in embryo extracts shows that the *ints5* morpholinos disrupt the synthesis of Ints5 proteins (see Fig. S1 in the supplementary material).

By 24 hpf, embryos injected with *ints5* splice-junction morpholinos showed severe defects, with a shortened anterior-posterior axis and no circulating blood cells (Fig. 1E,P), in comparison to control morpholino- or RNA-injected embryos (Fig. 1D,O), indicating defects in convergent-extension cell movement and hematopoiesis. These phenotypes were rescued by co-injecting *ints5* RNA with the *ints5* splice-junction morpholinos (Fig. 1F,Q).

To determine if specification of the germ layers is affected in the *ints5* morphant embryos, we examined the expression of various germ-layer and cell-type specific marker genes during gastrulation (see Figs S2 and S7 in the supplementary material). Analysis of the expression of *ntl* (*ntla* – ZFIN) and *spt* (*tbx16* – ZFIN) in the mesoderm, *gsc* in the dorsal organizer, *dlx3* (*dlx3b* – ZFIN) in the neural plate, *sox17* in the endoderm and *myoD* (*myod1* – ZFIN) in the myotome showed that knockdown of *ints5* does not affect germ-layer specification. Furthermore, the patterning of dorsoventral and anterior-posterior axes was largely normal, and the shortened axis in *ints5* morphant embryos is therefore likely to be a result of impaired convergent-extension cell movements.

Since blood circulation is impaired in *ints5* morphants, we examined the expression of the hematopoietic genes *stem cell leukemia* (*scl*) and *gata1* by whole-mount in situ hybridization. The expression of *scl* transcripts was severely reduced in *ints5* morphants (Fig. 1I,J; Fig. 2B; see Fig. S7B in the supplementary material) in comparison to control embryos (Fig. 1G,H; Fig. 2A; see Fig. S7A in the supplementary material). By contrast, the adjacent *pax2a*-expressing pronephric cells were not affected in *ints5* morphants (Fig. 2A,B) (Majumdar et al., 2000). The expression of *gata1*, which is crucial for the specification of erythrocytes, was also reduced in *ints5* morphants (Fig. 1P) (Orkin and Zon, 1997). This reduction is rescued by the co-injection of *ints5* RNA (Fig. 1M,N,Q), whereas overexpression of *ints5* RNA by itself does not affect *scl* or *gata1* expression (Fig. 1K,L; data not shown). Semi-quantitative RT-PCR to determine the levels of *scl* and *gata1* RNA also show reduced expression of these genes in *ints5* morphants (see Fig. S3A,B in the supplementary material), which is rescued by co-injection of *ints5* RNA. Together, these experiments show that Ints5 function is required during primitive hematopoiesis.

As *scl* expression is also crucial for the formation of vascular precursors, we examined the expression of the endothelial gene *flk1* (*kdrl* – ZFIN) at various stages (de Jong and Zon, 2005; Liao et al., 1997). We find that, although the early expression of *flk1* is reduced in *ints5* morphants (Fig. 2C,D; see Fig. S3C in the supplementary material), this seems to recover later, and by 24 hpf, with the exception of the inter-segmental vessels, *flk1* expression is detected in most domains observed in control embryos (Fig. 2E-J). The lack of *flk1* expression in inter-segmental vessels might reflect cell migration and/or vessel branching defects. These results suggest that the common progenitor of hematopoietic and endothelial cells, the hemangioblast precursors (Vogeli et al., 2006), are not affected in *ints5* morphants per se, and that Ints5 function is required for hematopoietic development.

Ints5 is required for erythrocyte differentiation

A previous study by Qian et al. (Qian et al., 2007) showed that *scl* isoforms function in the initiation of primitive hematopoiesis and regulate erythroid cell differentiation. Since *ints5* morpholino-injected embryos have reduced *scl* expression, we examined erythroid differentiation in Ints5-manipulated embryos. May-Grunwald Giemsa staining of blood smears from wild-type embryos revealed normal erythrocyte progenitors. These cells differentiate and are typically categorized as: stage I, basophilic erythroblast (30 hpf); stage II, polychromatophilic erythroblast (2 days post fertilization, dpf); stage III, orthochromatophilic erythroblast (4 dpf); stage IV, erythrocyte (5 dpf onwards) (Fig. 3A-C; data not shown), based on the shape of their nucleus, size and morphology of the cells, and staining of the cytoplasm (Qian et al., 2007).

Blood smear analysis showed that, whereas 98% of RBCs grow to the polychromatophilic erythroblast stage (stage II) in control embryos by 2 dpf (Fig. 3D,J), only 58% of RBCs in *ints5* morphants develop normally. In *ints5* morphant embryos, 42% of cells arrested at the basophilic erythroblast stage (stage I; Fig. 3E,J). To investigate the role of Ints5 in RBC differentiation, we reduced the dosage of the antisense morpholinos so as to allow embryos to survive to later stages. At 7 dpf, only 30% of RBCs in *ints5* morphant embryos differentiated normally in comparison to control embryos in which ~80% of the cells are fully developed mature RBCs with flattened elliptical shape (Fig. 3G,H,K). Normal differentiation of RBCs in *ints5* morphants was restored by co-injection of *ints5* RNA (Fig. 3F,I,J,K). Thus, Ints5 function is required for the differentiation of erythrocytes.

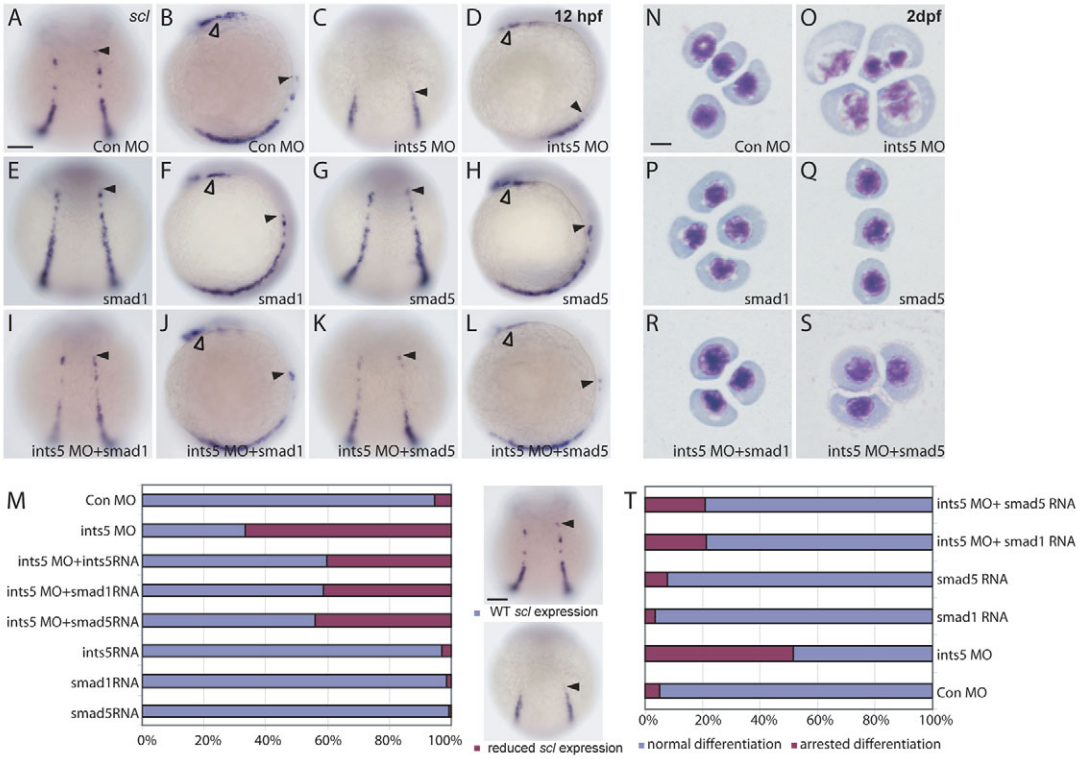

Fig. 5. The hematopoiesis defects induced by Ints5 knockdown are rescued by *smad1* and *smad5* RNA. (**A-L**) Whole-mount in situ hybridization to detect *scl* expression in 12 hpf embryos injected with control morpholinos (A,B), *ints5* morpholinos (C,D), *smad1* RNA (E,F), *smad5* RNA (G,H), *ints5* morpholinos with *smad1* RNA (I,J), or *ints5* morpholinos with *smad5* RNA (K,L). Black arrowheads indicate the anterior limit of *scl* expression in the ICM; open arrowheads indicate *scl* expression in the RBI. A,C,E,G,I,K show dorsal views of embryos with anterior to the top; B,D,F,H,J,L show lateral views of embryos with dorsal to the right. (**M**) Histogram showing the percentage of injected embryos with wild-type-like (blue) or reduced (magenta) *scl* expression. The total number of embryos for each staining is >180, and all experiments were carried out three independent times (see Table S1 in the supplementary material). (**N-S**) May-Grunwald Giemsa staining to show RBC differentiation in embryos injected with control morpholinos (N), *ints5* morpholinos (O), *smad1* RNA (P), *smad5* RNA (Q), *ints5* morpholinos with *smad1* RNA (R), or *ints5* morpholinos with *smad5* RNA (S) at 2 dpf. (**T**) Histogram showing the percentage of RBCs with normal (blue) or arrested (magenta) differentiation in injected embryos at 2 dpf. The total number of red blood cells counted for each sample is >200, and all experiments were carried out three independent times. Scale bars: 50 μm in A,M; 10 μm in N.

Ints5 is necessary for splicing of *smad1* and *smad5* transcripts

The Integrator complex is thought to be involved in snRNA processing (Baillat et al., 2005). As *ints5* morpholino-injected embryos have decreased *scl* expression, similar to *smad5* mutant embryos (McReynolds et al., 2007), we investigated whether the splicing of *smad5* and *smad1* is disrupted in *ints5* morphant embryos. Splicing of *smad2*, *smad3a*, *smad3b*, *cyclops* (*ndr2* – ZFIN), *squint* (*ndr1* – ZFIN) and actin (*bactin1* – ZFIN) RNAs was also examined as controls. Total RNA was extracted from embryos injected with control or *ints5* splice morpholinos, and RT-PCR was performed with primers for the various genes (Fig. 4A). In *ints5* morpholino-injected embryos, as early as gastrula stages we detected significant amounts of aberrantly spliced *smad5* transcripts that either lacked exon 4 or both exon 4 and exon 5 (Fig. 4B,C). To test the activity of the aberrant *smad5* splice products, we overexpressed capped synthetic mRNA encoding Smad5 lacking exon 4 (*smad5Δexon4*), or exons 4 and 5 (*smad5Δexon4,5*). Analysis of *scl* expression showed that embryos injected with *smad5Δexon4* or *smad5Δexon4,5* RNA have reduced expression, similar to *ints5* morphants (Fig. 4F,G). Furthermore, western blot analysis using antibodies to detect Smad5 protein in embryo extracts showed that the *ints5* morpholinos disrupted the synthesis of Smad5 proteins and led to the accumulation of truncated Smad5 proteins. The truncated Smad5 proteins correspond to proteins encoded by the aberrant transcripts, *smad5Δexon4* and *smad5Δexon4,5* (see Fig. S4 in the supplementary material). These truncated proteins might function as dominant-negative peptides that disrupt Smad5 function during development.

Similarly, unspliced *smad1* transcripts are also detected in *ints5* morpholino-injected embryos (Fig. 4D). However, we did not observe aberrant splicing of any exon-intron boundary of *smad2*, *smad3a* or *smad3b* transcripts, or other examined transcripts (Fig. 4E; see Fig. S5 in the supplementary material; data not shown). These results show that Ints5 is specifically required for the correct splicing of *smad1* and *smad5* RNA.

To understand the mechanism underlying the *smad1/5* splicing defects in *ints5* morphants, we examined the expression and processing of U1/U2 snRNA (see Fig. S6A in the supplementary material). Semi-quantitative RT-PCR analysis showed an accumulation of unprocessed primary U1/U2 snRNAs in *ints5* morpholino-injected embryos (see Fig. S6B,C,D in the supplementary material). In contrast to the increased primary U1/U2 snRNAs, the level of mature U1/U2 snRNAs was not significantly altered in *ints5* morphants (see Fig. S6E,F in the supplementary material). These results show that Ints5 regulation of *smad1/5* RNA splicing is mediated via U1/U2 snRNA processing.

Ints5 modulates hematopoiesis through Smad/BMP signaling

To determine the epistatic relationship between Ints5 and Smad1 or Smad5, we injected 10 pg of capped *smad1* or *smad5* RNA together with *ints5* morpholinos into 1-cell-stage embryos. We found that co-injected *smad1* or *smad5* RNA could restore *scl* expression and RBC differentiation in *ints5* morphants, similar to *ints5* RNA co-injections (Fig. 5C,D,I-L,M,O,R,S,T; see Fig. S7B,E,F in the supplementary material; see Table S1 in the supplementary material; $P \ll 0.01$). Control embryos injected with 10 pg of *smad1* or *smad5* RNA alone showed normal *scl* expression and RBC differentiation (Fig. 5E-H,M,P,Q,T; see Fig. S7C,D in the supplementary material), similar to those injected with control morpholinos (Fig. 5A,B,M,N,T; see Fig. S7A in the supplementary material). Blood circulation was also restored in *ints5* morphants upon rescue with *smad1* or *smad5* RNA (data not shown). These results, together with

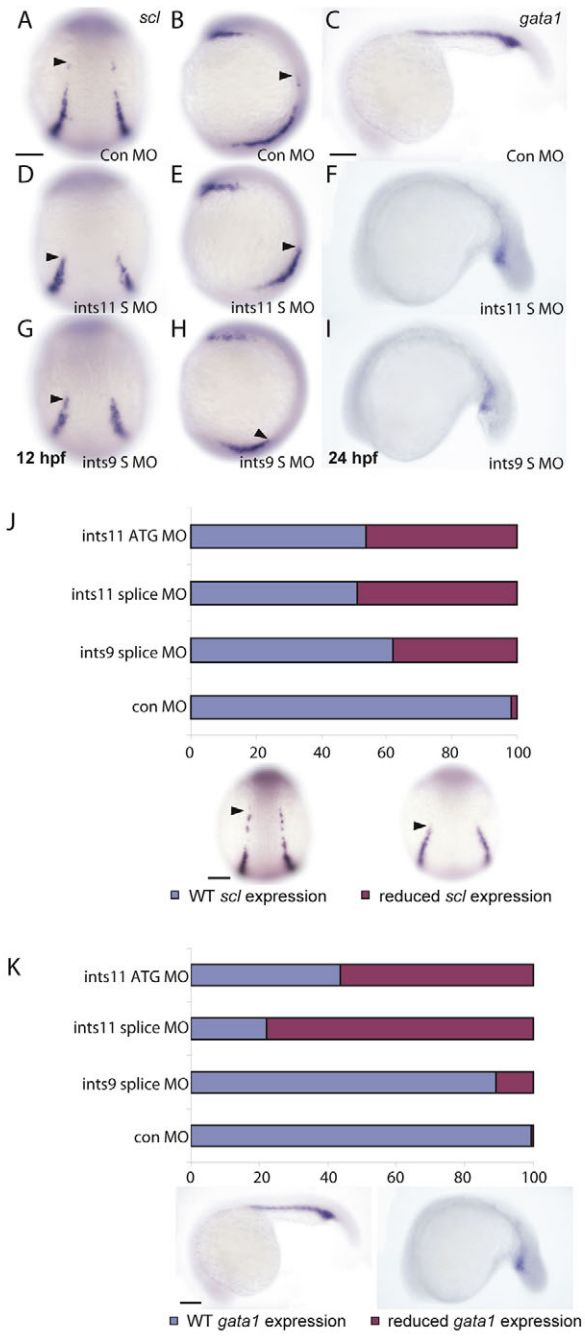

Fig. 6. Multiple subunits of the Integrator complex regulate primitive hematopoiesis. (**A-I**) Whole-mount in situ hybridization to detect *scl* (A,B,D,E,G,H) and *gata1* (C,F,I) expression in embryo injected with control morpholinos (A-C), *ints11* splice-junction morpholinos (S MO, D-F) and *ints9* splice-junction morpholinos (G-I). Black arrowhead indicates the anterior limit of *scl* expression in the ICM. The *ints9* and *ints11* morphants show substantially reduced *scl* and *gata1* expression in comparison to control morphants. (**J**,**K**) Histograms showing the percentage of injected embryos with wild-type (blue) or reduced (magenta) *scl* (J) and *gata1* (K) expression levels. Scale bars: 50 μm in A,J; 250 μm in C,K.

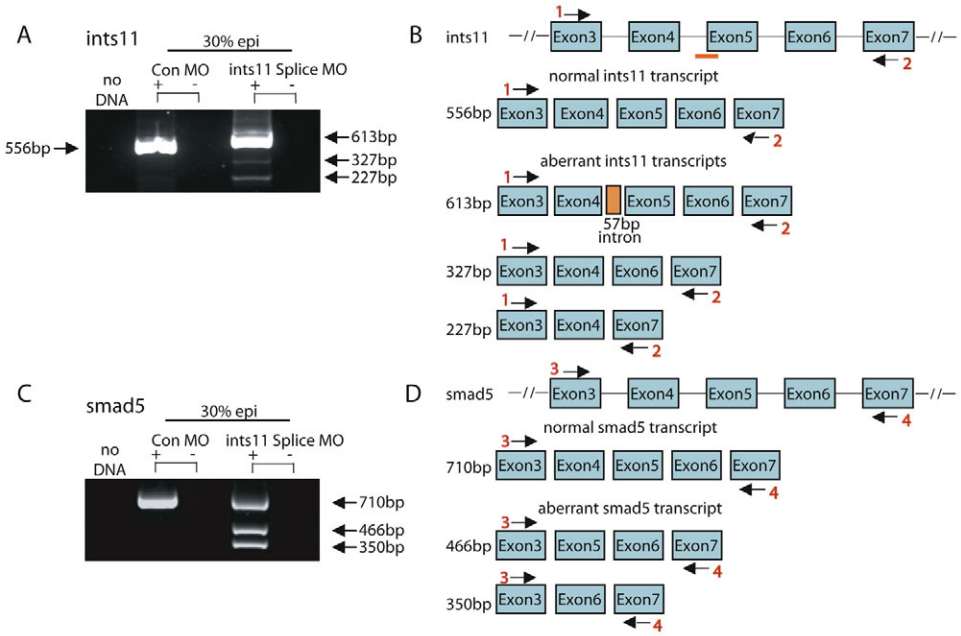

Fig. 7. Knockdown of *ints11* perturbs *smad5* splicing. (**A**) RT-PCR analysis shows that the *ints11* splice-junction morpholino efficiently blocks the correct splicing of *ints11* RNA, and several aberrant transcripts are detected. Transcripts are indicated by black arrows, with sizes indicated. (**B**) Schematic representation of the *ints11* genomic locus (upper panel); schematic representation of normal or aberrant *ints11* transcripts is shown in the lower panel. Numbered black arrows indicate the position of primers used in RT-PCRs to detect splicing. Orange bar shows the target site of the *ints11* splice-site morpholino. (**C**) RT-PCR analysis shows that splicing of *smad5* is impaired in *ints11* morphants. (**D**) Schematic representation of the *smad5* genomic locus (upper panel); the lower panel shows schematic representations of normal and aberrantly spliced *smad5* transcripts.

the results from semi-quantitative RT-PCR experiments (see Fig. S3 in the supplementary material), show that Ints5 functions in hematopoiesis by modulating *smad1/5* RNA splicing.

The Integrator complex regulates primitive hematopoiesis

As Ints5 is a subunit of the Integrator complex (Baillat et al., 2005), to find out whether Ints5 functions independently or as part of the Integrator complex in regulating hematopoiesis, we examined the activity of other Integrator subunits. We injected *ints11* (*zgc::110671* – ZFIN) ATG morpholinos and splice morpholinos targeting the boundary of intron 4 and exon 5 in the *ints11* gene into 1-cell-stage embryos. Both *ints11* morpholinos caused reduced expression of the hematopoietic markers *scl* and *gata1* (Fig. 6A-C,D-F,J,K; data not shown) in more than 50% embryos. In addition, embryos injected with *ints9* (*zgc::154012* – ZFIN) splice morpholinos targeting the boundary of intron 2 and exon 3 showed similar hematopoiesis defects (Fig. 6G-K). Morpholinos targeting the splice junction of *ints11* also caused defects in *smad5* splicing, U1/U2 snRNA processing and hematopoiesis (Figs 6 and 7; see Fig. S6B in the supplementary material). Therefore, multiple subunits of the Integrator complex, including Ints5, might be required for appropriate hematopoietic gene expression. These results suggest that the Integrator proteins function as a complex to regulate primitive hematopoiesis by modulating *smad1/5* splicing during zebrafish development.

DISCUSSION

Although hematopoiesis has been extensively studied, the molecular program of hematopoietic stem cell induction and self-renewal remains unclear. Recent work has revealed that the post-transcriptional processing of BMP Smads is involved in the maintenance of hematopoietic stem cell identity. Jiang et al. identified a C-terminal truncation in SMAD5, SMAD5β, which inactivates the protein. SMAD5β is expressed in both normal hematopoiesis and leukemogenesis (Jiang et al., 2000). Interestingly, the expression level of the SMAD5β isoform is higher in CD34+ hematopoietic stem cells than in terminally differentiated peripheral blood leukocytes, indicating that the alternative splicing of *SMAD5* is differentially regulated during the maturation of hematopoietic cells. Our work shows that the splicing of *smad1/5* is impaired by the knockdown of Ints5. Aberrant splicing of *smad5* leads to the production of dominant-negative forms of Smad5, the overexpression of which phenocopies the hematopoiesis phenotypes we observed in *ints5* morphants. These include reduced the expression of *scl* and, eventually, failure in erythrocyte differentiation. Thus, the accurate splicing of *smad5* is crucial for the normal progression of hematopoiesis and erythropoietic differentiation, and the failure to generate appropriate Smad5 products can lead to a reduction of hematopoietic progenitors.

The analysis of germ-layer specification and dorsoventral patterning suggests that these developmental processes are not affected in *ints5* morphant embryos. In addition, the expression of *pax2a*, *spt*, *myoD* and *ntl* suggests that anterior-posterior patterning is also largely normal (Fig. 2B; see Fig. S2F, Fig. S7B and Fig. S9C in the supplementary material). It may seem surprising that, although Ints5 knockdown affects *smad1/5* splicing, we do not observe early dorsoventral or anterior-posterior patterning, or germ-layer specification defects (see Fig. S2 in the supplementary material), as observed for *smad5* and other BMP pathway mutants (Dick et al., 2000; Hild et al., 1999; Kishimoto et al., 1997; Kodjabachian et al., 1999; Mullins et al., 1996; Schmid et al., 2000; Schulte-Merker et al., 1997). This can be explained by the maternal deposition of Integrator complex factors such as Ints5 (see Fig. S8 in the supplementary material). The maternal Ints products might allow normal functioning of the Integrator complex in early embryos, such that the early patterning events that are mediated by BMP signaling are not affected by the knockdown of Ints5. We also observe convergent-extension defects in *ints5* morphants (Fig 1E; see Fig. S2E,F,I,J and Fig. S9C,D,M in the supplementary material), leading to a shortened anterior-posterior axis in *ints5* morphants. It is possible that the Integrator subunits also regulate cell movements via Smad1/5 signaling, as co-injection of *smad1/5* RNA can restore normal cell movements in *ints5* morphants (see Fig. S9I-L,M in the supplementary material).

One interesting question is how the Integrator complex proteins, which are thought to function in RNA processing, might have such a specific effect on Smad/BMP signaling and hematopoiesis. Only *smad1* and *smad5* splicing is affected, whereas the expression of other Smads (e.g. *smad2*, *smad3a* and *smad3b*) is not disrupted, suggesting that the Integrator complex does not generally affect all splicing. Furthermore, our analysis of several genes [*chordin*, *vent*, *vox*, *ved*, *gata2a*, *eve1*, *smurf1* (*wwp1* – ZFIN), *bmp2b*, *bmp7a*, *ski* (*skia* – ZFIN), *sqt*, *cyc* and others] shows that the disruption of Integrator complex function does not generally affect genes expressed during gastrulation. This raises the possibility that the Integrator complex might be functioning specifically in the cells that respond to BMP signaling.

It is now known that mutations affecting some transcription or translation machinery components can have very specific effects on distinct cell types (Pellizzoni, 2007; van der Knaap et al., 2006). Recent work by Watanabe et al. has shown that Sf3b4, a subunit of Sf3b, which is a common RNA splicing complex, specifically binds to Bmpr1a and inhibits BMP signaling during osteochondral cell differentiation (Watanabe et al., 2007). There might be a potential connection between TGFβ/BMP signaling and the RNA processing machinery. So it is possible that Ints5, which is involved in U1/U2 snRNA maturation, which in turn is important for pre-mRNA splicing, might cooperate with other RNA splicing factors in specific cellular contexts (such as in hematopoietic progenitors), to specifically modulate BMP signaling via *smad1/smad5* RNA splicing. Alternatively, Ints5 itself might be post-transcriptionally regulated via factors that are specific to hematopoietic progenitors.

Deficiencies in RNA splicing have been shown to cause many genetic disorders (Pellizzoni, 2007; Solis et al., 2008). As the Integrator complex plays a vital role in the transcription and processing of snRNA, dysfunction of the Integrator subunits can lead to various developmental defects. In fact, recent work has shown that disruption of the murine integrator complex subunit 1 causes growth arrest and eventual apoptosis at early blastocyst stages (Hata and Nakayama, 2007). Integrator subunit 3 is a probable target for the amplification of chromosomal region 1q21 found in most hepatocellular carcinoma (HCC) tumors, and may be involved in the development and/or progression of this cancer (Inagaki et al., 2008). However, it is still unclear how these genes function, and how their malfunction leads to profound defects in specific biological processes. The study presented here reveals a potential link between snRNA processing and BMP signaling in hematopoiesis. Understanding the precise mechanisms by which the individual subunits function may provide insights into the roles played by the Integrator complex during development and tumorigenesis.

Acknowledgements

We thank Aniket Gore, Roland Dosch, Yun-Jin Jiang and members of the Sampath laboratory for discussions and suggestions; Helen Ngoc Bao Quach, Jiang Guanying and Leong Li Sun for technical assistance; Qian Feng for advice on blood smear analysis; Ge Ruowen for the *flk1* construct; and the TLL fish facility and sequencing facility. Work in the laboratory of Karuna Sampath is supported by the Temasek Life Sciences Laboratory, Singapore.

Competing interest statement

The authors have no competing interests.

Supplementary material

Supplementary material for this article is available at http://dev.biologists.org/cgi/content/full/136/16/2757/DC1

References

Akimenko, M. A., Ekker, M., Wegner, J., Lin, W. and Westerfield, M. (1994). Combinatorial expression of three zebrafish genes related to distal-less: part of a homeobox gene code for the head. *J. Neurosci.* **14**, 3475-3486.

Al-Adhami, M. A. and Kunz, Y. W. (1977). Ontogenesis of Hematopoietic sites in Brachydanio rerio. *Dev. Growth Differ.* **19**, 171-179.

Alexander, J. and Stainier, D. Y. (1999). A molecular pathway leading to endoderm formation in zebrafish. *Curr. Biol.* **9**, 1147-1157.

Baillat, D., Hakimi, M. A., Naar, A. M., Shilatifard, A., Cooch, N. and Shiekhattar, R. (2005). Integrator, a multiprotein mediator of small nuclear RNA processing, associates with the C-terminal repeat of RNA polymerase II. *Cell* **123**, 265-276.

Davidson, A. J. and Zon, L. I. (2004). The 'definitive' (and 'primitive') guide to zebrafish hematopoiesis. *Oncogene* **23**, 7233-7246.

de Jong, J. L. and Zon, L. I. (2005). Use of the zebrafish system to study primitive and definitive hematopoiesis. *Annu. Rev. Genet.* **39**, 481-501.

Detrich, H. W., 3rd, Kieran, M. W., Chan, F. Y., Barone, L. M., Yee, K., Rundstadler, J. A., Pratt, S., Ransom, D. and Zon, L. I. (1995). Intraembryonic hematopoietic cell migration during vertebrate development. *Proc. Natl. Acad. Sci. USA* **92**, 10713-10717.

Dick, A., Meier, A. and Hammerschmidt, M. (1999). Smad1 and Smad5 have distinct roles during dorsoventral patterning of the zebrafish embryo. *Dev. Dyn.* **216**, 285-298.

Dick, A., Hild, M., Bauer, H., Imai, Y., Maifeld, H., Schier, A. F., Talbot, W. S., Bouwmeester, T. and Hammerschmidt, M. (2000). Essential role of Bmp7 (snailhouse) and its prodomain in dorsoventral patterning of the zebrafish embryo. *Development* **127**, 343-354.

Fehling, H. J., Lacaud, G., Kubo, A., Kennedy, M., Robertson, S., Keller, G. and Kouskoff, V. (2003). Tracking mesoderm induction and its specification to the hemangioblast during embryonic stem cell differentiation. *Development* **130**, 4217-4227.

Gering, M., Rodaway, A. R., Gottgens, B., Patient, R. K. and Green, A. R. (1998). The SCL gene specifies haemangioblast development from early mesoderm. *EMBO J.* **17**, 4029-4045.

Griffin, K. J., Amacher, S. L., Kimmel, C. B. and Kimelman, D. (1998). Molecular identification of spadetail: regulation of zebrafish trunk and tail mesoderm formation by T-box genes. *Development* **125**, 3379-3388.

Hata, T. and Nakayama, M. (2007). Targeted disruption of the murine large nuclear KIAA1440/Ints1 protein causes growth arrest in early blastocyst stage embryos and eventual apoptotic cell death. *Biochim. Biophys. Acta* **1773**, 1039-1051.

Hild, M., Dick, A., Rauch, G. J., Meier, A., Bouwmeester, T., Haffter, P. and Hammerschmidt, M. (1999). The smad5 mutation somitabun blocks Bmp2b signaling during early dorsoventral patterning of the zebrafish embryo. *Development* **126**, 2149-2159.

Hsu, K., Kanki, J. P. and Look, A. T. (2001). Zebrafish myelopoiesis and blood cell development. *Curr. Opin. Hematol.* **8**, 245-251.

Inagaki, Y., Yasui, K., Endo, M., Nakajima, T., Zen, K., Tsuji, K., Minami, M., Tanaka, S., Taniwaki, M., Itoh, Y. et al. (2008). CREB3L4, INTS3, and SNAPAP are targets for the 1q21 amplicon frequently detected in hepatocellular carcinoma. *Cancer Genet. Cytogenet.* **180**, 30-36.

Jiang, Y., Liang, H., Guo, W., Kottickal, L. V. and Nagarajan, L. (2000). Differential expression of a novel C-terminally truncated splice form of SMAD5 in hematopoietic stem cells and leukemia. *Blood* **95**, 3945-3950.

Kishimoto, Y., Lee, K. H., Zon, L., Hammerschmidt, M. and Schulte-Merker, S. (1997). The molecular nature of zebrafish swirl: BMP2 function is essential during early dorsoventral patterning. *Development* **124**, 4457-4466.

Kodjabachian, L., Dawid, I. B. and Toyama, R. (1999). Gastrulation in zebrafish: what mutants teach us. *Dev. Biol.* **213**, 231-245.

Larsson, J. and Karlsson, S. (2005). The role of Smad signaling in hematopoiesis. *Oncogene* **24**, 5676-5692.

Liao, W., Bisgrove, B. W., Sawyer, H., Hug, B., Bell, B., Peters, K., Grunwald, D. J. and Stainier, D. Y. (1997). The zebrafish gene cloche acts upstream of a flk-1 homologue to regulate endothelial cell differentiation. *Development* **124**, 381-389.

Majumdar, A., Lun, K., Brand, M. and Drummond, I. A. (2000). Zebrafish no isthmus reveals a role for pax2.1 in tubule differentiation and patterning events in the pronephric primordia. *Development* **127**, 2089-2098.

McReynolds, L. J., Gupta, S., Figueroa, M. E., Mullins, M. C. and Evans, T. (2007). Smad1 and Smad5 differentially regulate embryonic hematopoiesis. *Blood* **110**, 3881-3890.

Mullins, M. C., Hammerschmidt, M., Kane, D. A., Odenthal, J., Brand, M., van Eeden, F. J., Furutani-Seiki, M., Granato, M., Haffter, P., Heisenberg, C. P. et al. (1996). Genes establishing dorsoventral pattern formation in the zebrafish embryo: the ventral specifying genes. *Development* **123**, 81-93.

Orkin, S. H. and Zon, L. I. (1997). Genetics of erythropoiesis: induced mutations in mice and zebrafish. *Annu. Rev. Genet.* **31**, 33-60.

Pellizzoni, L. (2007). Chaperoning ribonucleoprotein biogenesis in health and disease. *EMBO Rep.* **8**, 340-345.

Qian, F., Zhen, F., Xu, J., Huang, M., Li, W. and Wen, Z. (2007). Distinct functions for different scl isoforms in zebrafish primitive and definitive hematopoiesis. *PLoS Biol.* **5**, e132.
Schmid, B., Furthauer, M., Connors, S. A., Trout, J., Thisse, B., Thisse, C. and Mullins, M. C. (2000). Equivalent genetic roles for bmp7/snailhouse and bmp2b/swirl in dorsoventral pattern formation. *Development* **127**, 957-967.
Schulte-Merker, S., van Eeden, F. J., Halpern, M. E., Kimmel, C. B. and Nusslein-Volhard, C. (1994). no tail (ntl) is the zebrafish homologue of the mouse T (Brachyury) gene. *Development* **120**, 1009-1015.
Schulte-Merker, S., Lee, K. J., McMahon, A. P. and Hammerschmidt, M. (1997). The zebrafish organizer requires chordino. *Nature* **387**, 862-863.
Solis, A. S., Shariat, N. and Patton, J. G. (2008). Splicing fidelity, enhancers, and disease. *Front. Biosci.* **13**, 1926-1942.
Thisse, C., Thisse, B., Halpern, M. E. and Postlethwait, J. H. (1994). Goosecoid expression in neurectoderm and mesendoderm is disrupted in zebrafish cyclops gastrulas. *Dev. Biol.* **164**, 420-429.
Tian, J., Yam, C., Balasundaram, G., Wang, H., Gore, A. and Sampath, K. (2003). A temperature-sensitive mutation in the nodal-related gene cyclops reveals that the floor plate is induced during gastrulation in zebrafish. *Development* **130**, 3331-3342.
van der Knaap, M. S., Pronk, J. C. and Scheper, G. C. (2006). Vanishing white matter disease. *Lancet Neurol.* **5**, 413-423.
Vogeli, K. M., Jin, S. W., Martin, G. R. and Stainier, D. Y. (2006). A common progenitor for haematopoietic and endothelial lineages in the zebrafish gastrula. *Nature* **443**, 337-339.
von Bubnoff, A. and Cho, K. W. (2001). Intracellular BMP signaling regulation in vertebrates: pathway or network? *Dev. Biol.* **239**, 1-14.
Watanabe, H., Shionyu, M., Kimura, T. and Kimata, K. (2007). Splicing factor 3b subunit 4 binds BMPR-IA and inhibits osteochondral cell differentiation. *J. Biol. Chem.* **282**, 20728-20738.
Weinberg, E. S., Allende, M. L., Kelly, C. S., Abdelhamid, A., Murakami, T., Andermann, P., Doerre, O. G., Grunwald, D. J. and Riggleman, B. (1996). Developmental regulation of zebrafish MyoD in wild-type, no tail and spadetail embryos. *Development* **122**, 271-280.
Winnier, G., Blessing, M., Labosky, P. A. and Hogan, B. L. (1995). Bone morphogenetic protein-4 is required for mesoderm formation and patterning in the mouse. *Genes Dev.* **9**, 2105-2116.